INSTITUTO
UNIVERSITÁRIO
DE LISBOA

Three Essays on Modeling Energy Prices with Time-Varying Volatility and Jumps

Mário Jorge Correia Fernandes

PhD in Finance

Supervisors:

Doutor José Carlos Dias, Professor Associado com Agregação,

ISCTE-IUL

Doutor João Pedro Nunes, Professor Catedrático,

ISCTE-IUL

January, 2021

BUSINESS
SCHOOL

Department of Finance

Three Essays on Modeling Energy Prices with Time-Varying Volatility and Jumps

Mário Jorge Correia Fernandes

PhD in Finance

Jury:

Doutor Mohamed Azzim, Professor Catedártico , ISCTE-IUL

Doutor João Pedro Pereira, Professor Associado , Nova SBE-UNL

Doutor António Quintino, Professor Auxiliar Convidado , IST-UL

Doutor José Dias Curto, Professor Associado com Agregação, ISCTE-IUL

Doutor José Carlos Dias, Professor Associado com Agregação , ISCTE-IUL

January, 2021

Resume

This thesis addresses the modeling of energy prices with time-varying volatility and jumps in three separate and self-contained papers:

A. **Modeling energy futures volatility through stochastic volatility processes with Markov chain Monte Carlo**

This paper studies the volatility dynamics of futures contracts on crude oil, natural gas and electricity. To accomplish this purpose, an appropriate Bayesian model comparison exercise between seven stochastic volatility (SV) models and their counterpart GARCH models is performed, with both classes of time-varying volatility processes being estimated through a Markov chain Monte Carlo technique. A comparison exercise for hedging purposes is also considered by computing the extreme risk measures (using the Conditional Value-at-Risk) of simulated returns from the SV model with the best performance — i.e., the SV model with a t-distribution — and the standard GARCH(1,1) model for the hedging of crude oil, natural gas and electricity positions. Overall, we find that: (i) volatility plays an important role in energy futures markets; (ii) SV models generally outperform their GARCH-family counterparts; (iii) a model with t-distributed innovations generally improves the fitting performance of both classes of time-varying volatility models; (iv) the maturity of futures contracts matters; and (v) the correct specification for the stochastic behavior of futures prices impacts the extreme market risk measures of hedged and

unhedged positions.

B. **How does electrification under energy transition impact the portfolio management of energy firms?**

This paper presents a novel approach for structuring dependence between electricity and natural gas prices in the context of energy transition: a copula of mean-reverting and jump-diffusion processes. Based on historical day-ahead prices of the Nord Pool electricity market and the Henry Hub natural gas market, a stochastic model is estimated via the maximum likelihood approach and considering the dependency structure between the innovations of these two-dimensional returns. Given the role of natural gas in the global policy for energy transition, different copula functions are fit to electricity and natural gas returns. Overall, we find that: (i) using an out-of-sample forecasting exercise, we show that it is important to consider both mean-reversion and jumps; (ii) modeling correlation between the returns of electricity and natural gas prices, assuring nonlinear dependencies are satisfied, leads us to the adoption of Gumbel and Student-t copulas; and (iii) without government incentive schemes in renewable electricity projects, the usual maximization of the risk-return trade-off tends to avoid a high exposure to electricity assets.

C. **Modeling commodity prices under alternative jump processes and fat tails dynamics**

The recent fluctuations in commodity prices affected significantly Oil Gas (O&G) companies' returns. However, integrated O&G companies are not only exposed to the downturn of oil prices since a high level of integration allows these firms to obtain non-perfectly positive correlated portfolio. This paper aims to test several different stochastic processes to model the main strategic commodities in integrated O&G companies: brent, natural gas, jet fuel and diesel. The competing univariate models include the log-normal and double exponential jump-diffusion model,

the Variance-Gamma process and the geometric Brownian motion with nonlinear GARCH volatility. Given the effect of correlation between these assets, we also estimate multivariate models, such as the Dynamic Conditional Correlation (DCC) GARCH, DCC-GJR-GARCH and the DCC-EGARCH models. Overall, we find that: (i) the asymmetric conditional heteroskedasticity model substantially improves the performance of the univariate jump-diffusion models; and (ii) the multivariate approaches are the best models for our strategic energy commodities, in particular the DCC-GJR-GARCH model.

JEL Classification: C52, C58, Q40, Q41

Keywords: Bayesian econometrics, Commodity prices, Energy prices, Futures, Maximum likelihood.

Resumo

Esta tese aborda a modelação de preços de energia com modelos de volatilidade variável no tempo e saltos e encontra-se separada em três artigos distintos:

A. **Modelação da volatilidade de futuros de energia com processos de volatilidade estocástica utilizando "Markov chain Monte Carlo"**

   Este artigo estuda a dinâmica da volatilidade dos contratos futuros de petróleo bruto, gás natural e eletricidade. Para cumprir este propósito, um exercício apropriado de comparação de modelos Bayesianos entre sete modelos de volatilidade estocástica (VE) e os correspondentes modelos GARCH é realizado, com ambas as classes de processos de volatilidade variável no tempo tendo sido estimadas através de uma técnica de "Markov Chain Monte Carlo". Um exercício de comparação para fins de "hedging" também é considerado, calculando as medidas de risco extremo (usando o "Conditional Value-at-Risk") dos retornos simulados do modelo de VE com o melhor desempenho —ou seja, o modelo VE com uma distribuição-t— e o modelo GARCH (1,1) para hedging das posições de petróleo bruto, gás natural e eletricidade. No geral, descobrimos que: (i) a volatilidade desempenha um papel importante nos mercados futuros de energia; (ii) os modelos VE geralmente superam seus homólogos da família GARCH; (iii) um modelo com inovações t-distribuídas geralmente melhora o desempenho de ajuste de ambas as classes de modelos de volatilidade que variam no tempo; (iv) o vencimento de

contratos de futuros importa; e (v) a correta especificação do comportamento estocástico dos preços futuros impacta as medidas de risco extremo de mercado das posições “hedged” e “unhedged”.

B. **Como a eletrificação na transição energética impacta a gestão de portefólio das empresas de energia?**

Neste artigo apresentamos uma nova abordagem no contexto da transição energética: o modelo estocástico com reversão à média e difusão com saltos combinado com funções de cópula. Com base nos preços históricos do mercado de eletricidade (“Nord Pool”) e do mercado de gás natural (“Henry Hub”), estimamos um modelo estocástico com base no método de Máxima Verossimilhança. O modelo teórico é fornecido considerando a estrutura de dependência entre as inovações desses retornos bi-dimensionais. Dado o papel do gás natural na política global de transição energética, ajustamos diferentes funções de cópula aos retornos de eletricidade e gás natural. Descobrimos que: (i) Num exercício de previsão fora da amostra, confirmamos o desempenho de previsão do modelo estocástico de reversão à média e difusão com saltos; (ii) modelar a correlação entre os retornos de eletricidade e gás natural, garantindo que dependências não lineares sejam satisfeitas, conduz-nos às funções da cópula (principalmente a cópula de Gumbel e t-Student) e (iii) sem incentivos ou mecanismos governamentais de apoio a projetos renováveis, a habitual maximização do trade-off de risco-retorno tenderá a evitar elevadas exposições a ativos de eletricidade.

C. **Modelação do preço de “commodities” com base em processos alternativos de difusão em saltos e caudas pesadas**

As recentes flutuações nos preços das “commodities” afetaram fortemente os retornos das empresas de petróleo e gás (O&G). No entanto, as empresas integradas de O&G não estão apenas expostas ao decréscimo dos preços do petróleo, uma

vez que um elevado nível de integração permite obter carteiras correlacionadas, embora não perfeitamente positivas. Este artigo tem como objetivo testar diversos processos estocásticos para modelar as principais “Commodities” estratégicas em empresas integradas de O&G: “brent”, gás natural, “jet fuel” e “diesel”. Os modelos univariados concorrentes incluem o modelo log-normal e o modelo “double exponential jump-diffusion”, a abordagem Variância-Gama e o movimento browniano geométrico (GBM) com volatilidade GARCH não linear. Dado o efeito de correlação entre esses ativos, também estimamos modelos multivariados, como a Correlação Condicional Dinâmica (DCC) GARCH, DCC-GJR-GARCH e o DCC-EGARCH. Descobrimos que: (i) o modelo de heterocedasticidade condicional assimétrica melhora substancialmente o desempenho dos modelos univariados de difusão com saltos e (ii) no geral, as abordagens multivariadas são os melhores modelos para nossas “commodities” estratégicas, principalmente o DCC-GJR-GARCH.

Classificação JEL: C52, C58, Q40, Q41

Palavras-chave: Econometria bayesiana, Futuros, Máxima Verosimilhança, Preços de Commodities, Preços de energia.

Acknowledgements

I would like to thank my parents (Maria Alexandrina Fernandes and António da Fonseca Fernandes) and my wife Joana Caria Silva for their constant encouragement and unconditional support during this PhD program.

I take this opportunity to warmly thank Professors José Carlos Dias, PhD and João Pedro Nunes, PhD for their full availability and support. It has been a privilege working with both.

I would also like to thank to António and my Master José Paulo Oliveira for their support in my professional and academic career.

I wish to express my gratitude to my colleagues Tiago Mota Dutra and Luís Miguel Gaspar for their support during the PhD programme.

Contents

1. Introduction

This thesis addresses three essays on modeling energy prices with time-varying volatility and jumps in three separate and self-contained papers.

The first paper aims to study the volatility dynamics of futures contracts of crude oil, natural gas and electricity. To accomplish this goal, an appropriate Bayesian model comparison exercise between seven stochastic volatility (SV) models and the corresponding GARCH models is performed, with both classes of time-varying volatility processes being estimated using a Markov chain Monte Carlo (MCMC, hereafter) method.

This paper offers a twofold contribution for the current literature on modeling the volatility of futures for energy markets. First, we model futures contracts of crude oil, natural gas and electricity based on a list of SV and GARCH models and using the MCMC technique. The list of models includes not only the standard processes, but also models accommodating jumps, heavy-tails and leverage effects.

Second, we show the relevance of the accurate specification of the theoretical framework to be used when modeling futures contracts of energy markets. To the best of our knowledge, this problem has not been addressed yet in the energy economics and energy finance literature. To accomplish this goal, we compute the CVaR measure suggested by Rockafellar and Uryasev (2000) for each commodity/utility based on the model with best fit performances and then compare it with the standard GARCH

model. A short hedge strategy using futures contracts is suggested and implemented for this risk management formulation. Moreover, and beyond these two main contributions, this paper can be also considered as a natural extension of Chan and Grant (2016): the Bayesian approach suggested by these authors is extended to other energies (e.g., electricity to represent renewable energies); a higher level of frequency in data (daily data versus weekly data) is considered; besides spot prices of energy, derivatives contracts (in particular, futures) are also studied; and, finally, the relevance of the estimation framework under MCMC for risk management and hedging purposes is addressed.

The second paper provides a novel approach for structuring dependence between electricity and natural gas prices in the context of energy transition: a copula of mean-reverting and jump diffusion processes. For this purpose, we use historical day-ahead prices of the Nord Pool electricity market and the Henry Hub natural gas market, a stochastic model is estimated through the maximum likelihood estimation and considering the dependency structure between the innovations of these two-dimensional returns. The adoption of a stochastic process with mean-reversion and jumps is motivated by the stylized facts in the electricity (and natural gas) markets since they are recognized to be seasonal, mean-reverting and to exhibit frequent jumps in the spot data, as documented, for instance, in Benth et al. (2008) and Haugom (2011). These features in both markets not only contribute to higher volatility levels, but also for an increasing difficulty to estimate models governed by appropriate stochastic processes. In order to illustrate the relevance of the model, we first estimate several spot prices of one of the most significant European electricity day-ahead market and then we conduct an out-of-sample forecasting exercise against the competing standard geometric Brownian motion model with Poisson jumps proposed by Merton (1976) and a GARCH model adapted to the extreme value theory (henceforth, EVT). After modeling the be-

havior of the electricity returns, and given the recent predictions of an increasing global demand for natural gas and since this is the unique fossil fuel available in the context of energy transition, we propose a copula framework (incorporating mean reversion and jumps) to model a simulated portfolio of electricity (from renewable energy sources) and natural gas assets.

In a nutshell, we offer a twofold contribution to the current literature. First, we develop the theoretical framework to model electricity and natural gas spot prices based on a copula of mean-reverting and jump-diffusion processes. As a second contribution, our research generates multiple empirical findings. To the best of our knowledge, this is a novel development for exploring the effect of the nonlinear dependence between electricity and natural gas markets in a context of energy transition while maintaining the three most significant features of these assets: spikes/drops, jumps and seasonality. This new approach should be not only relevant for energy companies (with or without renewable energy assets) but also for policy makers.

Finally, the main concerning of the last paper is to compare a number of univariate and multivariate models using the most important strategic commodities in Oil & Gas (O&G) firms. For this purpose, the historical prices between 1990-2017 for brent, natural gas, jet fuel and diesel are tested. In fact, the recent fluctuations in commodity markets heavily affected O&G companies' returns. However, integrated O&G firms are not only exposed to the downturn of the crude oil prices since a high level of integration allows to obtain non perfectly positively correlated portfolio. In the first part of the paper, we estimate four univariate stochastic processes including jump-diffusion and fat-tails. The competing models include the log-normal model of Merton (1976), the double exponential jump-diffusion of Kou (2002), the Variance-Gamma (VG, hereafter) approach of Madan and Seneta (1990), Madan et al. (1998) and Seneta (2004) and the geometric Brownian motion (GBM, henceforth) with nonlinear GARCH (NGARCH, hereafter)

volatility suggested by Engle and Ng (1993). The second part of the paper aims modeling our main strategic commodities with three theoretical multivariate approaches: the Dynamic Conditional Correlation (DCC, henceforth) GARCH, DCC-GJR-GARCH and the DCC-EGARCH.

Therefore, the last paper offers three contributions for the current literature on modeling the spot prices of commodity markets. First, and most importantly, these models have not been explored for an integrated portfolio of an O&G firm. Although some researchers used the standard stochastic processes— GBM, Constant Elasticity of Variance and others— to model prices of some individual commodities (e.g. Geman and Shih (2009)), this paper studies different jump-diffusion processes on a real and not perfectly correlated portfolio of energy prices.

Second, we test four univariate jump-diffusion and fat tails stochastic models. To support the phenomenon of discontinuous variations in commodity prices, this research tests empirically the pertinence of jumps by incorporating the log-normal and the double exponential jump-diffusion models and others pure jumps processes of finite variations, however with infinitely jump-diffusion, such as the VG process. On the other hand, the traditional conditional heteroskedasticity phenomena is also tested by estimating the NGARCH volatility model to the standard GBM.

Third, since the correlation effects matters for integrated O&G firms, we suggest to test three different multivariate approaches based on the Dynamic Conditional Correlation: the DCC-GARCH, DCC-GJR-GARCH and the DCC-EGARCH. This is a natural empirical extension of Cappiello et al. (2006) since the authors provided the technical details to extended the research of Engle (2002) by allowing to incorporate the asymmetric effects in the standard DCC model and applied the multivariate models to stock markets. Additionally, we also provide several empirical findings since we extended the period of analysis in order to include the recent decreases in the prices of these commodity

markets.

This thesis proceeds as follows. Chapter 2 presents the first paper. Chapter 3 presents the second paper. Chapter 4 presents the third paper. Finally, Chapter 5 concludes.

2. Modeling energy futures volatility through stochastic volatility processes with Markov chain Monte Carlo

Abstract: This paper studies the volatility dynamics of futures contracts on crude oil, natural gas and electricity. To accomplish this purpose, an appropriate Bayesian model comparison exercise between seven stochastic volatility (SV) models and their counterpart GARCH models is performed, with both classes of time-varying volatility processes being estimated through a Markov chain Monte Carlo technique. A comparison exercise for hedging purposes is also considered by computing the extreme risk measures (using the Conditional Value-at-Risk) of simulated returns from the SV model with the best performance—i.e., the SV model with a t-distribution—and the standard GARCH(1,1) model for the hedging of crude oil, natural gas and electricity positions. Overall, we find that: (i) volatility plays an important role in energy futures markets; (ii) SV models generally outperform their GARCH-family counterparts; (iii) a model with t-distributed innovations generally improves the fitting performance of both classes of time-varying volatility models; (iv) the maturity of futures contracts matters; and (v) the correct specification for the stochastic behavior of futures prices impacts the extreme market risk measures of hedged and unhedged positions.

JEL Classification: C11, C52, C58, Q40, Q41

Keywords: Bayesian econometrics, Commodities, Energy markets, Futures contracts, Markov chain Monte Carlo, Stochastic volatility, Utilities.

2.1 Introduction

Modeling and forecasting commodities and utilities futures prices (and the corresponding volatility) have been receiving much attention in the literature over the years, since their dynamics have important economic and financial implications. A plausible motivation for this interest is the need for accurately measure the volatility of energy futures prices, since this variable plays a key role on the price connection between spot and futures markets—see, for example, Silvapulle and Moosa (1999), Lin and Tamvakis (2001), Hammoudeh et al. (2003), Hammoudeh and Li (2004) and Huang et al. (2009)—and on risk management problems—see, for instance, Sadorsky (2006) and Aloui and Mabrouk (2010).

The first attempts to remove the assumption of constant variance from the conventional time series and econometric models have been based on the autoregressive conditional heteroscedasticity (ARCH, hereafter) process proposed by Engle (1982), which allows the conditional variance to change over time as a function of past errors leaving the unconditional variance constant. A more general class of processes, known as generalized ARCH (GARCH, henceforth) processes, has been subsequently suggested by Bollerslev (1986). The main advantages of the GARCH model over the ARCH process is that it permits a more parsimonious description in many situations and provides a better fit for modeling time series data when the data exhibits heteroscedasticity and volatility clustering. However, in some situations there are specific

aspects of the model that can be improved so that it can better detect the features and dynamics of a particular time series. For instance, the standard GARCH model is not able to capture the leverage effects that are often observed in financial time series. Therefore, several GARCH extensions were proposed to make GARCH modeling more flexible. The most popular extensions of the traditional GARCH models include the possibility of accommodating jumps, heavy-tails and capturing the asymmetric behavior in volatility.

An alternative class of stochastic volatility (SV, henceforth) models has also emerged in the literature inspired in the prominent work of Taylor (1994). Even though GARCH and SV models can be both considered as time-varying volatility processes, they possess different assumptions and properties and, therefore, are nonnested. Nevertheless, it is possible to make formal comparison exercises between the models of each class. While in the primer class of models the conditional variance is a deterministic function of model parameters and historical data, in the latter class volatility is assumed to be a latent variable following a given stochastic process—see, for instance, Sadorsky (2006), Trolle and Schwartz (2009), Larsson and Nossman (2011) and Brooks and Prokopczuk (2013).

More recently, Chan and Grant (2016) compared a battery of GARCH and SV models for the spot prices of crude oil, refined products and natural gas prices under a Bayesian approach. The authors found that SV models outperform their GARCH counterpart models for their list of energy prices. To the best of our knowledge, however, such formal Bayesian model comparison exercise has not been addressed yet in the case of energy futures contracts. Hence, one of the purposes of this paper is to fill this gap in the literature on energy economics and energy finance.

The stochastic behavior of energy and derivatives prices is a relevant theme for modeling purposes and beyond; different assumptions for the stochastic path of energy

and derivative prices also affect risk management and hedging strategies. The original contribution of Markowitz (1952) on diversification of investments and selection of efficient portfolios (also known as the modern portfolio theory) potentiated the use of financial derivatives on the physical energy traded in the spot markets, in order to reduce the companies market risk exposure. In fact, years later, Artzner et al. (1999) and Rockafellar and Uryasev (2000) present the foundations of a coherent risk measure for portfolio and risk optimization: the Conditional Value-at-Risk (CVaR, hereafter). This coherent (extreme) risk measure represents a step forward compared with the standard deviation and the Value-at-Risk (VaR, hereafter) measures.

This paper offers two relevant contributions for the current literature on modeling the volatility of futures on energy products. First, we model futures contracts of crude oil, natural gas and electricity based on a list of SV and GARCH models and using the Markov chain Monte Carlo (MCMC, hereafter) technique. The battery of models includes not only the standard processes, but also models accommodating jumps, heavy-tails and leverage effects. Second, we show the relevance of correctly specifying the theoretical framework to be used when modeling futures contracts. To the best of our knowledge, this problem has not been addressed yet in the energy economics and energy finance literature. To accomplish this goal, we compute the CVaR measure suggested by Rockafellar and Uryasev (2000) for each commodity/utility based on the model with best fit performances and then compare it with the standard GARCH model. A short hedge strategy using futures contracts is adopted for this risk management problem. Moreover, and beyond these two main contributions, this paper can be also considered as a natural extension of Chan and Grant (2016): the Bayesian approach suggested by these authors is extended to other energies (e.g., renewable energies); a higher level of frequency in data (daily data versus weekly data) is considered; besides spot prices of energy, derivatives contracts (in particular, futures) are

also studied; and, finally, the relevance of the estimation framework under MCMC for risk management and hedging purposes is analyzed.

The remainder of the paper is organized as follows. Section 2.2 describes the list of time-varying volatility models to be tested and presents the Bayes factor to evaluate the fitting performance. Section 2.3 describes the futures contracts on crude oil, natural gas and electricity that will be used in our empirical analysis. Section 2.4 presents the numerical results and tests several futures maturities. Section 2.5 performs the numerical analysis for hedging applications. Section 2.6 concludes. Additional details and results are relegated to the appendixes.

2.2 Time-varying volatility models

For the analysis to remain self-contained, the next two subsections briefly outline the two classes of time-varying volatility models that will be considered for modeling the volatility of commodities and utilities futures contracts, that is: SV models and GARCH models. An excellent description of these two classes of processes is provided already in Chan and Grant (2016). Nevertheless, their main features are also collected in Appendixes A and B for the sake of completeness. This section ends with a short description of the Bayes approach that will be used in our empirical analysis. Details about the required estimation procedures for both time-varying volatility models under the MCMC technique are provided also in Chan and Grant (2016).

2.2.1 The class of stochastic volatility models

The first class of processes that will be used for analyzing the behavior of the volatility of commodities and utilities futures contracts is divided into seven different stochastic

volatility models, in which the volatility term is a random variable. The list of stochastic volatility models includes: (i) the standard stochastic volatility model (hereafter, SV model), where the log-volatility is assumed to follow a stationary auto-regressive model of first order, i.e. an AR(1) process; (ii) an extension to the standard stochastic volatility model, where now the log-volatility is assumed to follow a stationary auto-regressive model of second order (henceforth, SV-2 model); (iii) a stochastic volatility model accommodating the possibility of infrequent jumps (SV-J model); (iv) the stochastic volatility in mean model (SV-M model) proposed by Koopman and Hol Uspensky (2002); (v) the standard stochastic volatility model coupled with moving average innovations (SV-MA model) suggested by Chan (2013); (vi) a stochastic volatility process incorporating t innovations to capture extreme events in future contracts (SV-t model); and (vii) a stochastic volatility model with leverage effects (SV-L model). The technical details about these processes are presented in Appendix A.

2.2.2 The class of GARCH models

In order to compare the performance of the aforementioned SV models against their counterpart GARCH-family processes for modeling the behavior of volatility in commodities and utilities futures contracts, the following GARCH models will be also considered: (i) the standard GARCH model (hereafter, G model), where the conditional variance follows an AR(1) process; (ii) a GARCH model with the conditional variance following now an AR(2) process (henceforth, G-2 model); (iii) a GARCH model with jumps (G-J model); (iv) the traditional GARCH in mean model (G-M model); (v) the GARCH model incorporating innovations with a first-order moving average process (G-MA model); (vi) the GARCH model with t innovations (G-t model); and (vii) a GARCH model accommodating leverage effects, as suggested by Glosten et al. (1993). The technical details about these models can be consulted in Appendix B.

2.2.3 Evaluating the fitting performance of energy futures contracts

Following Chan and Grant (2016), our formal Bayesian model comparison exercise between the SV and GARCH processes is also performed through a Bayes factor (hereafter, BF) using importance sampling. In particular, given a specific set of models $\{M_1, ..., M_K\}$, each model M_k (for $k = 1, ..., K$) is defined by two components, namely: the likelihood function $p(y|\theta_k, M_k)$, which is dependent of the parameter vector θ_k with dimension p_k; and the prior density represented by $p(\theta_k|M_k)$. For $i, j \in \{1, ..., K\}$, one possible approach for model comparison is the BF defined by

$$BF_{ij} = \frac{p(y|M_i)}{p(y|M_j)}, \tag{2.1}$$

that is interpreted as the BF in favor of M_i against M_j. The marginal likelihood under model M_k is defined as

$$p(y|M_k) = \int p(y|\theta_k, M_k)p(\theta_k|M_k)d\theta_k. \tag{2.2}$$

The marginal likelihood (2.2) can be interpreted as a density prediction of our empirical data under model M_k evaluated at the actual observed data y. A $BF_{ij} > 1$ denotes that the observed data is more likely under the process M_i when compared to model M_j. Consequently, a $BF_{ij} > 1$ is interpreted as a Bayesian evidence in favor of model M_i where the dimension of superiority is proportional to the value determined by the BF. For instance, a $BF_{ij} = 5$ means that process M_i is 5 times more likely than model M_j, given the collected data to estimate both models.

We recall also that computing the marginal likelihood is a nontrivial exercise, since the integral appearing in equation (2.2) generally involves an high-dimensional inte-

gration problem and, hence, cannot be solved analytically. A plausible approach to overcome this issue is to use the cross-entropy method of Chan and Eisenstat (2015), which is an improved technique of an adaptive importance sampling method to compute the marginal likelihood—see also Rubinstein (1997) and Rubinstein and Kroese (2004). Additional technical details on the computation of the marginal likelihood for the time-varying volatility models considered in this paper are available in Chan and Grant (2016, Section 3 and Appendix B).

2.3 Data

In this section, we present the main features of the data set chosen for our empirical research. We are considering the most usual daily prices of futures contracts used by energy companies (non-renewable and renewable energies). This data set includes the daily prices of futures contracts on crude oil (West Texas Intermediate), natural gas (Henry Hub) and electricity. Crude oil and natural gas futures prices are collected from the US Energy Information Administration (EIA)/Thomson Reuters Eikon. The time series for our futures contracts are collected from January 2000 to November 2019, on a daily basis, but given the recent deregulation and integration in electricity markets in Europe, the time series for electricity futures prices is collected from January 2015 to November 2019, also on a daily basis. For this purpose, we use the electricity futures contracts of the Iberian market (MIBEL). This market belongs to the Internal Energy Market of the European Union, arising from the liberalisation of electricity production and commercialisation.

The crude oil futures prices are measured in dollars per barrel ($/bbl). The futures prices for crude oil represent daily closing prices at 2:30 p.m. from the trading floor of the New York Mercantile Exchange (NYMEX), for a specific delivery month. Each

of these futures contracts expires on the third business day prior to the 25th calendar day of the month preceding the delivery month. For natural gas high frequency data, (spot and futures) prices are based on delivery at the Henry Hub in Louisiana. These contracts are measured in dollars per million Btu ($/MMbtu). Once again, the official daily is based on the closing prices at 2:30 p.m. from the trading floor of the NYMEX, for a specific delivery month. Following the philosophy of crude oil futures contracts, natural gas contracts expire three business days prior to the first calendar day of the delivery month. Therefore, the delivery month for the derivatives contracts that we consider is the calendar month following the trade date. Electricity futures contracts are measured in €/MWh and the futures prices represent the settlement price for each trading day. To preserve the consistency of the previous futures contracts, we adopt electricity prices with one month of time to maturity. As usual, the prices of the futures contracts are converted into geometric returns by taking the first difference of the logs and multiplying by 100. Appendix C presents the plots of the daily returns of spot and 1 month futures prices of crude oil, natural gas and electricity.

2.4 Empirical results

To better explore and emphasize the major findings of our empirical work, this section is divided in three subsections. In the first, and following the insights of Chan and Grant (2016), we compare the performance of the seven stochastic volatility processes against their GARCH-family counterpart models using a formal Bayesian model comparison exercise. The main goal here is to examine which class of time-varying volatility models tends to provide a better fit to the price dynamics of futures contracts on crude oil, natural gas and electricity. Furthermore, we also want to highlight which particular (and more complex) model features should be included in the standard SV and GARCH

processes to obtain a superior model performance. To accomplish this purpose, all the models are estimated through the Bayesian techniques outlined in Chan and Grant (2016, Appendix A), whereas the required marginal likelihoods are computed via the improved cross-entropy method suggested in Chan and Eisenstat (2015) and Chan and Grant (2016, Appendix B). In the second, we report the posterior estimates of the model parameters of both classes of processes for our set of energy futures contracts. Finally, in the third, we provide some robustness tests regarding the use of alternative futures contracts possessing different expiry dates.

The econometric approach is implemented by adopting the *Matlab* code offered by Chan and Grant (2016), and all the numerical results are obtained by implementing the MCMC technique using *Matlab* (R2015a 32 bit) running on an Intel Core i7 2.40GHz personal computer.

2.4.1 Model comparison exercise results

Table 2.1 presents the (log) marginal likelihoods for stochastic volatility models (in Panel A) and GARCH models (in Panel B) to analyze the stochastic behavior of the price of each selected futures contract with a time to maturity of 1 month. The numerical standard errors are also reported in parentheses.

Table 2.1: Log marginal likelihoods corresponding to the estimated models.

	Crude oil	Natural gas	Electricity
Panel A: Stochastic volatility models			
SV	-10732.6	-12466.5	-2263.9
	(0.03)	(0.06)	(0.22)
SV-2	-10733.4	-12465.8	-2259.0
	(0.16)	(0.16)	(0.30)
SV-J	-10729.0	-12471.9	-2286.8
	(0.51)	(0.40)	(1.25)
SV-M	-10737.2	-12473.7	-2270.4
	(0.06)	(0.07)	(0.31)
SV-MA	-10734.4	-12466.3	-2265.5
	(0.02)	(0.06)	(0.18)
SV-t	-10721.1	-12451.2	-2233.2
	(0.02)	(0.01)	(1.06)
SV-L	-10720.6	-12468.0	-2265.8
	(0.04)	(0.04)	(0.24)
Panel B: GARCH models			
G	-10812.5	-12586.3	-2569.4
	(0.01)	(0.01)	(0.04)
G-2	-10812.6	-12583.7	-2570.6
	(0.05)	(0.16)	(0.04)
G-J	-10721.5	-12476.0	-2265.8
	(0.07)	(0.09)	(0.13)
G-M	-10819.4	-12592.5	-2577.6
	(0.02)	(0.03)	(0.06)
G-MA	-10815.4	-12587.3	-2571.3
	(0.01)	(0.01)	(0.03)
G-t	-10721.3	-12460.2	-2257.3
	(0.02)	(0.02)	(0.02)
G-L	-10794.5	-12589.8	-2531.1
	(0.03)	(0.03)	(0.04)

Several conclusions can be taken from the results contained in Table 2.1. We start noting that the SV-L model offers the best fitting performance for crude oil futures contracts, followed closely by the SV-t, G-t, G-J and SV-J models (in this specific ranking order). Clearly, both the t-distributed innovations and the jump component substantially

improve the performance of the standard SV and standard G models. Even though the inclusion of the leverage effect in stochastic volatility processes places the SV-L model at the top of all tested processes for crude oil futures contracts, such additional modeling complexity is much less important than the t-distributed innovations and the jump component in the case of GARCH models, though such feature still improves the standard G model.

In the case of natural gas and electricity futures contracts, the SV-t process is undoubtedly the one that provides the best fit to the corresponding data, while the G-t model is ranked in second place in this comparative model exercise. The comparison of crude oil futures contracts with the natural gas ones (for the same 1 month to maturity) reveals that the price paths of crude oil futures contracts behave more like equity high frequency data than natural gas futures contracts—we recall that there is supporting evidence in the literature that models with leverage effects achieve better performances for estimating equity returns. Moreover, the seasonality effect that is exhibited in the path of natural gas futures (and spot) prices can explain the better performance of the stochastic model that assumes the error follows a heavy-tailed distribution, such as the t-distribution. A similar conclusion is achieved also for electricity futures. A plausible reason for this finding is that such distribution captures the spikes (upward movements) and drops (downward movements) observed in the electricity futures prices.

Another relevant finding for our set of commodities/utilities futures contracts is related with the general performance of both classes of time-varying volatility models: the stochastic volatility processes generally outperform their corresponding GARCH models. A plausible explanation for this observation is that the log-volatility is assumed to follow a specific random variable in the case of stochastic volatility models, whereas GARCH models only assume a conditional variance that is a deterministic function of parameters estimated based on lagged data. The unique exceptions are observed

in the case of crude oil and electricity futures contracts when we consider the pair of models with a jump component. For this pair of models (i.e., SV-J versus G-J models), the log marginal likelihoods are -10729.0 (resp., -2286.8) and -10721.5 (resp., 2265.8) for crude oil (resp., electricity) futures contracts, respectively. Therefore, we obtain a Bayes factor of 1.8×10^3 (resp., 1.3×10^9) in favor of the GARCH process against its stochastic volatility counterpart model.

Furthermore, and despite the aforementioned disadvantage of the GARCH-family models against SV models, when GARCH models incorporate a heavy-tailed distribution (i.e., a t-distribution or a jump component) they attenuate misspecification and extreme events problems in crude oil, natural gas and electricity futures contracts and, therefore, the inherent over-performance of stochastic volatility models decreases. This fact also explains why both the G-t and G-J models show evidence of a much better performance than other GARCH processes in our model comparative exercise.

We also investigate which other features might be important when modeling the dynamics of energy futures contracts. For instance, comparing the standard SV model with the corresponding process in which the log-volatility follows a stationary AR(2) process, it follows that the SV-2 model provides only small improvements in the log marginal likelihood of natural gas and electricity futures contracts. By contrast, the SV-2 model deteriorates the fitting performance for crude oil futures contracts when compared with the standard SV model. In the case of GARCH models, the standard G model performs slightly better than the G-2 model for crude oil and electricity futures contracts, whereas the G-2 model is superior to the standard G model for natural gas futures contracts.

The relevance of the volatility feedback for modeling energy futures is also tested. Even though the empirical evidence suggests the importance of volatility feedback for the log returns of stocks, its inclusion when modeling futures contracts on energy seems to be

unimportant. Clearly, the log marginal likelihood decreases in all cases when the component of volatility feedback is added to stochastic volatility and GARCH processes. This finding in energy futures is consistent with the results documented in Sadorsky (2006) and Chan and Grant (2016), who highlight no evidence that the G-M model predicts better than the standard G model for several non-renewable energies, such as crude oil, heating oil and natural gas.

Another important issue is related with the possible inclusion of moving average components in both stochastic volatility and GARCH processes for modeling energy futures contracts. Overall, our results reveal that adding a moving average component does not improve the fitting performance of futures contracts on crude oil, natural gas and electricity. The only exception is the case of natural gas: the SV-MA process performs better than the standard SV model, though the differences are almost negligible. We note that this is not consistent with the findings of Chan and Grant (2016), who document that the SV-MA and G-MA models improve the performance fit of crude oil and natural gas spot prices, for the period of 1997-2015, when compared with the corresponding standard SV and G models, respectively.

Our last finding involves the introduction of leverage effects in both classes of models. As already mentioned, there is evidence supporting that adding leverage effects improves the fitting performance of both the standard SV and G models in the case of crude oil futures contracts. However, an opposite conclusion can be drawn in the case of natural gas futures contracts: the models incorporating leverage effects performed poorly when compared with their corresponding standard ones. The analysis for electricity futures prices shows mixed results: adding the leverage effect in stochastic volatility models contributes to a slightly worst performance than the standard SV model, whereas such additional complexity in the case of GARCH models improves the standard G model.

2.4.2 Estimation results

The numerical results from the estimation of SV models for crude oil, natural gas and electricity futures contracts are reported in Tables 2.2, 2.3 and 2.4, respectively. For comparative purposes, and given space constraints, the estimation of the GARCH-family counterpart models is shown in Tables D.1, D.2 and D.3 collected in Appendix D. In order to complement the parameter posterior mean estimations, the corresponding standard deviations are also presented in parentheses.

Table 2.2: Posterior means and standard deviations for the parameter set of stochastic volatility models estimated through MCMC and for crude oil futures contracts.

	SV	SV-2	SV-J	SV-M	SV-MA	SV-t	SV-L
μ	0.06	0.07	0.07	0.13	0.06	0.07	0.03
	(0.03)	(0.03)	(0.03)	(0.04)	(0.03)	(0.03)	(0.03)
μ_h	1.41	1.40	1.35	1.41	1.40	1.28	1.40
	(0.13)	(0.16)	(0.15)	(0.13)	(0.13)	(0.15)	(0.13)
ϕ_h	0.98	0.88	0.99	0.98	0.98	0.99	0.98
	(0.00)	(0.07)	(0.00)	(0.00)	(0.00)	(0.01)	(0.01)
ω_h^2	0.02	0.04	0.01	0.02	0.02	0.02	0.02
	(0.00)	(0.01)	(0.00)	(0.00)	(0.00)	(0.01)	(0.01)
ρ_h	-	0.08	-	-	-	-	-
	-	(0.08)	-	-	-	-	-
κ	-	-	0.02	-	-	-	-
	-	-	(0.01)	-	-	-	-
μ_k	-	-	-0.91	-	-	-	-
	-	-	(0.16)	-	-	-	-
σ_k^2	-	-	25.10	-	-	-	-
	-	-	(13.29)	-	-	-	-
λ	-	-	-	-0.02	-	-	-
	-	-	-	(0.01)	-	-	-
ψ	-	-	-	-	-0.03	-	-
	-	-	-	-	(0.01)	-	-
ν	-	-	-	-	-	15.39	-
	-	-	-	-	-	(3.30)	-
ρ	-	-	-	-	-	-	-0.36
	-	-	-	-	-	-	(0.08)
Q(20)	11.45	12.44	12.54	11.75	8.63	10.95	10.67
	(1.672)	(0.03)	(2.54)	(1.67)	(1.99)	(1.64)	(1.97)
Q^2(20)	25.86	27.15	21.90	25.35	25.55	23.69	27.53
	(4.87)	(0.08)	(5.40)	(4.73)	(4.67)	(4.55)	(4.22)

Notes: $Q(20)$ and $Q^2(20)$ are, respectively, the Ljung-Box and McLeod-Li statistics of order 20 computed on the standardized residuals and squared standardized residuals. The 5% and 1% critical values are 31.41 and 37.57, respectively.

Table 2.3: Posterior means and standard deviations for the parameter set of stochastic volatility models estimated through MCMC and for natural gas futures contracts.

	SV	SV-2	SV-J	SV-M	SV-MA	SV-t	SV-L
μ	-0.01	-0.01	-0.03	-0.02	-0.01	-0.02	0.00
	(0.04)	(0.04)	(0.04)	(0.06)	(0.04)	(0.04)	(0.04)
μ_h	2.12	2.08	2.06	2.12	2.11	1.98	2.12
	(0.11)	(0.22)	(0.12)	(0.10)	(0.11)	(0.12)	(0.11)
ϕ_h	0.98	0.89	0.98	0.98	0.98	0.98	0.98
	(0.00)	(0.09)	(0.00)	(0.00)	(0.00)	(0.00)	(0.00)
ω_h^2	0.02	0.04	0.02	0.03	0.02	0.02	0.02
	(0.00)	(0.01)	(0.00)	(0,00)	(0.00)	(0.00)	(0.00)
ρ_h	-	0.08	-	-	-	-	-
	-	(0.09)	-	-	-	-	-
κ	-	-	0.02	-	-	-	-
	-	-	(0.01)	-	-	-	-
μ_k	-	-	1.72	-	-	-	-
	-	-	(0.27)	-	-	-	-
σ_k^2	-	-	71.56	-	-	-	-
	-	-	(27.87)	-	-	-	-
λ	-	-	-	0.00	-	-	-
	-	-	-	(0.01)	-	-	-
ψ	-	-	-	-	-0.04	-	-
	-	-	-	-	(0.01)	-	-
ν	-	-	-	-	-	13.28	-
	-	-	-	-	-	(2.86)	-
ρ	-	-	-	-	-	-	0.09
	-	-	-	-	-	-	(0.06)
$Q(20)$	26.89	26.92	25.39	26.34	18.68	28.00	26.28
	(2.621)	(4.13)	(3.78)	(2.40)	(2.45)	(2.84)	(2.64)
$Q^2(20)$	48.47	55.94	42.69	50.02	48.42	35.90	48.71
	(7.56)	(8.90)	(8.64)	(7.36)	(7.57)	(7.83)	(8.05)

Notes: $Q(20)$ and $Q^2(20)$ are, respectively, the Ljung-Box and McLeod-Li statistics of order 20 computed on the standardized residuals and squared standardized residuals. The 5% and 1% critical values are 31.41 and 37.57, respectively.

Table 2.4: Posterior means and standard deviations for the parameter set of stochastic volatility models estimated through MCMC and for electricity futures contracts.

	SV	SV-2	SV-J	SV-M	SV-MA	SV-t	SV-L
μ	-0.04	-0.04	-0.07	-0.06	-0.03	-0.02	-0.02
	(0.04)	(0.04)	(0.05)	(0.06)	(0.04)	(0.05)	(0.04)
μ_h	0.87	0.88	1.30	0.86	0.87	0.89	0.89
	(0.11)	(0.12)	(0.26)	(0.12)	(0.12)	(0.35)	(0.11)
ϕ_h	0.77	0.94	0.97	0.78	0.78	0.77	0.77
	(0.03)	(0.15)	(0.01)	(0.04)	(0.03)	(0.01)	(0.03)
ω_h^2	0.61	0.51	0.04	0.64	0.61	0.61	0.61
	(0.06)	(0.16)	(0.00)	(0.11)	(0.08)	(0.00)	(0.07)
ρ_h	-	-0.16	-	-	-	-	-
	-	(0.12)	-	-	-	-	-
κ	-	-	0.03	-	-	-	-
	-	-	(0.01)	-	-	-	-
μ_k	-	-	2.63	-	-	-	-
	-	-	(0.96)	-	-	-	-
σ_k^2	-	-	76.84	-	-	-	-
	-	-	(25.13)	-	-	-	-
λ	-	-	-	0.01	-	-	-
	-	-	-	(0.02)	-	-	-
ψ	-	-	-	-	0.05	-	-
	-	-	-	-	(0.03)	-	-
ν	-	-	-	-	-	8.63	-
	-	-	-	-	-	(1.34)	-
ρ	-	-	-	-	-	-	0.08
	-	-	-	-	-	-	(0.05)
Q(20)	36.34	35.26	31.65	38.72	31.98	30.20	31.45
	(7.38)	(5.91)	(4.69)	(6.70)	(7.27)	(0.69)	(5.52)
Q^2(20)	23.39	20.72	17.58	17.42	18.29	7.09	19.50
	(11.81)	(6.98)	(5.16)	(4.00)	(4.89)	(0.03)	(5.94)

Notes: Q(20) and Q^2(20) are, respectively, the Ljung-Box and McLeod-Li statistics of order 20 computed on the standardized residuals and squared standardized residuals. The 5% and 1% critical values are 31.41 and 37.57, respectively.

The stochastic volatility processes applied to crude oil and natural gas futures contracts show that the posterior mean parameter ϕ_h is quite similar across all the models. Under the SV-2 model it is equal to 0.88 and 0.89 for crude oil and natural gas futures contracts, respectively. The posterior mean parameters governing the remaining stochastic volatility processes, for these two futures contracts, reveal a high persistence behavior by ranging between 0.98 and 0.99. For electricity futures contracts, however,

such persistence is less pronounced: the estimated ϕ_h ranges between 0.77 and 0.97 across the seven stochastic volatility models, which can be justified with the spikes and downturns observed in the underlying asset price. A similar persistent behavior across models is also generally observed for the remaining parameters governing the stochastic volatility process.

Similarly to the estimates of the stochastic volatility processes, the parameters governing the evolution of the conditional variance process associated to GARCH models are also highly persistent across all processes. For crude oil and natural gas futures contracts, the posterior mean of β_1 is estimated to be between 0.93 to 0.95 and to be equal to 0.91, respectively, if we do not consider the G-2 model—see Tables D.1 and D.2, respectively. In the case of the G-2 model, however, β_1 is much lower: 0.71 and 0.37 for crude oil and natural gas futures contracts, respectively. As shown in Table D.3, the persistence of the β_1 parameter is much weaker across all models for the case of electricity futures contracts.

As highlighted in Tables 2.2 and 2.3, the average jump size μ_k for the stochastic volatility model is negative for crude oil and positive for natural gas futures contracts. These results are coherent with the corresponding ones for the G-J model—see Tables D.1 and D.2. For electricity futures, the jump size is also positive, which is coherent with the dominance of the spikes (over downturns) in the futures markets—see Tables 2.4 and D.3. The estimates for the jump probability κ in the stochastic volatility models are lower than the corresponding ones for the GARCH processes.

The volatility feedback coefficient λ is estimated to be equal to -0.02, 0.00 and 0.01 for crude oil, natural gas and electricity futures contracts—see Tables 2.2, 2.3 and 2.4, respectively. Similar results are also observed for the corresponding GARCH models in Appendix D. We recall that when $\lambda = 0$ the SV-M model (resp., G-M model) reduces to the standard SV model (resp., standard G model). Hence, these results (very close to

0) reveal that the volatility feedback is not relevant for modeling non-renewable energy futures (more specifically, crude oil and natural gas futures) and electricity futures. As expected, this is consistent with the conclusions that have been already drawn for both SV-M and G-M models based on the analysis of the log marginal likelihood results from Table 2.1.

The estimate of the moving average component ψ in the SV-MA and G-MA models is also close to zero for the three futures contracts under analysis, as highlighted in Tables 2.2, 2.3, 2.4, D.1, D.2 and D.3. These parameter values justify also why the log marginal likelihoods for the crude oil, natural gas and electricity futures contracts highlighted in Table 2.1 for the SV-MA model (resp., G-MA model) are not too farther away from the corresponding ones reported for the standard SV model (resp., standard G model).

The degree of freedom parameter ν associated to crude oil, natural gas and electricity futures contracts is estimated to be equal to 15.39, 13.28 and 8.63—see Tables 2.2, 2.3 and 2.4, respectively. These results indicate that the tails of the t-distribution are relatively heavy, i.e. outliers tend to occur frequently. Clearly, this supports the better fitting performance already reported for both SV-t and G-t models. We recall that the SV-t process has been ranked at the top of all tested models in the case of natural gas and electricity futures contracts, as evidenced by the log marginal likelihoods reported in Table 2.1. We further note that these two models are always preferable than their counterpart standard SV and G models—see Appendix D for additional details on the GARCH processes.

The correlation ρ between observation and state innovations is negative for crude oil and positive for natural gas and electricity futures contracts: it is equal to -0.36, 0.09 and 0.08, respectively—see Tables 2.2, 2.3 and 2.4. In the case of crude oil, such parameter value implies that a negative shock at time t tends to augment the volatility

at time $t+1$. However, an opposite behavior is achieved in the case of natural gas and electricity futures markets.

Finally, we report the Ljung-Box and McLeod-Li statistics of twentieth order calculated on the standardized residuals and squared standardized residuals, respectively. In the case of crude oil, these diagnostic tests fail to reject the null hypothesis of no serial correlation in the standardized residuals and squared standardized residuals at the 5% level for all the SV and GARCH models—see Tables 2.2 and D.1, respectively. This indicates that both classes of processes adequately capture the time-varying volatility of the crude oil data. The Ljung-Box tests show that the null hypothesis of no serial correlation in the standardized residuals is not rejected at the 5% level for the SV and GARCH models when applied to natural gas data—see Tables 2.3 and D.2, respectively. The same conclusion is obtained also from the Q^2(20) tests reported in Table D.2 for the GARCH processes. However, with the exception of the SV-t model, all the McLeod-Li tests shown in Table 2.3 reject the null hypothesis of no serial correlation in the squared standardized residuals at the 1% level for the remaining stochastic volatility models. This result provides further evidence supporting the previous argument that the SV-t model is preferable to the standard SV model and other competing processes. Lastly, in the case of electricity, the McLeod-Li tests fail to reject the null hypothesis of no serial correlation in the squared standardized residuals at the 5% level for all the SV and GARCH models—see Tables 2.4 and D.3, respectively. The penultimate line of Table 2.4 reveals that the null hypothesis of no serial correlation in the standardized residuals is not rejected at the 5% level in the SV-t model and is not rejected at the 1% level for the remaining stochastic volatility models, with the exception of the SV-M model for which such null hypothesis is rejected also at the 1% level. The Q(20) tests reported in Table D.3 for the GARCH processes show that the null hypothesis of no serial correlation in the standardized residuals is not rejected at the 1% level only

in the case of the G-J and G-t models. These results support, again, the ranking of the marginal likelihood, which favours the SV-t model with respect to the remaining processes in the case of electricity futures contracts.

2.4.3 Testing different maturities

The energy futures contracts analyzed so far have a time to maturity of 1 month. However, it is well known that futures contracts on a given underlying asset generally have different expiry dates available. Therefore, we now extend our empirical analysis in order to test if the time to maturity of energy futures contracts influences our previous conclusions. To accomplish this purpose, we re-estimate each model using the MCMC technique and compute the corresponding log marginal likelihood for crude oil and natural gas futures contracts expiring in 2, 3 and 4 months. We only perform this empirical exercise for crude oil and natural gas futures contracts since these energy derivatives are both at the top of the ranking of the Chicago Mercantile Exchange in the sub-group of energy—in the Top 10+, crude oil and Henry Hub Natural Gas futures are the most liquid futures contracts (i.e., they are ranked in the first two positions, respectively); the remaining positions are composed by refining products and not electricity derivatives. Table 2.5 presents the (log) marginal likelihoods aiming to test if the use of alternative futures contracts on crude oil and natural gas with different expiry dates changes our previous results in terms of the model fitting performance. The numerical results from the estimation of SV models for crude oil and natural gas futures contracts expiring in 2, 3 and 4 months are reported in Appendix E.

Table 2.5: Log marginal likelihoods for different maturities of futures contracts on crude oil and natural gas.

	Crude oil futures			Natural gas futures		
	2 month	3 month	4 month	2 month	3 month	4month
Panel A: Stochastic volatility models						
SV	-10480.0	-10257.4	-10084.2	-5669.2	-5435.7	-5250.2
	(0.04)	(0.03)	(0.02)	(0.02)	(0.03)	(0.02)
SV-2	-10479.5	-10257.7	-10083.3	-5668.9	-5435.7	-5250.2
	(0.32)	(0.20)	(0.17)	(0.09)	(0.04)	(0.04)
SV-J	-10479.3	-10261.3	-10090.4	-5670.6	-5430.5	-5239.6
	(0.25)	(0.30)	(0.65)	(0.19)	(0.22)	(0.24)
SV-M	-10484.2	-10261.1	-10087.5	-5675.6	-5442.1	-5256.6
	(0.05)	(0.04)	(0.06)	(0.03)	(0.02)	(0.02)
SV-MA	-10481.7	-10258.8	-10084.3	-5670.4	-5438.2	-5253.1
	(0.02)	(0.02)	(0.04)	(0.04)	(0.01)	(0.02)
SV-t	-10471.5	-10249.8	-10072.9	-5666.4	-5432.3	-5242.8
	(0.01)	(0.05)	(0.05)	(0.05)	(0.02)	(0.01)
SV-L	-10465.7	-10286.8	-10072.7	-5670.7	-5437.7	-5252.2
	(0.02)	(0.68)	(0.08)	(0.01)	(0.01)	(0.02)
Panel B: GARCH models						
G	-10551.1	-10325.1	-10166.3	-5699.5	-5471,0	-5299.5
	(0.02)	(0.01)	(0.01)	(0.02)	(0.02)	(0.02)
G-2	-10551.8	-10324.1	-10165.0	-5700.5	-5471.9	-5300.7
	(0.03)	(0.09)	(0.04)	(0.09)	(0.10)	(0.02)
G-J	-10467.3	-10243.5	-10068.7	-5675.6	-5435.7	-5254.3
	(0.08)	(0.08)	(0.05)	(0.04)	(0.07)	(0.08)
G-M	-10557.7	-10331.7	-10172.5	-5705.5	-5477.2	-5306.1
	(0.02)	(0.02)	(0.02)	(0.02)	(0.03)	(0.02)
G-MA	-10554,0	-10328,0	-10168.5	-5701.9	-5473.8	-5302.6
	(0.01)	(0.01)	(0.01)	(0.01)	(0.01)	(0.01)
G-t	-10472.4	-10251,0	-10075.3	-5670.5	-5436.9	-5251.8
	(0.01)	(0.01)	(0.02)	(0.06)	(0.03)	(0.02)
G-L	-10532.5	-10307.2	-10152.4	-5701.4	-5474.4	-5302.2
	(0.03)	(0.03)	(0.02)	(0.02)	(0.03)	(0.03)

Overall, the best fitting performance is obtained by the stochastic volatility models for all tested expiry dates. The only exception is in the case of crude oil futures contracts for the pair of SV-J versus G-J models, in which the latter process is preferable (when compared with the corresponding SV-J model) independently of the time to maturity. We recall that this is consistent with the results reported for 1 month futures on crude

oil. Hence, these findings support our previous conclusions that stochastic volatility processes generally outperform their corresponding GARCH-family models.

Another salient feature is that the results for the futures contracts expiring in 2 months are similar to those observed with the 1 month futures contracts: the SV-L and the SV-t models are the ones offering the best fitting performance for crude oil and natural gas futures contracts, respectively. However, for the contracts expiring in 3 and 4 months such model ranking changes. In the case of crude oil futures, the G-J model is at the top for contracts expiring in 3 and 4 months, whereas the SV-J model is the best for natural gas futures contracts expiring in 3 and 4 months. Clearly, the time to maturity matters when one needs to choose a time-varying volatility model for modeling the volatility of energy futures contracts.

Once again, the general performance of stochastic volatility processes compared with their corresponding GARCH-family models can be explained with the fact that the primer processes assume that the log-volatility is following a specific random variable, while in the latter the conditional variance is a deterministic function of parameters estimated based on past continuous returns. The performance of the G-J model in crude oil futures with a time to maturity of 3 and 4 months can be justified by the inclusion of heavy-tailed distributions (i.e., by introducing a jump component). In other words, this jump component in the GARCH process introduces an extra dynamic in the path of futures contracts against extreme events and, therefore, turns the performance of stochastic volatility models less evident.

Finally, and given our aim of presenting a hedging exercise in the following section, we also estimate both time-varying volatility model classes for the spot prices (and assuming the same time horizon). Due to space constraints, we only present here the two main findings. First, the fitting performance of stochastic volatility processes also beats the GARCH-family models. Second, there is evidence that the SV-t model offers

the best fitting performance in the case of crude oil and natural gas, while the SV-MA process is preferable for electricity—see Appendix F for additional details on the log marginal likelihoods for the series of daily price changes on crude oil, natural gas and electricity spot prices. The corresponding posterior means and standard deviations estimations on these energy prices are available upon request.

2.5 Implications for hedging purposes

Integrated energy producers can hedge against (undesirable) falls in energy spot prices by taking positions in energy futures contracts. To mitigate the market risk, energy producers can adopt a short hedge approach by selling enough energy futures contracts in the derivatives market to cover the quantity of energy to be produced. Given this hedging strategy, the risk-reward trade-off is clear: the downside of the short hedge is that the energy seller would have been better off without the hedge if the price of the energy spot price went up.

Extreme risk measures, such as VaR and CVaR, have become essential tools for quantifying the market risk of energy firms. Even though there are other alternative methods for evaluating the market risk of energy firms, in this paper we use the VaR and CVaR as risk measures based on the simulated distributions estimated through MCMC and ranked by the BF approach.

Since the value of energy trades can change over time with the behavior of the underlying spot and derivatives prices, we choose the model with the best performance evaluated in the previous section with the BF method, i.e. the SV-t process. Under our Bayesian approach, and in order to show the relevance of the specification of the underlying behavior of prices, we compare the extreme risk measures of the SV-t model

with the most basic GARCH process, i.e. the standard G model.

Tables 2.6 and 2.7 show the results from our hedging optimization exercise with 1,000 Monte Carlo simulations, considering the SV-t model and the standard G process, respectively. The first part of each table presents the unhedged spot position (i.e., the simulation results from the calibration of the spot prices for crude oil, natural gas and electricity) with the corresponding extreme risk measures for losses with 90%, 95% and 97.5% confidence levels. The standard deviation is included to complement the CVaR and VaR results. Next, the results associated to the futures contracts for delivery after 1 month are also reported. Finally, we also show the same risk metrics for a hedged position that combines (with a unit hedge ratio) the previous spot and futures positions.

Table 2.6: Extreme risk measures simulated from a stochastic volatility model with a t-distribution.

		Crude oil	Natural gas	Electricity
Spot position	Standard deviation	0.0310	0.0677	0.0488
	VaR (10%)	-0.0324	-0.0428	-0.0332
	VaR (5%)	-0.0488	-0.0614	-0.0497
	VaR (2.5%)	-0.0668	-0.0945	-0.0825
	CVaR (10%)	-0.0563	-0.0989	-0.0821
	CVaR (5%)	-0.0722	-0.1469	-0.1223
	CVaR (2.5%)	-0.0879	-0.2206	-0.1818
1 month futures	Standard deviation	0.0290	0.0605	0.0552
	VaR (10%)	-0.0250	-0.0645	-0.0571
	VaR (5%)	-0.0427	-0.0888	-0.0789
	VaR (2.5%)	-0.0591	-0.1203	-0.1150
	CVaR (10%)	-0.0518	-0.1093	-0.0980
	CVaR (5%)	-0.0712	-0.1413	-0.1283
	CVaR (2.5%)	-0.0916	-0.1811	-0.1626
Hedged position	Standard deviation	0.0198	0.0387	0.0386
	VaR (10%)	-0.0202	-0.0592	-0.0421
	VaR (5%)	-0.0245	-0.0670	-0.0843
	VaR (2.5%)	-0.0248	-0.0820	-0.1187
	CVaR (10%)	-0.0241	-0.0854	-0.0841
	CVaR (5%)	-0.0255	-0.1069	-0.1191
	CVaR (2.5%)	-0.0261	-0.1317	-0.1239

Table 2.7: Extreme risk measures simulated from a standard GARCH model.

		Crude oil	Natural gas	Electricity
Spot position	Standard deviation	0.0190	0.0245	0.0375
	VaR (10%)	-0.0241	-0.0304	-0.0454
	VaR (5%)	-0.0328	-0.0381	-0.0573
	VaR (2.5%)	-0.0391	-0.0496	-0.0695
	CVaR (10%)	-0.0348	-0.0429	-0.0641
	CVaR (5%)	-0.0414	-0.0514	-0.0768
	CVaR (2.5%)	-0.0464	-0.0593	-0.0900
1 month futures	Standard deviation	0.0154	0.0160	0.0415
	VaR (10%)	-0.0159	-0.0202	-0.0458
	VaR (5%)	-0.0207	-0.0257	-0.0704
	VaR (2.5%)	-0.0287	-0.0319	-0.0849
	CVaR (10%)	-0.0258	-0.0282	-0.0759
	CVaR (5%)	-0.0334	-0.0334	-0.0959
	CVaR (2.5%)	-0.0429	-0.0379	-0.1141
Hedged position	Standard deviation	0.0180	0.0090	0.0184
	VaR (10%)	-0.0211	-0.0125	-0.0199
	VaR (5%)	-0.0282	-0.0157	-0.0204
	VaR (2.5%)	-0.0375	-0.0160	-0.0286
	CVaR (10%)	-0.0336	-0.0154	-0.0300
	CVaR (5%)	-0.0423	-0.0166	-0.0396
	CVaR (2.5%)	-0.0471	-0.0172	-0.0506

Several conclusions can be drawn from Tables 2.6 and 2.7. The first concluding remark is about the properties of the estimated CVaR against the VaR results. Tables 2.6 and 2.7 show that CVaR accounts for losses exceeding VaR for all scenarios (i.e., simulated unhedged returns, futures returns and returns from the hedged position) and for both models (i.e., SV-t and standard G models).

Second, the standard deviation and the risk measures for the unhedged spot and 1 month futures positions computed for the standard G model displayed in Table 2.7 reveal that electricity markets exhibit a higher volatility when compared with natural gas and crude oil markets, with natural gas markets being generally more volatile than crude oil markets. However, if we consider the results shown in Table 2.6 for the SV-t

model we observe that natural gas markets are riskier than electricity and crude oil markets. Hence, while both processes indicate that crude oil markets are less volatile than natural gas and electricity markets, they are not consistent with each other when ranking the riskier markets. Such ranking inconsistency between the two models is also found for the case of hedged positions. Hence, care must be taken when choosing the appropriate time-varying volatility model for risk management purposes.

Third, the extreme risk measures show a higher level for the maximum expected loss with the stochastic volatility model with a t-distribution compared with the GARCH (1,1) process. In fact, the combination of a stochastic volatility behaviour with a statistical feature that captures extreme events in energy markets (t-distribution) generates higher extreme risk measures, since the so-called heavy tails phenomenon is conveniently accommodated.

Fourth, the adoption of a monthly hedging strategy reduces the market risk exposure to energy spot prices. This finding is observed for both the SV-t and the standard G models. This is particularly relevant for risk management optimization purposes. Although similar conclusions are achieved using both models, when the results from the (unitary) hedging strategy are transposed to a real portfolio of integrated energy firms, the relevance of fitting the spot and derivatives prices/volatility using the most suitable model is crucial. For example, an energy firm that produces 2,000,000 barrels per day may observe (on average) a difference of $ 23,000,000/year in the $CVaR_{95\%}$ computed using the SV-t process and the standard G model (that does not capture several empirical features of the commodities/utilities markets). Hence, the adoption of the MCMC estimation method and the corresponding BF selection criteria should be also relevant for decision makers in risk management.

2.6 Conclusions

This paper tests a large number of time-varying volatility processes based on a formal Bayesian model comparison exercise for modeling the volatility of future contracts from a representative portfolio of energy firms: oil, natural gas and electricity. In summary, this paper offers four relevant findings for the literature. First, by adopting the Bayes factor criteria to rank our battery of models, we find that stochastic volatility models almost always outperform the most used GARCH-family models. This finding consolidates the conclusion of Chan and Grant (2016) for a battery of similar models but applied to spot prices. Second, the stochastic volatility model with a t-distribution seems to be the best model for computing the volatility of futures contracts on commodities/utilities. Third, the maturity of future contracts seems relevant since it impacts the fitting performance of our models. Finally, given the previous concluding remarks, these findings have relevant implications for hedging, particularly when computing extreme risk measures, such as the CVaR. We show the pertinence of using the accurate stochastic process for computing the corresponding risk measures for both hedged and unhedged positions.

Given our promising results, it would be interesting to test the pertinence of introducing alternative jump distributions to our stochastic volatility models or regime-shift models in order to capture structural breaks in futures contracts of energy markets. It would be also worthwhile to apply multivariate stochastic volatility models in fitting multiple futures contracts, given the linear and non-linear dependencies between them.

Appendix A

The first model that we consider is the standard stochastic volatility (SV) model represented by

$$y_t = \mu + \varepsilon_t^y, \qquad \varepsilon_t^y \sim \mathcal{N}(0, e^{h_t}), \tag{A.1}$$

and

$$h_t = \mu_h + \phi_h(h_{t-1} - \mu_h) + \varepsilon_t^h, \qquad \varepsilon_t^h \sim \mathcal{N}(0, \omega_h^2), \tag{A.2}$$

with $\mathcal{N}(a, b)$ denoting the Gaussian distribution (with mean a and variance b), and where the log-volatility h_t is governed by a stationary auto-regressive process of first order, AR(1), with $|\phi_h| < 1$ and unconditional mean μ_h. The process starts with $h_1 \sim \mathcal{N}\left(\mu_h, \frac{\omega_h^2}{1-\phi_h^2}\right)$.

The second stochastic volatility model is obtained by assuming equation $(\mathrm{A}.1)$ of the standard SV model, but considering now that the log-volatility h_t follows a stationary AR(2) process, that is

$$h_t = \mu_h + \phi_h(h_{t-1} - \mu_h) + \rho_h(h_{t-2} - \mu_h) + \varepsilon_t^h, \qquad \varepsilon_t^h \sim \mathcal{N}(0, \omega_h^2), \tag{A.3}$$

where the roots of the characteristic polynomial related with (ϕ_h, ρ_h) are assumed to lie outside the unit circle. Moreover, it is considered that h_1 and h_2 follow the unconditional distribution

$$h_1, h_2 \sim \mathcal{N}\left(\mu_h, \frac{(1-\rho_h)\omega_h^2}{(1+\rho_h)\left((1-\rho_h)^2 - \phi_h^2\right)}\right).$$

We recall that this alternative stochastic volatility model with a stationary AR(2) process, denoted hereafter as the SV-2 model, nests the standard SV model as a special case when $\rho_h = 0$.

Next we consider a stochastic volatility model accommodating the possibility of infrequent jumps (SV-J). In this model, a jump component is added to equation $(\mathrm{A}.1)$, thus resulting in

$$y_t = \mu + k_t q_t + \varepsilon_t^y, \qquad \varepsilon_t^y \sim \mathcal{N}(0, e^{h_t}), \tag{A.4}$$

while the log-volatility h_t follows, again, the AR(1) process shown in equation $(\mathrm{A}.2)$ and $q_t \in \{0, 1\}$ represents a jump variable with success probability $\mathbb{P}(q_t = 1) = \kappa$, where $\mathbb{P}$ denotes the real world (or physical) probability measure. Therefore, if $q_t = 1$, a jump occurs at time t and the jump size is determined by k_t, which is modeled as $k_t \sim \mathcal{N}(\mu_k, \sigma_k^2)$, where μ_k and σ_k^2 are the mean and the variance of the jump size, respectively.

The fourth model is the stochastic volatility in mean (SV-M) model proposed by Koopman and Hol Uspensky (2002). In contrast with the previous models, the stochastic volatility is now included in equation $(\mathrm{A}.1)$ as a covariate, that is

$$y_t = \mu + \lambda e^{h_t} + \varepsilon_t^y, \qquad \varepsilon_t^y \sim \mathcal{N}(0, e^{h_t}), \tag{A.5}$$

with the log-volatility h_t following the same AR(1) process highlighted in equation $(\mathrm{A}.2)$. The parameter λ included in equation $(\mathrm{A}.5)$ captures the extent of volatility feedback in futures contracts. Clearly, the SV-M model nests the standard SV model as a special case when $\lambda = 0$.

Following Chan (2013) and Chan and Grant (2016), we consider also stochastic volatility models with moving average innovations (SV-MA). More specifically, we adopt a first-order moving average model with stochastic volatility, that is

$$y_t = \mu + \varepsilon_t^y, \tag{A.6}$$

and

$$\varepsilon_t^y = u_t + \psi u_{t-1}, \qquad u_t \sim \mathcal{N}(0, e^{h_t}), \tag{A.7}$$

where $u_0 = 0$, $|\psi| < 1$ and with the log-volatility h_t being still modeled via equation (A.2).

A stochastic volatility model with t innovations (SV-t) is also considered. The economic rational for testing this model is that the t-distribution has heavier tails than the Gaussian distribution. Therefore, the SV-t model should be able to better capture more extreme events in commodities and utilities futures contracts when compared with the standard SV model. The observation equation for the SV-t model is given by

$$y_t = \mu + \varepsilon_t^y, \qquad \varepsilon_t^y \sim t_\nu(0, e^{h_t}), \tag{A.8}$$

where t_ν represents a t-distribution with ν degrees of freedom, while the log-volatility h_t is governed, again, through the stationary AR(1) process shown in equation (A.2).

Finally, we consider a stochastic volatility model with leverage (SV-L). This model is intended to test the existence of a potentially larger impact of negative excess returns on the conditional variance (i.e., the presence of a leverage effect). It might be particularly relevant since the innovations in the observed and state equations can be correlated, that is

$$y_t = \mu + \varepsilon_t^y, \tag{A.9}$$

and

$$h_{t+1} = \mu_h + \phi_h(h_t - \mu_h) + \varepsilon_t^h, \tag{A.10}$$

where the innovations ε_t^y and ε_t^h jointly follow a bivariate normal distribution, that is

$$\begin{pmatrix} \varepsilon_t^y \\ \varepsilon_t^h \end{pmatrix} \sim \mathcal{N}\left(0, \begin{pmatrix} e^{h_t} & \rho e^{\frac{1}{2}h_t}\omega_h \\ \rho e^{\frac{1}{2}h_t}\omega_h & \omega_h^2 \end{pmatrix}\right).$$

If $\rho < 0$, given a negative shock to y_t at time t, the volatility at time $t+1$ tends to be higher. The SV-L model nests the standard SV model when $\rho = 0$.

Appendix B

The first model that we adopt to model energy futures prices under the class of GARCH models is the standard GARCH(1,1) model, denoted hereafter as the G model for simplicity. This model is governed by

$$y_t = \mu + \varepsilon_t, \qquad \varepsilon_t \sim \mathcal{N}(0, \sigma_t^2), \tag{B.1}$$

and

$$\sigma_t^2 = \alpha_0 + \alpha_1 \varepsilon_{t-1}^2 + \beta_1 \sigma_{t-1}^2, \tag{B.2}$$

where $\varepsilon_0 = 0$ and σ_0^2 is a constant. To guarantee that the variance process σ_t^2 is straightly positive and stationary, it is necessary to assume that $\alpha_0 > 0$, $\alpha_1 \geq 0$, $\beta_1 \geq 0$ and $\alpha_1 + \beta_1 < 1$. Equation (B.2) highlights that the conditional variance σ_t^2 is modeled as a deterministic function of the model parameters and lagged data. The conditional variance σ_t^2 follows an AR(1) process.

The second model to be considered is the GARCH(2,1) model, henceforth the G-2 model, which is similar to the previous G model, though with the conditional variance

σ_t^2 following now an AR(2) process, that is

$$\sigma_t^2 = \alpha_0 + \alpha_1 \varepsilon_{t-1}^2 + \beta_1 \sigma_{t-1}^2 + \beta_2 \sigma_{t-2}^2, \tag{B.3}$$

where $\sigma_{-1}^2 = \varepsilon_0 = 0$ and σ_0^2 is a constant. The variance dynamics is now enriched for capturing the lagged periods of the volatility in futures contracts. Similarly to the standard G model, it is required that $\alpha_0 > 0$, $\alpha_1 \geq 0$, $\beta_1 \geq 0$, $\beta_2 \geq 0$ and $\alpha_1 + \beta_1 + \beta_2 < 1$.

The GARCH model with a jump component (G-J) accommodates the possibility of infrequent jumps in futures price contracts. Under this model specification, we have

$$y_t = \mu + k_t q_t + \varepsilon_t, \qquad \varepsilon_t \sim \mathcal{N}(0, \sigma_t^2), \tag{B.4}$$

and

$$\sigma_t^2 = \alpha_0 + \alpha_1 (y_{t-1} - \mu)^2 + \beta_1 \sigma_{t-1}^2, \tag{B.5}$$

where the jump indicator q_t and jump size k_t are modeled as in the counterpart SV-J model.

The GARCH in mean (G-M) model is the counterpart to the SV-M model. Under the G-M model, the conditional variance σ_t^2 appears in the conditional mean as a covariate, that is

$$y_t = \mu + \lambda \sigma_t^2 + \varepsilon_t, \qquad \varepsilon_t \sim \mathcal{N}(0, \sigma_t^2), \tag{B.6}$$

and

$$\sigma_t^2 = \alpha_0 + \alpha_1 (y_{t-1} - \mu - \lambda \sigma_{t-1}^2)^2 + \beta_1 \sigma_{t-1}^2. \tag{B.7}$$

The G-M model is particularly relevant for testing if the log-returns of futures contracts on energy depend on their volatility. It is possible to observe that the G-M model nests the standard G model when $\lambda = 0$.

The next model combines GARCH innovations with a first-order moving average process and it will be referred henceforth as the G-MA model. This model specification aims to better capture the short-run dynamics in high frequency data related with futures contracts. To accomplish this purpose, it allows the log-returns of energy futures price contracts to be correlated over time, that is

$$y_t = \mu + \varepsilon_t, \tag{B.8}$$

and

$$\varepsilon_t = u_t + \psi u_{t-1}, \qquad u_t \sim \mathcal{N}(0, \sigma_t^2), \tag{B.9}$$

where the condition $|\psi| < 1$ is required to ensure the invertibility condition and the variance equation is still modeled via equation (B.2).

The GARCH model with t innovations (G-t) is governed by

$$y_t = \mu + \varepsilon_t, \qquad \varepsilon_t \sim t_\nu(0, \sigma_t^2), \tag{B.10}$$

where the variance process is given again by equation (B.2). As before, the use of a t-distribution might better capture more extreme observations when compared with the Gaussian distribution.

Finally, we consider the GARCH model with leverage (G-L) suggested by Glosten et al. (1993). Similarly to its counterpart SV-L model, the G-L model is intended to capture the potential presence of an asymmetric leverage effect, which is known to potentially improve the forecast performance of the standard G model, as documented, for instance, in Wei et al. (2010). In this model specification, the observation equation is still

equation $(\mathrm{B}.1)$ and the variance equation is given by

$$\sigma_t^2 = \alpha_0 + (\alpha_1 + \delta_1 \mathbf{1}_{\{\varepsilon_{t-1}<0\}})\varepsilon_{t-1}^2 + \beta_1 \sigma_{t-1}^2, \tag{B.11}$$

where δ_1 is the parameter that controls the asymmetric leverage effect and $\mathbf{1}_{\{.\}}$ is the indicator function. When $\delta_1 = 0$, the G-L model is reduced to the standard G model.

Appendix C

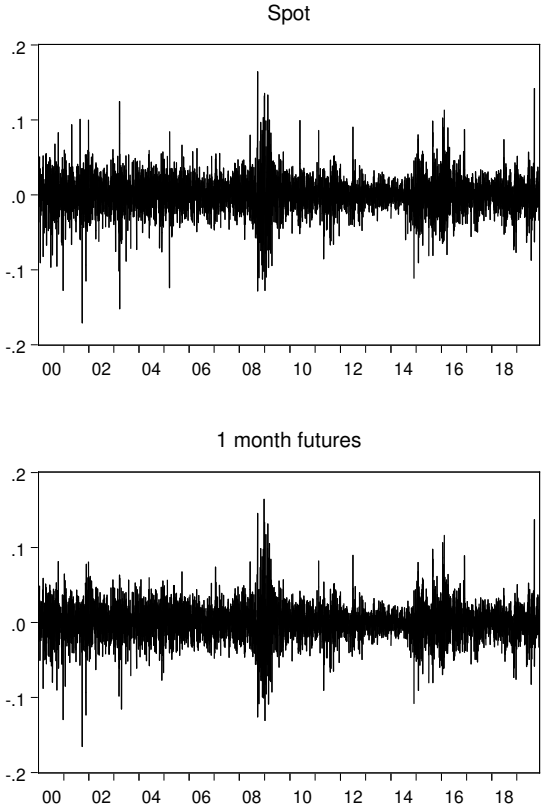

Figure C.1: Daily returns of spot and 1 month futures prices of crude oil from January 2000 to November 2019.

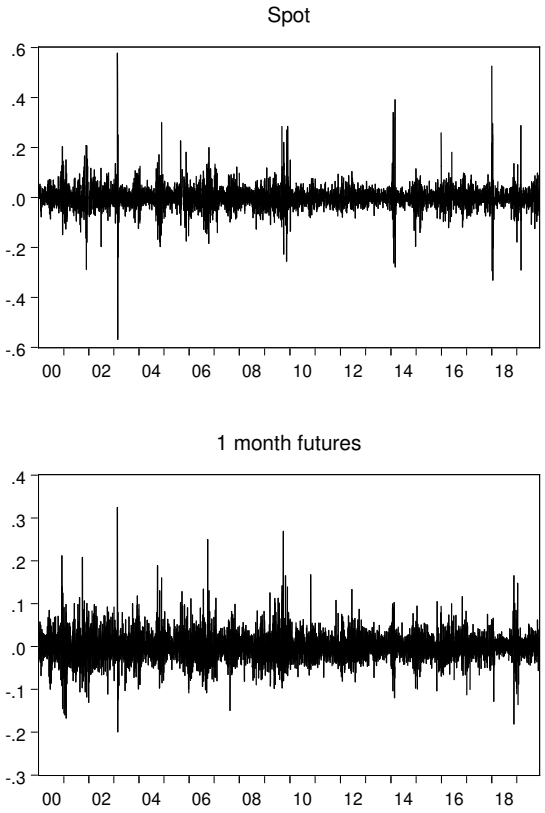

Figure C.2: Daily returns of spot and 1 month futures prices of natural gas from January 2000 to November 2019.

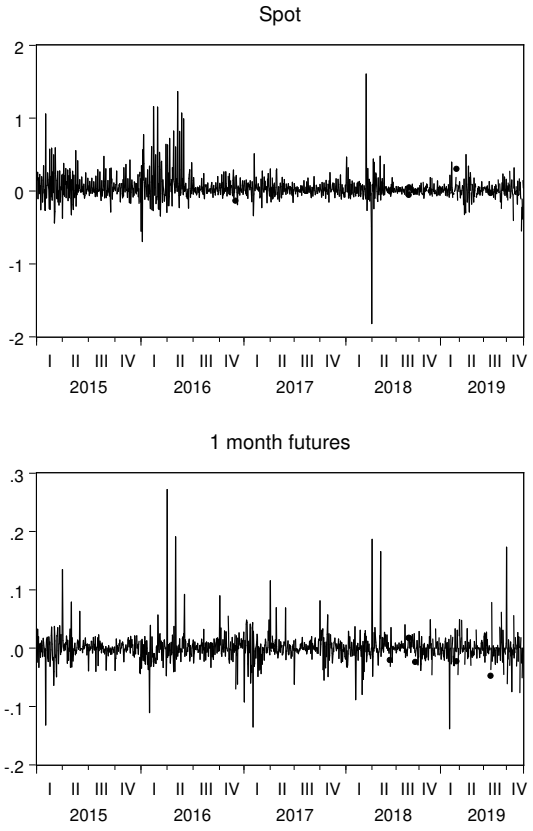

Figure C.3: Daily returns of spot and 1 month futures prices of electricity from January 2015 to November 2019.

Appendix D

Table D.1: Posterior means and standard deviations for the parameter set of GARCH models estimated through MCMC and for crude oil futures contracts.

	G	G-2	G-J	G-M	G-MA	G-t	G-L
μ	0.05	0.05	0.08	-0.01	0.04	0.06	0.02
	(0.03)	(0.03)	(0.03)	(0.04)	(0.03)	(0.03)	(0.03)
α_0	0.04	0.04	0.02	0.04	0.04	0.02	0.03
	(0.01)	(0.01)	(0.01)	(0.01)	(0.01)	(0.01)	(0.01)
α_1	0.06	0.07	0.05	0.06	0.06	0.04	0.02
	(0.01)	(0.01)	(0.00)	(0.01)	(0.01)	(0.00)	(0.01)
β_1	0.94	0.71	0.94	0.93	0.94	0.94	0.95
	(0.01)	(0.02)	(0.01)	(0.01)	(0.01)	(0.01)	(0.00)
β_2	-	0.21	-	-	-	-	-
	-	(0.02)	-	-	-	-	-
κ	-	-	0.05	-	-	-	-
	-	-	(0.01)	-	-	-	-
μ_k	-	-	-1.11	-	-	-	-
	-	-	(0.18)	-	-	-	-
σ_k^2	-	-	13.06	-	-	-	-
	-	-	(2.98)	-	-	-	-
λ	-	-	-	0.01	-	-	-
	-	-	-	(0.01)	-	-	-
ψ	-	-	-	-	-0.02	-	-
	-	-	-	-	(0.01)	-	-
ν	-	-	-	-	-	8.32	-
	-	-	-	-	-	(0.79)	-
δ_1	-	-	-	-	-	-	0.05
	-	-	-	-	-	-	(0.01)
Q(20)	7.98	8.03	7.71	8.07	7.03	7.84	7.95
	(0.26)	(0.19)	(0.24)	(0.25)	(1.41)	(0.29)	(0.28)
Q^2(20)	18.07	16.35	19.02	18.14	18.04	19.21	24.97
	(0.70)	(0.50)	(0.71)	(0.70)	(0.73)	(1.23)	(1.10)

Notes: Q(20) and Q^2(20) are, respectively, the Ljung-Box and McLeod-Li statistics of order 20 computed on the standardized residuals and squared standardized residuals. The 5% and 1% critical values are 31.41 and 37.57, respectively.

Table D.2: Posterior means and standard deviations for the parameter set of GARCH models estimated through MCMC and for natural gas futures contracts.

	G	G-2	G-J	G-M	G-MA	G-t	G-L
μ	0.03	0.03	-0.05	0.03	0.02	-0.03	0.03
	(0.04)	(0.04)	(0.04)	(0.04)	(0.04)	(0.04)	(0.04)
α_0	0.14	0.21	0.14	0.16	0.15	0.12	0.16
	(0.03)	(0.04)	(0.02)	(0.03)	(0.03)	(0.03)	(0.03)
α_1	0.09	0.13	0.06	0.09	0.09	0.05	0.09
	(0.01)	(0.01)	(0.01)	(0.01)	(0.01)	(0.01)	(0.01)
β_1	0.91	0.37	0.91	0.91	0.91	0.91	0.91
	(0.01)	(0.03)	(0.01)	(0.01)	(0.01)	(0.01)	(0.01)
β_2	-	0.49	-	-	-	-	-
	-	(0.03)	-	-	-	-	-
κ	-	-	0.04	-	-	-	-
	-	-	(0.01)	-	-	-	-
μ_k	-	-	1.95	-	-	-	-
	-	-	(0.10)	-	-	-	-
σ_k^2	-	-	40.27	-	-	-	-
	-	-	(5.42)	-	-	-	-
λ	-	-	-	-0.01	-	-	-
	-	-	-	(0.01)	-	-	-
ψ	-	-	-	-	-0.04	-	-
	-	-	-	-	(0.02)	-	-
ν	-	-	-	-	-	7.10	-
	-	-	-	-	-	(0.66)	-
δ_1	-	-	-	-	-	-	-0.01
	-	-	-	-	-	-	(0.01)
Q(20)	21.19	20.91	22.14	20.81	17.10	22.21	21.39
	(0.32)	(0.28)	(0.37)	(0.37)	(1.34)	(0.44)	(0.32)
Q^2(20)	16.90	18.95	15.10	16.45	16.54	15.39	17.22
	(0.98)	(1.20)	(0.53)	(1.21)	(0.96)	(0.67)	(0.93)

Notes: Q(20) and Q^2(20) are, respectively, the Ljung-Box and McLeod-Li statistics of order 20 computed on the standardized residuals and squared standardized residuals. The 5% and 1% critical values are 31.41 and 37.57, respectively.

Table D.3: Posterior means and standard deviations for the parameter set of GARCH models estimated through MCMC and for electricity futures contracts.

	G	G-2	G-J	G-M	G-MA	G-t	G-L
μ	0.01	0.01	0.00	0.43	0.03	0.00	0.06
	(0.08)	(0.08)	(0.05)	(0.20)	(0.08)	(0.05)	(0.07)
α_0	3.57	3.47	0.12	3.65	3.07	0.10	0.08
	(0.61)	(0.51)	(0.01)	(0.55)	(0.60)	(0.03)	(0.02)
α_1	0.05	0.04	0.05	0.11	0.11	0.02	0.01
	(0.03)	(0.03)	(0.00)	(0.05)	(0.07)	(0.01)	(0.00)
β_1	0.43	0.39	0.84	0.37	0.46	0.86	0.95
	(0.08)	(0.07)	(0.00)	(0.06)	(0.09)	(0.03)	(0.01)
β_2	-	0.06	-	-	-	-	-
	-	(0.03)	-	-	-	-	-
κ	-	-	0.08	-	-	-	-
	-	-	(0.01)	-	-	-	-
μ_k	-	-	0.77	-	-	-	-
	-	-	(0.25)	-	-	-	-
σ_k^2	-	-	53.15	-	-	-	-
	-	-	(9.76)	-	-	-	-
λ	-	-	-	-0.06	-	-	-
	-	-	-	(0.03)	-	-	-
ψ	-	-	-	-	0.06	-	-
	-	-	-	-	(0.05)	-	-
ν	-	-	-	-	-	2.60	-
	-	-	-	-	-	(0.21)	-
δ_1	-	-	-	-	-	-	0.08
	-	-	-	-	-	-	(0.01)
Q(20)	44.66	44.81	32.55	45.46	44.13	34.33	38.66
	(0.50)	(0.57)	(0.22)	(1.21)	(1.47)	(1.08)	(0.83)
Q^2(20)	9.12	8.90	10.09	8.87	10.51	8.20	7.87
	(0.44)	(0.41)	(0.32)	(2.51)	(1.29)	(1.83)	(0.43)

Notes: Q(20) and Q^2(20) are, respectively, the Ljung-Box and McLeod-Li statistics of order 20 computed on the standardized residuals and squared standardized residuals. The 5% and 1% critical values are 31.41 and 37.57, respectively.

Appendix E

Table E.1: Posterior means and standard deviations for the parameter set of SV models estimated through MCMC and for 2-month crude oil futures contracts.

	SV	SV-2	SV-J	SV-M	SV-MA	SV-t	SV-L
μ	0.06	0.07	0.06	0.14	0.06	0.06	0.03
	(0.02)	(0.03)	(0.02)	(0.04)	(0.02)	(0.02)	(0.03)
μ_h	1.30	1.29	1.27	1.30	1.30	1.20	1.30
	(0.12)	(0.13)	(0.14)	(0.12)	(0.12)	(0.14)	(0.12)
ϕ_h	0.98	0.91	0.99	0.98	0.98	0.99	0.98
	(0.00)	(0.08)	(0.00)	(0.00)	(0.00)	(0.00)	(0.00)
ω_h^2	0.02	0.04	0.01	0.02	0.02	0.01	0.02
	(0.00)	(0.01)	(0.00)	(0.00)	(0.00)	(0.00)	(0.00)
ρ_h	-	0.05	-	-	-	-	-
	-	(0.09)	-	-	-	-	-
κ	-	-	0.01	-	-	-	-
	-	-	(0.01)	-	-	-	-
μ_k	-	-	-0.09	-	-	-	-
	-	-	(0.11)	-	-	-	-
σ_k^2	-	-	27.53	-	-	-	-
	-	-	(12.13)	-	-	-	-
λ	-	-	-	-0.02	-	-	-
	-	-	-	(0.00)	-	-	-
ψ	-	-	-	-	-0.03	-	-
	-	-	-	-	(0.01)	-	-
ν	-	-	-	-	-	18.75	-
	-	-	-	-	-	(4.29)	-
ρ	-	-	-	-	-	-	-0.41
	-	-	-	-	-	-	(0.06)
Q(20)	11.94	13.11	11.26	12.38	8.59	11.84	11.63
	(2.00)	(2.07)	(2.27)	(1.98)	(2.00)	(1.97)	(1.81)
Q^2(20)	28.42	31.14	26.88	29.37	29.07	26.10	28.80
	(5.15)	(6.12)	(5.35)	(5.13)	(4.95)	(4.87)	(4.99)

Notes: Q(20) and Q^2(20) are, respectively, the Ljung-Box and McLeod-Li statistics of order 20 computed on the standardized residuals and squared standardized residuals. The 5% and 1% critical values are 31.41 and 37.57, respectively.

Table E.2: Posterior means and standard deviations for the parameter set of SV models estimated through MCMC and for 3-month crude oil futures contracts.

	SV	SV-2	SV-J	SV-M	SV-MA	SV-t	SV-L
μ	0.06	0.07	0.11	0.15	0.06	0.07	0.05
	(0.02)	(0.02)	(0.05)	(0.04)	(0.02)	(0.02)	(0.02)
μ_h	1.21	1.20	1.11	1.21	1.21	1.11	1.14
	(0.12)	(0.14)	(0.13)	(0.11)	(0.12)	(0.14)	(0.06)
ϕ_h	0.98	0.91	0.98	0.98	0.98	0.99	0.91
	(0.00)	(0.07)	(0.00)	(0.00)	(0.00)	(0.00)	(0.01)
ω_h^2	0.02	0.04	0.02	0.02	0.02	0.01	0.11
	(0.00)	(0.01)	(0.00)	(0.00)	(0.00)	(0.00)	(0.01)
ρ_h	-	0.05	-	-	-	-	-
	-	(0.07)	-	-	-	-	-
κ	-	-	0.06	-	-	-	-
	-	-	(0.03)	-	-	-	-
μ_k	-	-	-1.02	-	-	-	-
	-	-	(0.67)	-	-	-	-
σ_k^2	-	-	5.25	-	-	-	-
	-	-	(5.08)	-	-	-	-
λ	-	-	-	-0.03	-	-	-
	-	-	-	(0.00)	-	-	-
ψ	-	-	-	-	-0.03	-	-
	-	-	-	-	(0.01)	-	-
ν	-	-	-	-	-	18.93	-
	-	-	-	-	-	(5.25)	-
ρ	-	-	-	-	-	-	-0.25
	-	-	-	-	-	-	(0.02)
Q(20)	13.65	14.27	15.51	13.89	9.77	13.51	11.53
	(2.06)	(2.11)	(3.58)	(2.07)	(2.00)	(1.97)	(2.96)
Q^2(20)	28.72	30.54	25.12	29.18	29.20	29.38	28.44
	(4.85)	(6.70)	(6.04)	(5.33)	(4.93)	(5.14)	(6.08)

Notes: Q(20) and Q^2(20) are, respectively, the Ljung-Box and McLeod-Li statistics of order 20 computed on the standardized residuals and squared standardized residuals. The 5% and 1% critical values are 31.41 and 37.57, respectively.

Table E.3: Posterior means and standard deviations for the parameter set of SV models estimated through MCMC and for 4-month crude oil futures contracts.

	SV	SV-2	SV-J	SV-M	SV-MA	SV-t	SV-L
μ	0.06	0.07	0.13	0.15	0.06	0.07	0.04
	(0.02)	(0.02)	(0.03)	(0.04)	(0.02)	(0.02)	(0.02)
μ_h	1.14	1.13	1.02	1.14	1.13	1.03	1.13
	(0.11)	(0.13)	(0.14)	(0.11)	(0.11)	(0.13)	(0.11)
ϕ_h	0.98	0.95	0.99	0.98	0.98	0.98	0.98
	(0.00)	(0.07)	(0.00)	(0.01)	(0.00)	(0.01)	(0.01)
ω_h^2	0.02	0.04	0.02	0.03	0.02	0.02	0.02
	(0.00)	(0.01)	(0.00)	(0.01)	(0.00)	(0.01)	(0.01)
ρ_h	-	0.01	-	-	-	-	-
	-	(0.07)	-	-	-	-	-
κ	-	-	0.07	-	-	-	-
	-	-	(0.02)	-	-	-	-
μ_k	-	-	-1.27	-	-	-	-
	-	-	(0.39)	-	-	-	-
σ_k^2	-	-	4.01	-	-	-	-
	-	-	(2.30)	-	-	-	-
λ	-	-	-	-0.03	-	-	-
	-	-	-	(0.01)	-	-	-
ψ	-	-	-	-	-0.04	-	-
	-	-	-	-	(0.01)	-	-
ν	-	-	-	-	-	18.47	-
	-	-	-	-	-	(7.44)	-
ρ	-	-	-	-	-	-	-0.34
	-	-	-	-	-	-	(0.07)
Q(20)	19.68	19.78	20.38	20.02	13.06	19.45	18.40
	(2.57)	(3.20)	(4.18)	(2.39)	(2.30)	(2.21)	(2.24)
Q^2(20)	26.46	25.37	22.71	25.04	26.66	28.34	27.81
	(5.20)	(5.26)	(5.92)	(5.07)	(4.94)	(7.59)	(5.24)

Notes: Q(20) and Q^2(20) are, respectively, the Ljung-Box and McLeod-Li statistics of order 20 computed on the standardized residuals and squared standardized residuals. The 5% and 1% critical values are 31.41 and 37.57, respectively.

Table E.4: Posterior means and standard deviations for the parameter set of SV models estimated through MCMC and for 2-month natural gas futures contracts.

	SV	SV-2	SV-J	SV-M	SV-MA	SV-t	SV-L
μ	-0.03	-0.03	-0.06	-0.01	-0.03	-0.03	-0.02
	(0.04)	(0.04)	(0.05)	(0.09)	(0.04)	(0.04)	(0.04)
μ_h	1.68	1.69	1.62	1.68	1.68	1.61	1.68
	(0.12)	(0.23)	(0.12)	(0.11)	(0.12)	(0.12)	(0.11)
ϕ_h	0.97	0.93	0.97	0.97	0.97	0.97	0.97
	(0.01)	(0.08)	(0.01)	(0.01)	(0.01)	(0.01)	(0.01)
ω_h^2	0.02	0.03	0.02	0.03	0.02	0.02	0.02
	(0.01)	(0.01)	(0.00)	(0.01)	(0.00)	(0.00)	(0.00)
ρ_h	-	0.03	-	-	-	-	-
	-	(0.09)	-	-	-	-	-
κ	-	-	0.03	-	-	-	-
	-	-	(0.02)	-	-	-	-
μ_k	-	-	1.53	-	-	-	-
	-	-	(0.86)	-	-	-	-
σ_k^2	-	-	17.47	-	-	-	-
	-	-	(16.54)	-	-	-	-
λ	-	-	-	-0.00	-	-	-
	-	-	-	(0.01)	-	-	-
ψ	-	-	-	-	-0.04	-	-
	-	-	-	-	(0.02)	-	-
ν	-	-	-	-	-	32.57	-
	-	-	-	-	-	(16.74)	-
ρ	-	-	-	-	-	-	0.08
	-	-	-	-	-	-	(0.10)
Q(20)	22.34	22.51	21.22	22.80	19.49	23.05	22.59
	(2.35)	(2.53)	(3.36)	(2.65)	(2.48)	(2.34)	(2.26)
Q^2(20)	27.47	28.94	27.26	27.76	26.19	23.37	28.06
	(5.86)	(6.20)	(6.70)	(5.66)	(5.76)	(5.74)	(5.97)

Notes: Q(20) and Q^2(20) are, respectively, the Ljung-Box and McLeod-Li statistics of order 20 computed on the standardized residuals and squared standardized residuals. The 5% and 1% critical values are 31.41 and 37.57, respectively.

Table E.5: Posterior means and standard deviations for the parameter set of SV models estimated through MCMC and for 3-month natural gas futures contracts.

	SV	SV-2	SV-J	SV-M	SV-MA	SV-t	SV-L
μ	-0.03	-0.03	-0.04	0.00	-0.03	-0.03	-0.03
	(0.04)	(0.04)	(0.04)	(0.08)	(0.04)	(0.04)	(0.04)
μ_h	1.51	1.53	1.44	1.51	1.51	1.42	1.51
	(0.11)	(0.23)	(0.12)	(0.12)	(0.11)	(0.12)	(0.11)
ϕ_h	0.97	0.92	0.97	0.97	0.97	0.97	0.97
	(0.01)	(0.09)	(0.01)	(0.01)	(0.01)	(0.01)	(0.01)
ω_h^2	0.02	0.03	0.02	0.02	0.02	0.02	0.02
	(0.00)	(0.01)	(0.00)	(0.00)	(0.00)	(0.00)	(0.01)
ρ_h	-	0.04	-	-	-	-	-
	-	(0.09)	-	-	-	-	-
κ	-	-	0.02	-	-	-	-
	-	-	(0.01)	-	-	-	-
μ_k	-	-	0.75	-	-	-	-
	-	-	(0.58)	-	-	-	-
σ_k^2	-	-	25.76	-	-	-	-
	-	-	(12.96)	-	-	-	-
λ	-	-	-	-0.01	-	-	-
	-	-	-	(0.00)	-	-	-
ψ	-	-	-	-	-0.03	-	-
	-	-	-	-	(0.02)	-	-
ν	-	-	-	-	-	29.58	-
	-	-	-	-	-	(20.20)	-
ρ	-	-	-	-	-	-	-0.03
	-	-	-	-	-	-	(0.09)
Q(20)	26.07	26.04	24.50	25.90	24.91	26.29	26.06
	(2.60)	(2.53)	(3.38)	(2.54)	(2.80)	(2.62)	(2.54)
Q^2(20)	24.40	25.19	27.29	23.71	24.01	18.98	24.66
	(5.59)	(5.89)	(7.58)	(5.54)	(5.90)	(5.22)	(5.54)

Notes: Q(20) and Q^2(20) are, respectively, the Ljung-Box and McLeod-Li statistics of order 20 computed on the standardized residuals and squared standardized residuals. The 5% and 1% critical values are 31.41 and 37.57, respectively.

Table E.6: Posterior means and standard deviations for the parameter set of SV models estimated through MCMC and for 4-month natural gas futures contracts.

	SV	SV-2	SV-J	SV-M	SV-MA	SV-t	SV-L
μ	-0.03	-0.03	-0.03	-0.01	-0.03	-0.03	-0.03
	(0.04)	(0.04)	(0.04)	(0.07)	(0.04)	(0.04)	(0.04)
μ_h	1.34	1.35	1.28	1.34	1.34	1.20	1.34
	(0.10)	(0.20)	(0.10)	(0.11)	(0.11)	(0.11)	(0.10)
ϕ_h	0.96	0.92	0.97	0.97	0.97	0.97	0.97
	(0.01)	(0.08)	(0.01)	(0.01)	(0.01)	(0.01)	(0.01)
ω_h^2	0.03	0.03	0.02	0.03	0.03	0.02	0.03
	(0.01)	(0.01)	(0.00)	(0.01)	(0.01)	(0.00)	(0.01)
ρ_h	-	0.04	-	-	-	-	-
	-	(0.09)	-	-	-	-	-
κ	-	-	0.01	-	-	-	-
	-	-	(0.00)	-	-	-	-
μ_k	-	-	-0.87	-	-	-	-
	-	-	(0.32)	-	-	-	-
σ_k^2	-	-	135.82	-	-	-	-
	-	-	(58.24)	-	-	-	-
λ	-	-	-	-0.00	-	-	-
	-	-	-	(0.01)	-	-	-
ψ	-	-	-	-	-0.02	-	-
	-	-	-	-	(0.02)	-	-
ν	-	-	-	-	-	14.50	-
	-	-	-	-	-	(4.96)	-
ρ	-	-	-	-	-	-	-0.00
	-	-	-	-	-	-	(0.11)
Q(20)	24.67	24.48	22.80	24.58	24.52	25.08	24.76
	(2.61)	(2.54)	(2.86)	(2.50)	(2.69)	(2.51)	(2.59)
Q^2(20)	26.46	26.91	37.72	26.26	26.63	38.62	26.27
	(4.98)	(5.49)	(8.81)	(4.96)	(5.04)	(22.49)	(4.96)

Notes: Q(20) and Q^2(20) are, respectively, the Ljung-Box and McLeod-Li statistics of order 20 computed on the standardized residuals and squared standardized residuals. The 5% and 1% critical values are 31.41 and 37.57, respectively.

Appendix F

Table F.1: Log marginal likelihoods corresponding to the estimated models.

	Crude oil	Natural gas	Electricity
Panel A: Stochastic volatility models			
SV	-10804.4	-12221.2	-5531.5
	(0.09)	(0.08)	(0.02)
SV-2	-10805.3	-12221.6	-5559.0
	(0.29)	(0.25)	(0.30)
SV-J	-10805.2	-12226.5	-5570.4
	(0.59)	(0.37)	(0.31)
SV-M	-10808.3	-12228.8	-5534.5
	(0.05)	(0.11)	(0.02)
SV-MA	-10806.2	-12224.2	-5019.4
	(0.06)	(0.13)	(0.20)
SV-t	-10784.1	-12220.5	-5535.9
	(0.01)	(0.18)	(0.02)
SV-L	-10796.2	-12222.3	-5533.0
	(0.09)	(0.20)	(0.02)
Panel B: GARCH models			
G	-10912.3	-12387.8	-5482.6
	(0.01)	(0.02)	(0.02)
G-2	-10912.3	-12381.7	-5472.0
	(0.04)	(0.07)	(0.08)
G-J	-10786.5	-12260.5	-5360.1
	(0.05)	(0.08)	(0.03)
G-M	-10919.8	-12395.8	-5490.0
	(0.02)	(0.05)	(0.02)
G-MA	-10914.7	-12389.2	-5222.7
	(0.01)	(0.04)	(0.02)
G-t	-10784.5	-12230.4	-5372.8
	(0.01)	(0.01)	(0.02)
G-L	-10903.1	-12589.8	-5485.0
	(0.05)	(0.03)	(0.02)

3. How does electrification under energy transition impact the portfolio management of energy firms?

Abstract: This paper presents a novel approach for structuring dependence between electricity and natural gas prices in the context of energy transition: a copula of mean-reverting and jump-diffusion processes. Based on historical day-ahead prices of the Nord Pool electricity market and the Henry Hub natural gas market, a stochastic model is estimated via the maximum likelihood approach and considering the dependency structure between the innovations of these two-dimensional returns. Given the role of natural gas in the global policy for energy transition, different copula functions are fit to electricity and natural gas returns. Overall, we find that: (i) using an out-of-sample forecasting exercise, we show that it is important to consider both mean-reversion and jumps; (ii) modeling correlation between the returns of electricity and natural gas prices, assuring nonlinear dependencies are satisfied, leads us to the adoption of Gumbel and Student-t copulas; and (iii) without government incentive schemes in renewable electricity projects, the usual maximization of the risk-return trade-off tends to avoid a high exposure to electricity assets.

JEL Classification: C52, C58, Q40, Q41, Q48

Keywords: Energy transition, Electricity, Natural gas, Copula functions, Jump-diffusion,

Mean reversion.

3.1 Introduction

Energy firms are challenged to move for energy transition with ambitious targets to enhance the decarbonization. To accomplish this purpose, two main assets come forward: electricity assets from renewable sources and natural gas.

Electricity assets from renewable sources are the main key drivers for energy firms. The shift from an electricity mix from fossil-based electricity (e.g., coal and oil) to non-fossil electricity (e.g., biomass, hydro, solar and wind) has been considered as a key strategy for mitigating the emissions of carbon dioxide (hereafter, CO_2)—see, for example, Ang and Su (2016). Moreover, the recent and quick growth of renewable energies in the European power market has turn the electricity markets more complex and dynamic since many sources of renewable energy are intermittent—see, for instance, European Wind Energy Association (2012) and Wind Europe (2019) for additional details.

In these circumstances, natural gas is continuing to assume a relevant role in a context of energy transition for diversified energy portfolios. Gas-fired power plants are commonly used as a back-up technology to ensure security of supply and provide short-term flexibility in energy systems with high-shares of weather-driven renewable power sources. According to the recent report from the U.S. Energy Information Administration (2016), natural gas is expected to remain a key fuel in the worldwide electric power and industrial sectors.

The co-existence of these two types of power production plants provides a promising

combination for a smooth transition to sustainable future energy systems that are flexible enough to accommodate high shares of renewable energy sources. Even though the interdependence between electricity and natural gas systems—with a focus on the need of increasing the operational flexibility of both energy systems in an integrated manner—has been studied recently by Ordoudis et al. (2019) and Ordoudis et al. (2020), the presence and importance of nonlinear interdependencies between the returns of electricity and natural gas market prices, in the context of energy transition, is not explored yet in the literature. This is the main purpose of this paper.

More specifically, we propose a theoretical framework to capture the prices specifications and interdependencies of relevant energy sources in a context of energy transition. The goal of modeling correlation and structuring dependence between the spot prices of commodities/utilities with different paths and features leads us to the adoption of copula functions. We first recall that even though the terms *correlation* and *dependence* are often used interchangeably, the primer is a rather particular kind of dependence measure between random variables. Hence, the strict use of correlation prevents the possibility of capturing other forms of dependence. The main advantage of using copula functions is that it is possible to separate the statistical properties of each variable from their dependence structure. To the best of our knowledge, our paper is the first to apply a stochastic-copula approach in an energy transition context.

Electricity spot markets are known to possess several stylized facts. In particular, they are recognized to be seasonal, mean-reverting and to exhibit frequent jumps in the spot data, as documented, for instance, in Benth et al. (2008) and Haugom (2011). These features in the electricity spot data not only contribute to higher volatility levels, but also for an increasing difficulty to calibrate models governed by appropriate stochastic processes. The first attempts to incorporate realistic models have been proposed by Schwartz (1997), Schwartz and Smith (2000) and Lucia and Schwartz (2002). These

authors focused on alternative stochastic processes to capture the mean-reverting effects, the long-term uncertainty and the seasonality patterns observed in spot prices. The suggestion of considering a jump component to model electricity prices is made by Kaminski (1997) and Clewlow and Strickland (2000). Following these initial insights, various factors characterizing the dynamics of electricity prices have been considered and a wide range of functional forms with different time-varying specifications and stochastic shocks has been suggested afterwards in the literature—e.g., Huisman and Mahieu (2003), Geman and Roncoroni (2006), Seifert and Uhrig-Homburg (2007), Lindström and Regland (2012), Zhou et al. (2016), Gianfreda and Bunn (2018), Zhou et al. (2019) and Wozabal and Rameseder (2020), among others.

The principal distinct feature of our modeling approach in comparison with the aforementioned relevant contributions is that we consider a copula of two mean-reverting and jump-diffusion stochastic processes. In a nutshell, we offer two main contributions to the literature. First, we develop the theoretical framework to model electricity and natural gas spot prices based on a copula of mean-reverting and jump-diffusion processes using a Maximum Likelihood (henceforth, ML) estimation procedure. As a second contribution, our paper generates multiple empirical findings. In order to illustrate the relevance of the model, we first estimate several spot prices of one of the most significant European electricity day-ahead market and then we conduct an out-of-sample forecasting exercise against the competing standard geometric Brownian motion model with Poisson jumps proposed by Merton (1976).

Given the recent interest in many energy markets applications of combining copula functions with generalized autoregressive conditional heteroscedasticity (hereafter, GARCH) models to construct conditional joint distributions—e.g., Chan and Gray (2006), Ghorbel and Trabelsi (2014), Lu et al. (2014), Kayalar et al. (2017) and Quintino et al. (2019)—, we also test a GARCH model adapted to the extreme value theory (hence-

forth, EVT) approach against the proposed mean-reverting and jump-diffusion stochastic model and the Merton (1976) model. The combination of GARCH and EVT is intended to use a GARCH modeling framework that is better able to model the tails of the returns distribution when compared with the simple GARCH specification.

Overall, we find that the mean-reverting and jump-diffusion stochastic process yields a better performance than the two competing models—i.e., Merton (1976) and GARCH-EVT. In addition, we apply a list of elliptical (Gaussian and Student-t) and Archimedean (Clayton, Frank and Gumbel) copula functions to electricity and natural gas spot returns. Our results show that the Gumbel and Student-t copula functions are the most appropriate for fitting the dependency structure between electricity and natural gas assets.

In summary, the recent predictions on the increasing global demand of natural gas and the relevant role of the natural gas in the context of energy transition (pressured by the global targets for decreasing the CO_2 emissions) allow us to propose a new approach to model a simulated portfolio of electricity (representing the renewable energies) and of natural gas: a copula of mean-reverting and jump-diffusion processes. To the best of our knowledge, this is a novel development for exploring the effect of the nonlinear dependence between electricity and natural gas markets in a context of energy transition while maintaining the three most significant features of these assets: spikes/drops, jumps and seasonality. This new framework should be relevant for energy firms (with or without renewable energy assets) given the implications for integrated portfolios in energy transition.

Furthermore, the high levels of uncertainty observed in electricity prices and the available renewable generation turns risk management a fundamental decision-making problem. Such prices tend to act as the underlying references in financial derivatives. Hence, a better comprehension of the dependency structure between electricity prices

and natural gas prices should be important for designing (new) financial contracts aiming to structure hedging strategies—see, for example, Kaminski (1997), Clewlow and Strickland (2000) and Deng and Oren (2006) for more details on the importance of pricing and risk managing electricity derivatives.

The results of this paper are also useful from the regulators' and investors perspective because most prevailing regulation schemes are incentive-based in the form of feed-in tariffs and use benchmarking—see, for example, Couture and Gagnon (2010), Ritzenhofen and Spinler (2016), Barbosa et al. (2018) and Kök et al. (2018), just to name a few. Although the goal of this paper is not to discuss which feed-in tariff policy should be used to provide effective policies aiming to increase investments in renewable energy, it calls at least the policymakers' attention on the importance of considering the dependence structure between the spot prices of electricity and natural gas when defining policy instruments to promote investments in renewable energy sources.

The remainder of the paper is organized as follows. Section 3.2 presents the data. Section 3.3 provides the theoretical framework for modeling the prices through a mean-reverting and jump-diffusion process and shows the model parameters estimated via a ML approach. Section 3.4 reports the estimation of copula functions and the corresponding fitting for the returns of electricity and natural gas. Section 3.5 implements a portfolio risk analysis and optimization problem and Section 3.6 concludes. Appendixes G and H contain additional results.

3.2 Data

This paper uses daily spot prices of electricity markets in Europe. More specifically, we adopt the *Nord Pool* market, which operates in power trading in several countries—

e.g., Norway, Denmark, Sweden, Finland, Estonia, Latvia, Lithuania, Germany, Netherlands, Belgium, Austria, Luxembourg, France and United Kingdom—and represents a turnover of 494 TWh of traded power (more than 90% of the total power consumption in the Nordic and Baltic market). This is the Europe's largest and most liquid market for electricity.

The Nord Pool market operates in the day-ahead spot market (also known as the Elspot market) for physical exchange of production and consumption. In the period 2015-2020, the Elspot market contains 17 day-ahead markets from 7 countries, namely Norway, Denmark, Sweden, Finland, Estonia, Latvia and Lithuania.[3.1] Nord Pool Spot computes the reference price used for financial trading purposes that is known as the System Price (henceforth, SYS) and represents the price that would be charged if there were no transmission restrictions within the Nordic region. SE1, SE2, SE3 and SE4 represent the four bidding areas in Sweden. FI denotes the bidding area in Finland, while DK1 and DK2 stand for the two bidding areas in Denmark. Oslo, Kristiansand, Bergen, Molde, Trondheim and Tromsø represent the five bidding areas in Norway (Molde and Trondheim belong to the same bidding area NO3). EE, LV and LT correspond to the bidding areas of Estonia, Latvia and Lithuania, respectively. An additional variable (price) has been created to represent the arithmetic average of the Elspot prices. We also consider the UK N2EX day-ahead market to represent the auction prices in the United Kingdom. All these prices are presented in EUR/MWh.

Our data set includes also the daily spot prices of natural gas. For this commodity, the prices represent the spot prices of the distribution hub on the natural gas pipeline system in Louisiana. These prices are measured in dollars per Million Btu (USD/MMBtu) and represent the prices for the production of natural gas assets—e.g., natural gas

[3.1] We note that market data for Germany, Netherlands, Belgium, Austria, Luxembourg and France became available only after the 3rd of July, 2019 and, therefore, these countries are excluded from our analysis due to the lack of sufficient data.

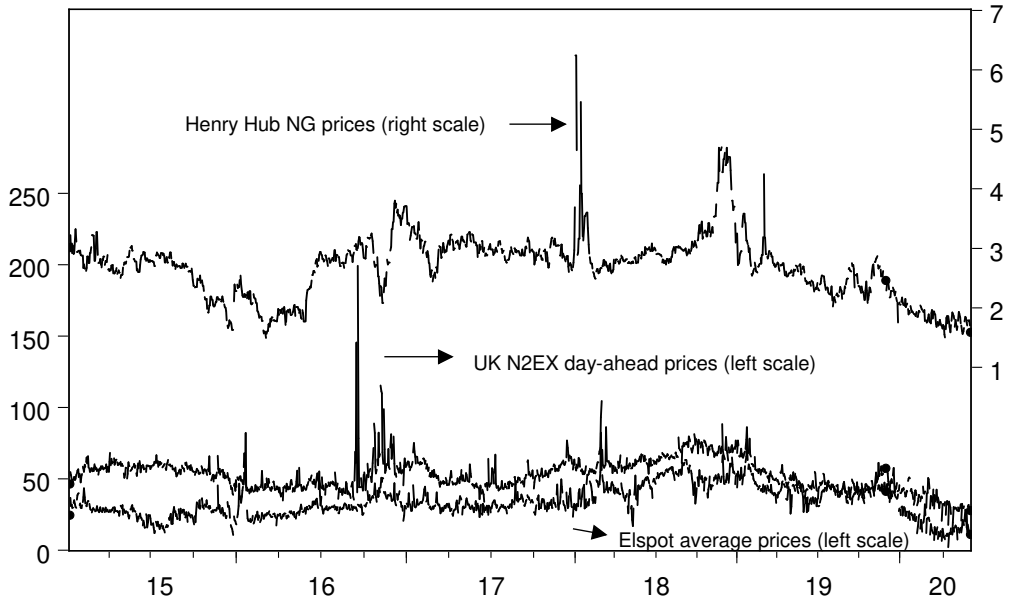

Figure 3.1: Average Elspot, UK N2EX day-ahead and natural gas historical prices between 01-Jan-2015 and 01-Jun-2020.

fields in upstream operations and used as indexing prices to natural gas commercialization in deregulated markets in the downstream operations.

While electricity prices were obtained from the Nord Pool market data, natural gas prices were collected from the U.S. Energy Information Administration (EIA)/Thomson Reuters Eikon. The time series for the prices of electricity and natural gas are daily-based and collected from 01-Jan-2015 to 01-Jun-2020. Figure 3.1 shows the graphical representation of the average Elspot, UK N2EX day-ahead and natural gas historical prices for this time period.

3.3 The general setup of the model

This section presents the general setup of the model aiming to accommodate the observed empirical properties of electricity and natural gas prices. The discretized version of the model for ML estimation purposes is also discussed in order to estimate the parameters of the stochastic and seasonal components. Finally, an out-of-sample analysis is conducted for assessing the forecasting performance of the proposed model. In this section, however, no conditional dependency between electricity and natural gas will be considered and tested. Such novelty, in the context of energy transition, will be analyzed in Section 3.4 using alternative copula distribution functions.

3.3.1 Modeling spikes, drops, seasonality and mean reversion

Realistic approaches for modeling the behavior of spot prices in electricity (and natural gas) markets contain mean-reversion, seasonality, diffusion and jump components. In order to model our prices, we adopt the modeling framework considered in Lucia and Schwartz (2002) and Seifert and Uhrig-Homburg (2007), that is

$$\ln P_t = f(t) + X_t, \tag{3.1}$$

where P_t represents the spot price of electricity (or natural gas), $f(t)$ denotes the deterministic seasonal part of the model and X_t is the stochastic component of the model.[3.2]

The deterministic part of the model is modeled through sinusoidal functions expressed as

$$f(t) = c_1 \sin(2\pi t) + c_2 \cos(2\pi t) + c_3 \sin(4\pi t) + c_4 \cos(4\pi t) + c_5 + \mu t, \tag{3.2}$$

[3.2] As argued by Seifert and Uhrig-Homburg (2007, Page 62), the use of log-prices (instead of prices) is preferable since the seasonality is less affected by extreme prices and it also facilitates the modeling of jumps.

where $c_i \in \mathbb{R}$, for $i \in \{1, ..., 5\}$, are constant parameters, $\mu \in \mathbb{R}$ is the linear trend of the deterministic component of the model and t represents the annualized time factors. We recall that time series of electricity day-ahead and natural gas prices exhibit a number of stylized patterns, that are mainly driven by the balance between supply and demand of power over time. The seasonality component considered in equation (3.2) is essentially driven by the evolution of temperature and daylight variations over the calendar year. Even though it should be possible to augment the continuous-time periodical component (3.2) by including also weekly, daily and hourly patterns—see, for instance, Lucia and Schwartz (2002), Seifert and Uhrig-Homburg (2007), Zhou et al. (2016), Zhou et al. (2019) and Wozabal and Rameseder (2020)—, we consider the determinist component as given in equation (3.2) for the sake of simplicity and to be better able to analyze the dependency structure via copulas in a more parsimony way.

Removing the deterministic component in the log-prices results in a stochastic behavior of prices. Since deseasonalised spot prices still exhibit a high volatility, jumps in data and a mean-reversion feature, the stochastic part X_t is modeled as in Seifert and Uhrig-Homburg (2007, Equation 6), that is as an Ornstein-Uhlenbeck (mean-reverting) process with a jump component in the context of a stochastic intertemporal economy that is characterized by continuous trading on the period $[t_0, T]$, for some fixed time period $T > t_0$, and where t_0 denotes the current time:

$$dX_t = (\alpha - \kappa X_t)dt + \sigma dW_t + J_t dN_t, \tag{3.3}$$

where $\kappa \in \mathbb{R}_+$ is the speed of mean reversion, α/κ denotes the long-run level of the process, $\sigma \in \mathbb{R}_+$ represents the usual volatility parameter and $\{W_t; t \geq t_0\}$ is a standard Brownian motion. The jump size is denoted by J_t and follows a normal distribution with mean $\mu_J \in \mathbb{R}$ and standard deviation $\sigma_J \in \mathbb{R}_+$, while $\{N_t; t \geq t_0\}$ is a Poisson process

with a jump intensity λ that is independent from the Brownian motion.[3.3] Since the pricing of energy derivatives is outside the scope of this study, this model is developed only under the physical (real world) measure.

3.3.2 Estimation through the ML procedure

We estimate the parameter set of the model in a two-step procedure. First, we estimate the deterministic component of the model by running the Least Squares (hereafter, LS) method as

$$\min_{\{c_1,c_2,c_3,c_4,c_5,\mu\}} \sum_{m=1}^{M} \left(\ln P_{m/365} - f(m/365)\right)^2, \tag{3.4}$$

where M represents the number of (daily) data points of the time series of prices.

After performing this estimation, the seasonality component is removed from the logarithm of the spot price by subtracting the deterministic component $f(t)$ from the logarithmic prices of electricity ($\ln P_t$) in equation (3.1).

Second, it is necessary to estimate the stochastic component. However, a discretization of the process is required under the ML estimation procedure. To accomplish this purpose, we adopt the Euler discretization scheme and the Bernoulli jump approach for the jump component. The discretized procedure is applied as follows to equation (3.3):

$$X_t = \alpha\Delta t + \phi X_{t-1} + \sigma\zeta, \tag{3.5}$$

with probability $(1 - \lambda\Delta t)$ and

$$X_t = \alpha\Delta t + \phi X_{t-1} + \sigma\zeta + \mu_J + \sigma_J\zeta_J, \tag{3.6}$$

[3.3] We note that we are incorporating jumps as in Merton (1976), but other jump specifications can be also used in the our general framework.

with probability $\lambda\Delta t$, where Δt represents a discrete time-period, $\phi = 1 - \kappa\Delta t$, while ζ and ζ_J represent independent standard normal random variables. Under this setup, the density function of X_t given X_{t-1} is equal to

$$f(X_t|X_{t-1}) = (\lambda\Delta t)N_1(X_t|X_{t-1}) + (1 - \lambda\Delta t)N_2(X_t|X_{t-1}), \tag{3.7}$$

with

$$N_1(X_t|X_{t-1}) := (2\pi(\sigma^2 + \sigma_J^2))^{-\frac{1}{2}} \exp\left[\frac{-(X_t - \alpha\Delta t - \phi X_{t-1} - \mu_J)^2}{2(\sigma^2 + \sigma_J^2)}\right] \tag{3.8}$$

and

$$N_2(X_t|X_{t-1}) := (2\pi\sigma^2)^{-\frac{1}{2}} \exp\left[\frac{-(X_t - \alpha\Delta t - \phi X_{t-1})^2}{2\sigma^2}\right]. \tag{3.9}$$

The parameter set to be estimated under the ML approach is $\theta \equiv (\alpha, \kappa, \sigma, \mu_j, \sigma_j, \lambda)$, where θ is an unknown parameter in a bounded set $\Theta \subset \mathbb{R}^6$. Therefore, we need to solve the following minimization problem

$$\min_{\{\theta\}} -\sum_{t=1}^{T} \ln(f(X_t|X_{t-1})), \tag{3.10}$$

subject to

$$\phi < 1, \tag{3.11}$$

$$\sigma^2 > 0, \tag{3.12}$$

$$\sigma_J^2 > 0 \tag{3.13}$$

and

$$0 \leq \lambda\Delta t \leq 1. \tag{3.14}$$

It is important to mention a few additional notes regarding these constraints. Given the relationship between ϕ and κ, the inequality constraint (3.11) is equivalent to $\kappa > 0$.

As usual, the volatility of the process and the volatility of the jump component must be positive, as shown in inequalities (3.12) and (3.13). Finally, inequality (3.14) is required because $\lambda\Delta t$ is the probability of a jump occurring at the period Δt. In order to solve this optimization problem, we adopt the following initial values: $\alpha = 0$, $\phi = 0$, $\mu_J = 0$, $\sigma_J^2 = Var(X_t)$, $\sigma^2 = Var(X_t)$ and $\lambda = 0.5$.

3.3.3 Estimation of the parameters

This subsection provides the calibration results to the aforementioned electricity and natural gas market data using the ML estimation approach and considering the full sample, i.e., the period between 01-Jan-2015 and 01-Jun-2020.[3.4] Table 3.1 provides the parameter estimates associated with the stochastic component of our model for all the Elspot day-ahead prices series, the N2EX day-ahead prices and natural gas prices. The corresponding parameters estimates obtained for each year of the electricity time series are reported in Tables G.1 to G.5 of the corresponding appendix. The annual results for the natural gas series are collected in Table G.6 of the Appendix G.[3.5]

Several relevant observations can be drawn from these calibration results. We first recall that modeling the logarithm of the spot electricity price as shown in equation (3.1) requires strict positive prices. Hence, the existence of negative (spot) prices in the series DK1 and DK2 in 2019, 2017 and 2016—see, respectively, Tables G.1, G.3 and G.4 of the Appendix G—prevents the calibration of the model for the full sample period from 01-Jan-2015 and 01-Jun-2020. We note, however, that the existence of negative electricity prices is frequently observed in practice and is well documented in the literature, e.g. in Zhou et al. (2016), Gianfreda and Bunn (2018) and Zhou et al. (2019).

[3.4] We note that all the results of this paper have been obtained through *Matlab* (R2015a 32 bit) running on an Intel Core i7 2.40GHz personal computer.

[3.5] The corresponding results for the electricity and natural gas market data for the period between 01-Jan-2020 and 01-Jun-2020 are also available upon request.

As expected, this problem can be easily avoided by modeling the price of electricity instead of the log-price. Results not reported here (but available upon request), show, however, that the latter assumption provides better out-of-sample forecasts, which is consistent with the observations documented in Seifert and Uhrig-Homburg (2007).

Overall, we find a very strong mean reversion parameter κ (speed of mean reversion), ranging from 2.647 to 114.718. All the estimates are statistically significant at the 0.1% level. Although the mean reversion speed of natural gas (3.229) is lower than the ones associated to UK day-ahead (23.458) and average Elspot prices (31.266), it is similar to the mean reversion observed in other electricity prices series—namely, Oslo, Kristiansand and Bergen. The parameter α can be simply interpreted as the product of the long-run level of the stochastic process and the mean reversion speed. The inclusion of mean reversion is important when modeling electricity and natural gas market data. Moreover, in the following subsection an out-of-sample exercise is presented to further validate the relevance of including a mean reversion feature in the Elspot market.

Some comments can be also made with respect to volatility. First, the estimations for volatility range from 0.793 to 2.622 in the electricity series. The estimated volatility of the average Elspot prices (1.912) is higher than the one for the UK day-ahead (1.114) and the Henry Hub natural gas prices (0.545). We note also that all the estimates are statistically significant at the 0.1% level. Second, we also find an higher volatility in the Elspot market not only in the full sample, but also in each annual subsample—see Tables G.1 to G.6 in the Appendix G. Third, natural gas exhibits lower historical volatility than all electricity markets.

The estimated jump intensities λ, ranging between 22.894 and 102.102, indicate the significant prevalence of jumps in the series, thus emphasizing the need of a well designed risk management policy for energy firms. However, an additional deep dive ex-

ercise is needed: (i) natural gas has a lower jump intensity; and (ii) Elspot prices show a higher jump intensity than the UK day-ahead market. The estimates associated to electricity markets are statistically significant at the 0.1% level, while the estimate for natural gas is statistically significant at the 1% level.

Still concerning the jump components, we analyze next the parameters μ_J and σ_J. The mean jump size ranges from -0.077 to 0.017. We note that the mean jump sizes of the average Elspot prices (-0.017) and UK day-ahead prices (0.017) are symmetric, whereas μ_J is zero in the case of natural gas. A deeper analysis to the subsamples of 2016 and 2017 reveals only positive mean jumps in these markets. By contrast, the subsample of 2019 shows only negative mean jumps in electricity and natural gas markets. Although the mean jump size estimates are not shown to be statistically significant at any of the tested levels, the range of (negative and positive) values encountered in μ_J is consistent with the presence of spikes and drops observed in these markets.

Finally, the standard deviation of the jump component is ranging between 0.203 and 0.451 in the Elspot day-ahead markets—the σ_J of the average Elspot market is 0.319. This jump volatility is similar to the volatility of the jumps in the UK day-ahead market (0.306). The estimate for σ_J of natural gas is lower (0.138) than the corresponding volatilities in both electricity markets. We observe also that all these estimates are statistically significant at the 0.1% level.

Even though our main focus is on the stochastic behavior and the nonlinear interdependencies between returns, the corresponding seasonality parameters estimates for the full sample are presented in Table 3.2. Figure 3.1 also supports the interpretation of the numerical results, since we can clearly see the yearly seasonality with highest prices in winter months for the average Elspot prices and UK N2EX day-ahead prices.

Table 3.1: Estimation of the parameters from the stochastic component for electricity and natural gas markets between 01-Jan-2015 and 01-Jun-2020 and via the ML approach.

	α	κ	σ	μ_J	σ_J	λ
SYS	-1.042	7.756***	1.128***	0.007	0.232***	101.302***
SE1	-1.428	9.831***	1.536***	0.015	0.329***	87.309***
SE2	-1.395	9.908***	1.545***	0.015	0.329***	86.793***
SE3	0.553	23.427***	1.730***	-0.006	0.410***	91.495***
SE4	-0.001	33.038***	2.156***	-0.000	0.450***	88.061***
FI	3.586*	83.008***	2.622***	-0.043	0.451***	84.199***
DK1	-	-	-	-	-	-
DK2	-	-	-	-	-	-
Oslo	-1.193*	2.647***	0.919***	0.008	0.232***	87.256***
Kristiansand	-0.698	3.040***	0.801***	0.002	0.203***	98.102***
Bergen	-0.839	2.719***	0.891***	0.005	0.244***	75.060***
Molde	-0.261	6.476***	1.048***	-0.000	0.227***	102.102***
Trondheim	-0.261	6.476***	1.048***	-0.000	0.227***	102.102***
Tromsø	0.428	6.319***	0.793***	-0.009	0.227***	81.840***
EE	5.662***	114.718***	2.608***	-0.077**	0.409***	73.315***
LV	1.532	83.707***	2.350***	-0.022	0.384***	68.126***
LT	2.023	87.336***	2.373***	-0.028	0.377***	71.784***
Average Elspot prices	1.016	31.266***	1.912***	-0.017	0.319***	64.119***
UK day-ahead prices	-0.629	23.458***	1.114***	0.017	0.306***	36.852***
Natural gas prices	-0.128	3.229***	0.545***	0.000	0.138***	22.894**

Notes: κ is the speed of mean reversion, α/κ denotes the long-run level of the process, σ represents the volatility, μ_J and σ_J are, respectively, the mean and the standard deviation of the jump size and λ is the jump intensity of the Poisson process. The Nord Pool Spot computes the reference price used for financial trading purposes that is known as the System Price (SYS), i.e., the price that would be charged if there were no transmission restrictions within the Nordic region. SE1, SE2, SE3 and SE4 represent the four bidding areas in Sweden. FI denotes the bidding area in Finland. DK1 and DK2 stand for the two bidding areas in Denmark. Oslo, Kristiansand, Bergen, Molde, Trondheim and Tromsø represent the five bidding areas in Norway (Molde and Trondheim belong to the same bidding area NO3). EE, LV and LT correspond to the bidding areas of Estonia, Latvia and Lithuania, respectively. Average Elspot prices express an additional variable (price) representing the arithmetic average of the Elspot prices. UK day-ahead prices represent the auction prices in the United Kingdom. Finally, the Henry Hub natural gas prices represent the spot prices of the distribution hub on the natural gas pipeline system in Louisiana. The existence of negative (spot) prices in the series DK1 and DK2 in 2019, 2017 and 2016—see, respectively, Tables G.1, G.3 and G.4 of the Appendix G—prevents the calibration of the model in the period from 01-Jan-2015 to 01-Jun-2020. The symbols $*$, $**$, $***$ indicate if the estimate is statistically significant at 5%, 1% and 0.1% level, respectively.

Table 3.2: Estimation of the seasonal parameters of electricity and natural gas markets between 01-Jan-2015 and 01-Jun-2020 and via the LS approach.

	c_1	c_2	c_3	c_4	c_5	μ
SYS	-0.144	0.151	0.010	0.025	0.040	3.206
SE1	-0.176	0.110	0.029	0.024	0.037	3.237
SE2	-0.176	0.110	0.029	0.024	0.037	3.237
SE3	-0.150	0.106	0.027	0.010	0.056	3.218
SE4	-0.147	0.098	0.012	0.007	0.067	3.226
FI	-0.150	0.036	0.052	0.006	0.046	3.405
DK1	-	-	-	-	-	-
DK2	-	-	-	-	-	-
Oslo	-0.128	0.182	-0.002	0.035	0.044	3.165
Kristiansand	-0.126	0.171	0.001	0.034	0.046	3.152
Bergen	-0.116	0.178	-0.005	0.035	0.047	3.142
Molde	-0.159	0.130	0.012	0.013	0.033	3.238
Trondheim	-0.159	0.130	0.012	0.013	0.033	3.238
Tromsø	-0.135	0.145	0.001	0.013	0.052	3.129
EE	-0.112	0.010	0.032	0.015	0.015	3.414
LV	-0.153	-0.021	0.018	0.046	0.004	3.656
LT	-0.151	-0.019	0.016	0.045	0.002	3.666
Average Elspot prices	-0.141	0.070	0.015	0.024	0.045	3.305
UK day-ahead prices	-0.062	0.055	-0.027	0.023	-0.029	4.025
Natural gas prices	-0.074	0.009	-0.004	0.041	-0.016	1.019

Notes: c_i, for $i \in \{1, ..., 5\}$, are constant parameters and μ is the linear trend of the deterministic component of the model. The Nord Pool Spot computes the reference price used for financial trading purposes that is known as the System Price (SYS), i.e., the price that would be charged if there were no transmission restrictions within the Nordic region. SE1, SE2, SE3 and SE4 represent the four bidding areas in Sweden. FI denotes the bidding area in Finland. DK1 and DK2 stand for the two bidding areas in Denmark. Oslo, Kristiansand, Bergen, Molde, Trondheim and Tromsø represent the five bidding areas in Norway (Molde and Trondheim belong to the same bidding area NO3). EE, LV and LT correspond to the bidding areas of Estonia, Latvia and Lithuania, respectively. Average Elspot prices express an additional variable (price) representing the arithmetic average of the Elspot prices. UK day-ahead prices represent the auction prices in the United Kingdom. Finally, the Henry Hub natural gas prices represent the spot prices of the distribution hub on the natural gas pipeline system in Louisiana. The existence of negative (spot) prices in the series DK1 and DK2 in 2019, 2017 and 2016—see, respectively, Tables G.1, G.3 and G.4 of the Appendix G—prevents the calibration of the model in the period from 01-Jan-2015 to 01-Jun-2020.

3.3.4 Forecasting performance

This subsection performs an out-of-sample forecasting analysis to evaluate the fitting performance of the mean-reverting and jump-diffusion stochastic process (henceforth, MR-JD) stated in equation (3.3) against the classic geometric Brownian motion with

jumps model (hereafter, JGBM) offered by Merton (1976), which does not take into account the presence of mean reversion in the series.

Additionally, we also estimate the GARCH-EVT model—see, for instance, Ghorbel and Trabelsi (2014) for additional details—to compare its performance against the estimated MR-JD model. To implement the GARCH-EVT model, first captures the residuals from the return series are captured using the asymmetric GARCH model suggested by Glosten et al. (1993) and then the sample marginal cumulative distribution function of each electricity series is created based on a Gaussian kernel estimate for the interior and a generalized Pareto distribution estimate for the (upper and lower) tails.

To apply this out-of-sample exercise, we use the average Elspot prices (that capture the path of the 17 Elspot prices). The evaluation period for the out-of-sample forecasting exercise corresponds to the following 1, 3 and 5 trading days in the average Elspot market of our sample and at the beginning of each year. We compare the three models by computing the mean absolute percentage error (hereafter, MAPE). The results are reported in Table 3.3.

Table 3.3: Out-of-sample forecasting performance.

	2016	2017	2018	2019	2020
	Panel A: 5 days				
MR-JD	16.8%	**15.7%**	**6.7%**	13.4%	**10.7%**
JGBM	28.5%	28.0%	22.0%	11.4%	11.1%
GARCH-EVT	**9.3%**	19.4%	29.6%	**5.3%**	12.2%
	Panel B: 3 days				
MR-JD	11.7%	**13.3%**	**5.5%**	14.2%	**6.4%**
JGBM	19.5%	24.2%	18.0%	**6.7%**	7.4%
GARCH-EVT	**11.2%**	18.2%	18.2%	7.0%	12.8%
	Panel C: 1 day				
MR-JD	**3.2%**	**9.7%**	6.0%	**2.3%**	**6.2%**
JGBM	11.4%	16.8%	**0.3%**	8.2%	9.3%
GARCH-EVT	14.8%	23.3%	6.3%	4.8%	17.7%

Notes: This table shows the mean absolute percentage errors. JGBM represents the classic standard geometric Brownian motion with jumps model offered by Merton (1976). MR-JD is the mean-reverting stochastic process with jumps proposed in equation (3.3). The GARCH-EVT model stands for the modeling framework described, for example, in Ghorbel and Trabelsi (2014). The values in bold highlight which model offers a best fitting performance.

To sum up, this out-of-sample forecasting exercise confirms the better fitting performance of the MR-JD model compared with the JGBM and GARCH-EVT models. The MAPE values highlight that the adoption of a stochastic process capturing the three stylized facts commonly found in the electricity markets allows a better fitting performance in 10 times—forecasting in the next 3 and 5 days achieves a better performance in 2017, 2018 and 2020 and the best forecasting for the next trading day is achieved in 2016, 2017, 2019 and 2020. These errors are in line with the ones reported, for instance, in Conejo et al. (2005) and explained by the high volatility feature of electricity markets.

3.4 The copula approach in the context of energy transition

This section aims to test the presence and importance of nonlinear interdependencies between the returns of electricity and natural gas prices in the context of energy transition. To accomplish this purpose, we propose a novel approach based on a copula between the returns of electricity and natural gas, assuming each one of them follows a mean-reverting and jump-diffusion process as described by equations (3.1), (3.2) and (3.3).

3.4.1 Copula functions

An important theorem offered by Sklar (1959) provides the groundwork to the theory of copulas and the foundation for many of the applications to statistics and to financial

modeling problems—for a comprehensive overview of this theorem see, for instance, Nelsen (2006, Section 2.3). In a nutshell, a d-dimensional copula C is a mathematical function representing a joint distribution F as a function of the corresponding marginal distributions F_j, for $j = 1, \ldots, d$, that is

$$F(x_1, \ldots, x_d) = C(F_1(x_1), \ldots, F_d(x_d)). \tag{3.15}$$

This means that any copula C may be used to join any collection of univariate distribution functions $F_1, \ldots, F_d$, creating a multivariate distribution function F with margins $F_1, \ldots, F_d$. The copula C of their joint distribution function may be extracted from equation (3.15) by evaluating

$$\begin{aligned} C(\mathbf{u}) &:= C(u_1, \ldots, u_d) \\ &= F\left(F_1^{-1}(u_1), \ldots, F_d^{-1}(u_d)\right), \end{aligned} \tag{3.16}$$

where F_j^{-1}, for $j = 1, \ldots, d$, are the quantile functions of the margins.

Our novel approach suggests the use of a copula (with $d = 2$) for the joint modeling of electricity and natural gas prices assuming the dynamic behavior of each asset is governed by the mean-reverting and jump-diffusion process proposed in equations (3.1), (3.2) and (3.3). This should be of interest for practitioners and academics since the classical covariance matrix setup is based on a linear dependency structure. The advantage of the copula approach is that other forms of dependence can be captured.

Figure 3.2 shows the graphical representation of the returns that will be used in our copula application. The left-hand side figures plot the historical log-returns for average Elspot, UK N2EX day-ahead and natural gas prices from 01-Jan-2015 to 01-Jun-2020. The right-hand figures plot the corresponding histograms. The continuous line is the normal density. Clearly, the normal distribution is not able to fit the higher peaks near

the origin and the heavy tails of the empirical distributions. This observation further enhances the importance of considering stochastic processes moving away from the standard GBM assumption.

We suggest testing two of the most popular copula families used in finance: (i) elliptical copulas and (ii) Archimedean copulas. Elliptical copula functions are the copulas of elliptical distributions. The most used elliptical copulas are the Gaussian and Student-t copulas. The primer was firstly suggested by Lee (1983) and then generalized by Van Ophem (1999), whereas the latter has been initially discussed in Embrechts et al. (2002) and Fang et al. (2002). The main advantage of using elliptical copula functions is that one can specify different levels of correlation between the margins. However, the main disadvantages include: (i) the absence of closed-form solutions; and (ii) these copulas are restricted to have radial symmetry. In contrast to the Gaussian copula, the t-copula has (symmetric) tail dependence, which is useful in models of the joint movements of the log-returns. More specifically, it should be better able to accommodate the empirical properties highlighted in Figure 3.2.

We also test the most used three Archimedean copula functions: the Gumbel (1960), Clayton (1978) and Frank (1979) copulas. Archimedean copulas represent an important class of copula functions given their analytical tractability and ability to reproduce a wide variety of dependence structures. The Gumbel copula function is an asymmetric copula and, therefore, reproduces nonlinear positive dependence in the data set. Consequently, this copula shows greater dependence in the positive tail than in the negative tail. In opposition to the Gumbel copula, the Frank copula function is a plausible copula when the data shows significant positive or negative dependence and describes circumstances of symmetric tail independence. Finally, the Clayton copula function is an asymmetric copula that is appropriate when nonlinear positive dependence is observed in the data. However, in opposition to the Gumbel copula function,

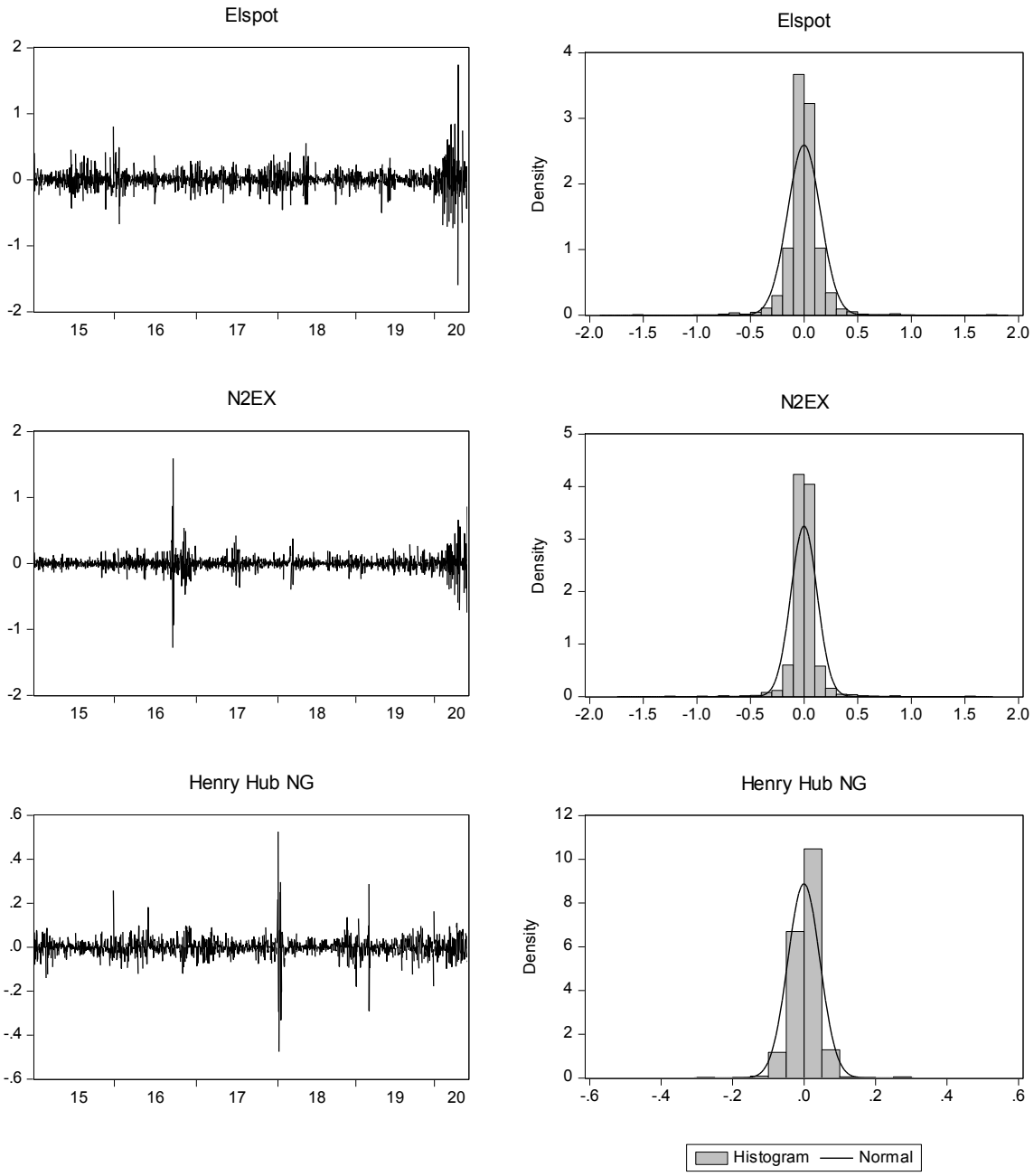

Figure 3.2: The left-hand side figures plot the historical log-returns for average Elspot, UK N2EX day-ahead and natural gas prices from 01-Jan-2015 to 01-Jun-2020. The right-hand side figures plot the corresponding histograms. The continuous line is the normal density.

this copula shows greater dependence in the negative tail than in the positive tail. For the sake of completeness, Table 3.4 shows the functional form of each of the five bivariate copula functions under our two-dimensional modeling setup (i.e., $d = 2$ in our case).[3.6]

Table 3.4: Bivariate copula functions.

Copula	Copula function
Panel A: Elliptical copula functions	
Gaussian	$C_\rho(u_1, u_2) := \Phi_\rho\left(\Phi^{-1}(u_1), \Phi^{-1}(u_2)\right)$
Student-t	$C_{\rho,\nu}(u_1, u_2) := t_{\rho,\nu}\left(t_\nu^{-1}(u_1), t_\nu^{-1}(u_2)\right)$
Panel B: Archimedean copula functions	
Clayton	$C_\alpha(u_1, u_2) := \left(u_1^{-\alpha} + u_2^{-\alpha} - 1\right)^{-\frac{1}{\alpha}}$
Frank	$C_\alpha(u_1, u_2) := -\frac{1}{\alpha}\ln\left[1 + \frac{(\exp[-\alpha u_1]-1)(\exp[-\alpha u_2]-1)}{\exp[-\alpha]-1}\right]$
Gumbel	$C_\alpha(u_1, u_2) := \exp\left[-((-\ln u_1)^\alpha + (-\ln u_2)^\alpha)^{\frac{1}{\alpha}}\right]$

Notes: $\Phi_\rho(.)$ denotes the standardized bivariate normal distribution with correlation ρ, whereas $\Phi^{-1}(.)$ is the inverse of the univariate standard normal distribution function. $t_{\rho,\nu}(.)$ denotes the standardized bivariate Student-t distribution with correlation ρ and $\nu(\geq 1)$ degrees of freedom, while $t_\nu^{-1}(.)$ is the inverse of the univariate Student-t cumulative distribution function with ν degrees of freedom. Finally, α is the parameter attached to the generator of each of the Archimedean copula functions.

3.4.2 Numerical results

Our copulas are estimated through the ML approach that is implemented in *Matlab* using the *copulafit* function.[3.7] Table 3.5 shows the elliptical and Archimedean copula functions parameter estimates, and Table 3.6 presents the corresponding Akaike Information Criterion (hereafter, AIC) to choose the copula function with better fitting performance. These results are computed for the entire sample (01-Jan-2015 to 01-Jun-2020) and using the returns of electricity and natural gas contracts.[3.8]

[3.6] We note that the theory of copulas has a long list of important contributions and a complete literature review on the topic is out of the scope of the present paper. Hence, further details on this theme may be consulted, for instance, in Joe (1997), Nelsen (2006) or Fusai and Roncoroni (2008, Chapter 8).

[3.7] Technical details of this copula-based parametric approach can be consulted, for instance, in Fusai and Roncoroni (2008, Chapter 8) and Choroś et al. (2010).

[3.8] Tables H.1 and H.2 contained in the corresponding appendix show the historical correlations for the returns and prices, respectively.

According to the AIC criteria, the Gumbel copula is the family selected for 10 time series: SE1, SE2, SE3, SE4, DK1, Oslo, Bergen, Molde, Trondheim and average Elspot prices. These results highlight the nonlinear positive dependence between the returns of the series, i.e., a greater dependence in the positive tail rather than in the negative tail of the distributions. Ghorbel and Trabelsi (2014) also find that the Gumbel copula is the appropriate one in some energy markets, in particular for modeling the dependency structure between crude oil, heating oil and natural gas.

The second copula with the best fitting performance is the Student-t copula that is the most appropriate for 8 time series: SYS, FI, Kristiansand, Tromsø, EE, LT, LV and UK N2EX, thus showing that there exists a symmetric dependence between the returns of these series. This is in line with the observations of Lu et al. (2014), who document that the Student-t copula is the most appropriate copula function for fitting the dependence structure between crude and natural gas futures.

We further note that we have also tested the Bayesian Information Criterion (hereafter, BIC) for each copula function under the MR-JD process and the obtained results confirm the selection of the same copula functions. The outputs for the BIC and Log-Likelihoods are available upon request.

Table 3.5: Parameters estimated via the ML approach and for each copula function from Table 3.4, for the period between 01-Jan-2015 and 01-Jun-2020.

	Student's-t	Gaussian	Clayton	Frank	Gumbel
SYS	0.039	0.030	0.019	0.300	1.030
SE1	0.013	0.011	0.015	0.152	1.017
SE2	0.013	0.011	0.015	0.152	1.017
SE3	0.038	0.035	0.028	0.266	1.030
SE4	0.053	0.045	0.042	0.398	1.037
FI	-0.019	-0.023	0.015	-0.071	1.013
DK1	0.023	0.018	0.004	0.190	1.021
DK2	0.041	0.036	0.027	0.349	1.024
Oslo	0.031	0.023	0.015	0.247	1.031
Kristiansand	0.038	0.027	0.015	0.300	1.031
Bergen	0.037	0.031	0.015	0.303	1.030
Molde	0.029	0.027	7.369	0.220	1.024
Trondheim	0.029	0.027	7.369	0.220	1.024
Tromsø	0.024	0.020	0.006	0.186	1.029
EE	-0.004	-0.010	0.015	0.021	1.016
LV	0.002	-0.007	0.015	0.044	1.014
LT	0.002	-0.009	0.015	0.039	1.016
Average Elspot prices	0.024	0.015	4.948	0.212	1.027
UK day-ahead prices	0.028	0.024	0.015	0.180	1.033

Notes: The second and third columns show the ρ parameters associated to the Student's-t and Gaussian copula functions, whereas the remaining columns to the right present the α parameters of Clayton, Frank and Gumbel copula functions. The Nord Pool Spot computes the reference price used for financial trading purposes that is known as the System Price (SYS), i.e., the price that would be charged if there were no transmission restrictions within the Nordic region. SE1, SE2, SE3 and SE4 represent the four bidding areas in Sweden. FI denotes the bidding area in Finland. DK1 and DK2 stand for the two bidding areas in Denmark. Oslo, Kristiansand, Bergen, Molde, Trondheim and Tromsø represent the five bidding areas in Norway (Molde and Trondheim belong to the same bidding area NO3). EE, LV and LT correspond to the bidding areas of Estonia, Latvia and Lithuania, respectively. Average Elspot prices express an additional variable (price) representing the arithmetic average of the Elspot prices. UK day-ahead prices represent the auction prices in the United Kingdom. All copulas are constructed using the returns of each electricity contract and the Henry Hub natural gas contract associated to the distribution hub on the natural gas pipeline system in Louisiana.

Table 3.6: Akaike Information Criterion (AIC) for each copula function from Table 3.4.

	Student's-t	Gaussian	Clayton	Frank	Gumbel
SYS	**-6.650**	-0.226	0.634	-2.125	-5.124
SE1	1.445	0.830	1.000	0.185	**-1.208**
SE2	1.480	0.829	1.000	0.192	**-1.181**
SE3	-1.643	-0.651	0.086	-1.476	**-3.296**
SE4	-4.425	-1.839	-0.899	-4.517	**-4.901**
FI	**-2.239**	0.269	1.000	0.826	-1.295
DK1	-0.962	0.549	0.986	-0.274	**-1.221**
DK2	-1.014	-0.746	0.250	**-3.302**	-1.519
Oslo	-3.779	0.261	1.000	-1.121	**-5.074**
Kristiansand	**-6.203**	-0.038	1.000	-2,128	-5.154
Bergen	-1.648	-0.321	1.000	-2.221	**-4.409**
Molde	-1.104	0.021	0.999	-0.692	**-3.499**
Trondheim	-1.104	0.021	0.999	-0.692	**-3.499**
Tromsø	**-7.153**	0.453	0.957	-0,188	-4.639
EE	**-2.473**	0.874	1.000	0.984	-1.573
LV	**-4.851**	0.939	1.000	0.932	-0.207
LT	**-7.653**	0.893	1.000	0.947	-0.532
Average Elspot prices	-2.838	0.677	0.999	-0.555	**-3.918**
UK day-ahead prices	**-4.604**	0.238	1.000	-0.131	-4.380

Notes: The Nord Pool Spot computes the reference price used for financial trading purposes that is known as the System Price (SYS), i.e., the price that would be charged if there were no transmission restrictions within the Nordic region. SE1, SE2, SE3 and SE4 represent the four bidding areas in Sweden. FI denotes the bidding area in Finland. DK1 and DK2 stand for the two bidding areas in Denmark. Oslo, Kristiansand, Bergen, Molde, Trondheim and Tromsø represent the five bidding areas in Norway (Molde and Trondheim belong to the same bidding area NO3). EE, LV and LT correspond to the bidding areas of Estonia, Latvia and Lithuania, respectively. Average Elspot prices express an additional variable (price) representing the arithmetic average of the Elspot prices. UK day-ahead prices represent the auction prices in the United Kingdom. All copulas are constructed using the returns of each electricity contract and the Henry Hub natural gas contract associated to the distribution hub on the natural gas pipeline system in Louisiana. The values in bold highlight which copula should be used for each of the series.

3.5 Risk analysis and portfolio optimization

After modeling the dependence structure through copula functions, we simulate the returns of an energy firm (whose portfolio incorporates electricity and natural gas assets) and compute extreme risk measures for a two-dimensional portfolio. For this purpose, 1,000 simulations of returns are used and the Value-at-Risk (hereafter, VaR) and Conditional Value-at-Risk (henceforth, CVaR) are adopted as extreme risk measures (for a

level of confidence of $1-\alpha$).

Table 3.7 tests several specifications of weights of electricity (ω_{elect}) and natural gas (ω_{ng}). We begin with a combination of 10% in electricity assets and 90% in natural gas—to represent a leveraged portfolio in a fossil fuel energy—and adopt subsequent changes in the weights until achieving a high level of investment in electricity. Electricity is assumed to come from renewable projects for all the combinations of these two assets. Under our copula approach, and in order to show the relevance of the specification adopted for the underlying behavior of electricity and natural gas prices, we compare the extreme risk measures produced by the MR-JD copula with the ones generated by the GARCH-EVT copula, i.e., by the process yielding the second best fitting performance, as shown in Table 3.3.[3.9]

Several remarks can be drawn from Table 3.7. In Table 3.7 CVaR accounts for losses exceeding VaR for all scenarios (i.e., for each combination of weights of electricity and natural gas) and for both copula models (i.e., MR-JD and GARCH-EVT). By definition, CVaR is the weighted average of the extreme losses which investors are exposed in the left tail of the distribution of returns beyond the VaR level. Table 3.7 shows that VaR represents only between 60% (for $1-\alpha=0.99$) to 80% (for $1-\alpha=0.90$) of the CVaR. This finding is valid for all (discrete) combinations of the assets. The quantification of losses exceeding VaR is particularly relevant for risk managers since these results arise from the fat tails feature of these energy returns.

[3.9] We note that we have also performed the estimation of the copula functions based on the residuals of the GARCH-EVT. The results confirm that the Gumbel copula is the one with best fitting performance for the average Elspot and natural gas returns—yielding an AIC value of -6.338. The AIC values for Gaussian, Student-t, Clayton and Frank copula functions are -0.538, -3.887, 0.886 and -3.194, respectively.

Table 3.7: Computation of the CVaR and VaR based on the Gumbel copula for different portfolios of electricity and natural gas.

		CVaR		VaR	
$\omega_{elec};\omega_{ng}$	$1-\alpha$	MR-JD	GARCH-EVT	MR-JD	GARCH-EVT
10%;90%	90%	-0.1051	-0.1116	-0.0577	-0.0600
	95%	-0.1395	-0.1513	-0.0800	-0.0852
	99%	-0.2692	-0.3147	-0.1654	-0.1883
20%;80%	90%	-0.1330	-0.1391	-0.0725	-0.0749
	95%	-0.1772	-0.1886	-0.1006	-0.1058
	99%	-0.3462	-0.3891	-0.2133	-0.2415
30%;70%	90%	-0.1558	-0.1620	-0.0847	-0.0873
	95%	-0.2080	-0.2196	-0.1175	-0.1229
	99%	-0.4085	-0.4513	-0.2520	-0.2849
40%;60%	90%	-0.1755	-0.1820	-0.0952	-0.0981
	95%	-0.2346	-0.2467	-0.1322	-0.1380
	99%	-0.4622	-0.5059	-0.2853	-0.3225
50%;50%	90%	-0.1932	-0.2000	-0.1047	-0.1078
	95%	-0.2584	-0.2711	-0.1453	-0.1515
	99%	-0.5100	-0.5550	-0.3149	-0.3561
60%;40%	90%	-0.2092	-0.2165	-0.1133	-0.1168
	95%	-0.2799	-0.2934	-0.1572	-0.1639
	99%	-0.5534	-0.6001	-0.3419	-0.3868
70%;30%	90%	-0.2240	-0.2318	-0.1212	-0.1250
	95%	-0.2998	-0.3141	-0.1682	-0.1754
	99%	-0.5934	-0.6420	-0.3666	-0.4151
80%;20%	90%	-0.2378	-0.2461	-0.1285	-0.1328
	95%	-0.3184	-0.3335	-0.1784	-0.1862
	99%	-0.6306	-0.6813	-0.3897	-0.4417
90%;10%	90%	-0.2507	-0.2596	-0.1355	-0.1401
	95%	-0.3357	-0.3518	-0.1880	-0.1963
	99%	-0.6656	-0.7183	-0.4114	-0.4667

Notes: ω_{elect} and ω_{ng} are the weights of electricity and natural gas assets in each portfolio, respectively. The second column presents the confidence level $1-\alpha$. The third and fourth columns show, respectively, the CVaR for the MR-JD and GARCH-EVT processes under the Gumbel copula. Finally, the fifth and sixth columns exhibit the corresponding VaR for each model also under the Gumbel copula.

The second finding concerns the variability of the extreme risk measures for different combinations of electricity and natural gas. The results highlight that both risk measures increase with higher stakes on electricity. This finding is coherent with the empirical results reported in Section 3.3., where we found that electricity markets exhibit a higher volatility when compared with the Henry Hub natural gas market.

The last finding is related with the choice of the best stochastic process. Although similar extreme risk measures are obtained using both copula models, when the results are transposed from the (unitary) risk measures to a real portfolio of an energy firm the importance of fitting the underlying prices/volatility based on the most suitable approach becomes crucial. For example, an energy firm that has available a capital expenditure budget of $2.0 billion may observe (on average) a difference of $23,626,808 in the $\text{CVaR}_{95\%}$ computed using the MR-JD copula and the GARCH-EVT copula (for the allocation $(\omega_{elect}, \omega_{ng}) = (10\%, 90\%)$). This finding highlights the relevance of adopting a stochastic process that accommodates the features of the underlying energy prices, i.e., for electricity and natural gas, spikes/drops, mean reversion and seasonality effects should be included.

To complement the previous risk analysis, we also perform an optimization exercise to find the optimal energy mix for a portfolio manager that seeks the maximization of the risk-return trade-off. Since risk managers of energy firms aim to maximize their return-risk ratio, we perform the optimization of the historical return of our portfolio (including natural gas as a fuel fossil energy and electricity from renewable assets such as photovoltaic or wind projects) adjusted by the corresponding standard deviation as:

$$\max_{\{\omega_{elect}, \omega_{ng}\}} \frac{r_p}{\sigma_p} \tag{3.17}$$

subject to

$$\omega_{elect} + \omega_{ng} = 1, \tag{3.18}$$

and

$$\omega_{elect}, \omega_{ng} \geq 0, \tag{3.19}$$

where r_p denotes the average (historical) return of the portfolio and σ_p represents the corresponding standard deviation. While the first restriction ensures the full investment

in both assets, the second condition is needed to require only long positions in each asset. The results of this optimization exercise are available in Table 3.8.

Table 3.8: Portfolio optimization and corresponding extreme risk measures from the MR-JD Gumbel copula.

Optimal weights	Risk measure	Simulated extreme risk measure
	CVaR(90%)	-0.1097
	CVaR(95%)	-0.1458
$\omega_{elec} = 0.115$	CVaR(99%)	-0.2821
$\omega_{ng} = 0.885$	VaR(90%)	-0.0602
	VaR(95%)	-0.0834
	VaR(99%)	-0.1735

Notes: ω_{elect} and ω_{ng} are the weights of electricity and natural gas assets in the optimal portfolio, respectively. The second column identifies the used extreme risk measure for the level of confidence $1-\alpha$. The third column shows the extreme optimal extreme risk measures based on the MR-JD processes under the Gumbel copula.

The findings taken from Table 3.8 are relevant for energy transition policies. In a context of a two-dimensional portfolio of natural gas and electricity assets, decision makers tend to avoid a high level of exposure to electricity prices, since electricity is known to be an high-volatility utility. This finding has implications in energy transition since the most relevant investments enhancing carbon neutrality involve electricity production with renewable energy sources. In addition to the large required capital expenditures in renewable projects, the high level of volatility in electricity markets highlights that the existence of incentive schemes provided by governments to new investments in renewable projects are of pivotal importance or, in the absence of such mechanisms, an accurate risk management policy is required for hedging electricity positions as long as energy transition is done based on electricity assets.

3.6 Conclusions and policy implications

In this paper, we have proposed a stochastic framework for modeling electricity (and natural gas) prices in a context of energy transition. The model captures the three most relevant features in these markets: mean reversion in the prices, spikes and drops (modeled as a jump process) and seasonality effects. Our empirical analysis was addressed for the day-ahead prices of the Nord Pool electricity market and natural gas prices. Using a ML approach, the model parameters are estimated for multiple day-ahead prices. Based on Monte Carlo simulations, an out-of-sample exercise is run to show that the mean-reverting model with jumps outperforms the corresponding standard geometric Brownian motion with jumps and the GARCH-EVT model.

Given the recent forecasts of an increasing global demand for natural gas (and liquefied natural gas) and since this is the unique fossil fuel available in the context of energy transition (to meet the goals for decreasing CO_2 emissions), we propose a copula framework (incorporating mean reversion and jumps) to model a simulated portfolio of electricity (from renewable energy sources) and natural gas assets. Several copula functions are tested and Gumbel and Student-t copulas emerge as the most suitable ones. These findings are relevant for risk management purposes, given the historical low or null correlations in these energy returns. Using extreme risk measures, our portfolio risk analysis simulates multiple energy portfolios in a context of energy transition by reducing the energy sources from fossil fuels (i.e., natural gas) and increasing the weight of electricity assets/projects (from renewable energy sources). We conclude that the use of government incentive schemes in renewable electricity projects is important for energy firms, because the usual maximization of the risk-return trade-off tends to avoid a high exposure to electricity assets.

For future research and as a natural extension of this work, we intend to study the optimal weights problem of energy assets. The use of a more realistic formulation of portfolio optimization requires additional inputs, such as the investments in renewable assets, disinvestments in fossil fuels and the modeling of operations in the renewable business (feed-in tariffs, hourly pricing management, operations and maintenance costs, etc.). This issue is out of the scope of the present paper and will be addressed in future research.

Appendix G

Table G.1: Estimation of the parameters from the stochastic component for Elspot and N2EX day-ahead markets in 2019 and via the ML approach.

	α	κ	σ	μ_J	σ_J	λ
SYS	2.110	103.234***	1.155***	-0.093	0.295*	21.164*
SE1	1.909	67.587***	1.303***	-0.031	0.474***	42.500***
SE2	1.909	67.580***	1.303***	-0.031	0.474***	42.505***
SE3	2.632	91.459***	1.697***	-0.074	0.556**	27.010***
SE4	5.211*	151.133***	2.085***	-0.208	0.608**	21.546**
FI	6.284	192.152***	2.761***	-0.178	0.496**	31.044**
DK1	-	-	-	-	-	-
DK2	-	-	-	-	-	-
Oslo	0.514	65.879***	0.790***	-0.010	0.171**	47.429**
Kristiansand	0.394	65.358***	0.768***	-0.008	0.180**	44.737***
Bergen	0.412	63.998***	0.768***	-0.008	0.170**	48.648**
Molde	0.928	49.574***	0.931***	-0.043	0.281*	23.738**
Trondheim	0.928	49.574***	0.931***	-0.043	0.281*	23.738**
Tromsø	1.094	43.843***	0.860***	-0.054	0.285**	22.534**
EE	4.654	220.575***	2.526***	-0.110	0.393	34.520
LV	3.629	215.143***	2.538***	-0.117	0.443	23.499
LT	3.327	212.197***	2.565***	-0.114	0.459	21.586
Average Elspot prices	3.453	143.360***	1.693***	-0.142	0.267*	20.826*
UK day-ahead prices	0.568	134.902***	1.223***	-0.018	0.194	24.536

Notes: κ is the speed of mean reversion, α/κ denotes the long-run level of the process, σ represents the volatility, μ_J and σ_J are, respectively, the mean and the standard deviation of the jump size and λ is the jump intensity of the Poisson process. The Nord Pool Spot computes the reference price used for financial trading purposes that is known as the System Price (SYS), i.e., the price that would be charged if there were no transmission restrictions within the Nordic region. SE1, SE2, SE3 and SE4 represent the four bidding areas in Sweden. FI denotes the bidding area in Finland. DK1 and DK2 stand for the two bidding areas in Denmark. Oslo, Kristiansand, Bergen, Molde, Trondheim and Tromsø represent the five bidding areas in Norway (Molde and Trondheim belong to the same bidding area NO3). EE, LV and LT correspond to the bidding areas of Estonia, Latvia and Lithuania, respectively. Average Elspot prices express an additional variable (price) representing the arithmetic average of the Elspot prices. Finally, UK day-ahead prices represent the auction prices in the United Kingdom. The existence of negative (spot) prices in the series DK1 and DK2 in 2019 prevents the calibration of the model in this year. The symbols $*$, $**$, $***$ indicate if the estimate is statistically significant at 5%, 1% and 0.1% level, respectively.

Table G.2: Estimation of the parameters from the stochastic component for Elspot and N2EX day-ahead markets in 2018 and via the ML approach.

	α	κ	σ	μ_J	σ_J	λ
SYS	0.888	103.449***	0.888***	-0.010	0.203***	91.555***
SE1	0.863	106.626***	1.207***	-0,013	0.267***	69.283***
SE2	0.863	106.626***	1.207***	-0.013	0.267***	69.283***
SE3	0.382	106.386***	1.229***	-0.005	0.262***	74.916***
SE4	-0.638	133.194***	1.651***	0.009	0.287***	76.080***
FI	2.730	184.358***	1.741***	-0.039	0.325***	66.043***
DK1	16.590***	232.547***	2.598***	-0.444***	0.561***	36.722***
DK2	9.986***	208.980***	2.333***	-0.178*	0.431***	54.902***
Oslo	0.914	96.596***	1.013***	-0.017	0.254***	59.738***
Kristiansand	1.190	85.434***	0.798***	-0.014	0.189***	93.386***
Bergen	1.830	83.992***	1.028***	-0.044	0.371***	44.204***
Molde	0.955	85.709***	0.918***	-0.015	0.239***	69.380***
Trondheim	0.955	85.709***	0.918***	-0.015	0.239***	69.380***
Tromsø	-1.043	62.770***	0.608***	0.012	0.190***	81.333***
EE	2.841	180.738***	1.771***	-0.043	0.328***	61.948***
LV	-0.581	181.760***	1.962***	0.020	0.360**	39.878***
LT	-0.749	181.703***	1.999***	0.024	0.355**	41.324**
Average Elspot prices	1.762	140.018***	1.237***	-0.020	0.218***	85.320***
UK day-ahead prices	-2.082*	139.716***	0.624***	0.026	0.102***	79.565**

Notes: κ is the speed of mean reversion, α/κ denotes the long-run level of the process, σ represents the volatility, μ_J and σ_J are, respectively, the mean and the standard deviation of the jump size and λ is the jump intensity of the Poisson process. The Nord Pool Spot computes the reference price used for financial trading purposes that is known as the System Price (SYS), i.e., the price that would be charged if there were no transmission restrictions within the Nordic region. SE1, SE2, SE3 and SE4 represent the four bidding areas in Sweden. FI denotes the bidding area in Finland. DK1 and DK2 stand for the two bidding areas in Denmark. Oslo, Kristiansand, Bergen, Molde, Trondheim and Tromsø represent the five bidding areas in Norway (Molde and Trondheim belong to the same bidding area NO3). EE, LV and LT correspond to the bidding areas of Estonia, Latvia and Lithuania, respectively. Average Elspot prices express an additional variable (price) representing the arithmetic average of the Elspot prices. Finally, UK day-ahead prices represent the auction prices in the United Kingdom. The symbols $*$, $**$, $***$ indicate if the estimate is statistically significant at 5%, 1% and 0.1% level, respectively.

Table G.3: Estimation of the parameters from the stochastic component for Elspot and N2EX day-ahead markets in 2017 and via the ML approach.

	α	κ	σ	μ_J	σ_J	λ
SYS	-4.353**	122.576***	0.857***	0.033*	0.119***	132.055***
SE1	-8.134**	146.671***	1.050**	0.042**	0.156***	194.439***
SE2	-8.134**	146.671***	1.050**	0.042**	0.156***	194.439***
SE3	-12.215***	155.280***	1.134**	0.058***	0.159***	210.956***
SE4	-15.462**	159.045***	1.447*	0.065**	0.155***	240.725***
FI	-7.702	206.719***	1.764**	0.041	0.166***	190.163***
DK1	-	-	-	-	-	-
DK2	-	-	-	-	-	-
Oslo	-1.757	79.455***	0.570***	0.014	0.120***	126.310***
Kristiansand	-1.021	73.804***	0.587***	0.008	0.122***	110.704***
Bergen	-1.291	72.893***	0.541***	0.010	0.114***	113.986***
Molde	-4.260*	142.482***	1.389***	0.288***	0.021	149.316*
Trondheim	-4.260*	142.482***	1.389***	0.288***	0.021	149.316*
Tromsø	-0.958	66.305***	0.621***	0.012	0.158***	78.621***
EE	-6.818	203.848***	1.798**	0.040	0.167***	174.341**
LV	-3.535	175.610***	1.912***	0.026	0.171***	147.479*
LT	-1.599	174.774***	2.030**	0.012	0.166***	156.237*
Average Elspot prices	-7.269	162.829***	1.287*	0.040*	0.121***	182.791**
UK day-ahead prices	-0.986	150.624***	0.803***	0.019	0.133***	51.391***

Notes: κ is the speed of mean reversion, α/κ denotes the long-run level of the process, σ represents the volatility, μ_J and σ_J are, respectively, the mean and the standard deviation of the jump size and λ is the jump intensity of the Poisson process. The Nord Pool Spot computes the reference price used for financial trading purposes that is known as the System Price (SYS), i.e., the price that would be charged if there were no transmission restrictions within the Nordic region. SE1, SE2, SE3 and SE4 represent the four bidding areas in Sweden. FI denotes the bidding area in Finland. DK1 and DK2 stand for the two bidding areas in Denmark. Oslo, Kristiansand, Bergen, Molde, Trondheim and Tromsø represent the five bidding areas in Norway (Molde and Trondheim belong to the same bidding area NO3). EE, LV and LT correspond to the bidding areas of Estonia, Latvia and Lithuania, respectively. Average Elspot prices express an additional variable (price) representing the arithmetic average of the Elspot prices. Finally, UK day-ahead prices represent the auction prices in the United Kingdom. The existence of negative (spot) prices in the series DK1 and DK2 in 2017 prevents the calibration of the model in this year. The symbols $*$, $**$, $***$ indicate if the estimate is statistically significant at 5%, 1% and 0.1% level, respectively.

Table G.4: Estimation of the parameters from the stochastic component for Elspot and N2EX day-ahead markets in 2016 and via the ML approach.

	α	κ	σ	μ_J	σ_J	λ
SYS	-1.167	82.267***	1.296***	0.027	0.206**	62.748*
SE1	-4.381*	137.591***	2.066***	0.545***	0.131	8.697*
SE2	-4.381*	137.591***	2.066***	0.545***	0.131	8.697*
SE3	-5.156*	120.914***	1.903***	0.115	0.265**	48.949
SE4	-4.992	142.059***	2.335***	0.521***	0.110	10.406*
FI	-3.251	185.328***	2.346**	0.041	0.252**	96.940
DK1	-	-	-	-	-	-
DK2	-	-	-	-	-	-
Oslo	-0.936	74.903***	0.864***	0.016	0.207***	93.800***
Kristiansand	-0.153	69.679***	0.645***	0.001	0.123***	122.165***
Bergen	0.143	63.456***	0.657***	0.003	0.125***	114.226***
Molde	-1.975	90.824***	1.578***	0.073	0.268*	32.771*
Trondheim	-1.975	90.824***	1.578***	0.073	0.268*	32.771*
Tromsø	-0.265	87.068***	0.684***	0.014	0.244*	48.914*
EE	-0.723	189.669***	2.212***	0.020	0.276**	69.486**
LV	-2.178	184.162***	2.068***	0.041	0.281**	67.883
LT	-4.189	191.764***	1.940***	0.049	0.264***	97.815*
Average Elspot prices	-2.971	138.514***	1.967***	0.416***	0.119	8.379
UK day-ahead prices	-6.474***	211.043***	1.491***	0.251**	0.392**	26.511***

Notes: κ is the speed of mean reversion, α/κ denotes the long-run level of the process, σ represents the volatility, μ_J and σ_J are, respectively, the mean and the standard deviation of the jump size and λ is the jump intensity of the Poisson process. The Nord Pool Spot computes the reference price used for financial trading purposes that is known as the System Price (SYS), i.e., the price that would be charged if there were no transmission restrictions within the Nordic region. SE1, SE2, SE3 and SE4 represent the four bidding areas in Sweden. FI denotes the bidding area in Finland. DK1 and DK2 stand for the two bidding areas in Denmark. Oslo, Kristiansand, Bergen, Molde, Trondheim and Tromsø represent the five bidding areas in Norway (Molde and Trondheim belong to the same bidding area NO3). EE, LV and LT correspond to the bidding areas of Estonia, Latvia and Lithuania, respectively. Average Elspot prices express an additional variable (price) representing the arithmetic average of the Elspot prices. Finally, UK day-ahead prices represent the auction prices in the United Kingdom. The existence of negative (spot) prices in the series DK1 and DK2 in 2016 prevents the calibration of the model in this year. The symbols $*$, $**$, $***$ indicate if the estimate is statistically significant at 5%, 1% and 0.1% level, respectively.

Table G.5: Estimation of the parameters from the stochastic component for Elspot and N2EX day-ahead markets in 2015 and via the ML approach.

	α	κ	σ	μ_J	σ_J	λ
SYS	-1.964	84.651***	1.369***	0.017	0.224***	135.241***
SE1	-5.988**	82.084***	0.986*	0.034	0.239***	187.595***
SE2	-6.634**	90.383***	0.941	0.036	0.236***	193.751***
SE3	-7.194*	105.804***	2.222***	0.078	0.371***	96.601***
SE4	-9.765**	94.793***	2.192***	0.077	0.384***	131.106***
FI	4.584	157.498***	2.732***	-0.029	0.385***	146.582***
DK1	-4.367	198.133***	1.871**	0.020	0.410***	240.503***
DK2	-18.397***	169.986***	1.105	0.068**	0.331***	280.442***
Oslo	-1.059	68.060***	0.998***	0.010	0.225***	135.280***
Kristiansand	-0.553	66.814***	1.004***	0.007	0.225***	126.908***
Bergen	-1.255	61.210***	1.011***	0.013	0.229***	122.692***
Molde	-3.206*	74.941***	0.780***	0.020	0.202***	176.438***
Trondheim	-3.206*	74.941***	0.779***	0.020	0.202***	176.438***
Tromsø	0.661*	54.640***	0.860***	-0.003	0.183***	130.475***
EE	16.586***	244.115***	3.073***	-0,201*	0.393***	80.340**
LV	3.972	167.847***	1.502***	-0,029	0.212***	127.480***
LT	3.472	163.395***	1.393**	-0,022	0.208***	147.721***
Average Elspot prices	0.653	145.193***	1.397**	-0.002	0.166***	212.358***
UK day-ahead prices	1.553	171.116***	0.554***	-0.009	0.069***	154.748***

Notes: κ is the speed of mean reversion, α/κ denotes the long-run level of the process, σ represents the volatility, μ_J and σ_J are, respectively, the mean and the standard deviation of the jump size and λ is the jump intensity of the Poisson process. The Nord Pool Spot computes the reference price used for financial trading purposes that is known as the System Price (SYS), i.e., the price that would be charged if there were no transmission restrictions within the Nordic region. SE1, SE2, SE3 and SE4 represent the four bidding areas in Sweden. FI denotes the bidding area in Finland. DK1 and DK2 stand for the two bidding areas in Denmark. Oslo, Kristiansand, Bergen, Molde, Trondheim and Tromsø represent the five bidding areas in Norway (Molde and Trondheim belong to the same bidding area NO3). EE, LV and LT correspond to the bidding areas of Estonia, Latvia and Lithuania, respectively. Average Elspot prices express an additional variable (price) representing the arithmetic average of the Elspot prices. Finally, UK day-ahead prices represent the auction prices in the United Kingdom. The symbols $*$, $**$, $***$ indicate if the estimate is statistically significant at 5%, 1% and 0.1% level, respectively.

Table G.6: Estimation of the parameters from the stochastic component for Henry Hub natural gas prices in the period 2015-2019 and via the ML approach.

	α	κ	σ	μ_J	σ_J	λ
2015	0.458	20.304***	0.162***	-0.001	0.047***	181.808**
2016	1.538	52.323***	0.067***	-0.086	0.001***	13.833**
2017	0.861	60.123***	0.521***	-0.004	0.044***	143.919**
2018	0.287	25.646***	0.424***	-0.036	0.167***	31.439**
2019	0.246	49.245***	0.499***	-0.008	0.111***	37.864**

Notes: κ is the speed of mean reversion, α/κ denotes the long-run level of the process, σ represents the volatility, μ_J and σ_J are, respectively, the mean and the standard deviation of the jump size and λ is the jump intensity of the Poisson process. The Henry Hub natural gas prices represent the spot prices of the distribution hub on the natural gas pipeline system in Louisiana. The symbols $*$, $**$, $***$ indicate if the estimate is statistically significant at 5%, 1% and 0.1% level, respectively.

Appendix H

Table H.1: Historical correlation between the listed electricity prices and the Henry Hub natural gas prices.

	2015	2016	2017	2018	2019	All
SYS	0.270	0.018	-0.017	-0.058	-0.055	0.012
SE1	0.200	0.024	-0.036	-0.019	-0.059	0.001
SE2	0.200	0.024	-0.036	-0.019	-0.059	0.001
SE3	0.199	0.018	-0.036	-0.045	-0.061	0.020
SE4	0.197	0.013	-0.037	-0.027	-0.024	0.015
FI	0.177	-0.028	-0.017	-0.052	-0.061	-0.013
DK1	0.192	0.009	-0.070	-0.077	-0.264	-0.017
DK2	0.178	0.017	-0.037	-0.067	-0.167	-0.004
Oslo	0.273	-0.012	0.003	-0.055	-0.050	0.002
Kristiansand	0.267	0.030	-0.030	-0.067	-0.063	0.002
Bergen	0.257	0.031	-0.013	-0.031	-0.033	0.004
Molde	0.240	0.012	-0.038	-0.029	-0.047	0.017
Trondheim	0.240	0.012	-0.038	-0.029	-0.047	0.017
Tromsø	0.256	-0.013	0.024	-0.008	-0.058	0.013
EE	0.188	-0.009	-0.022	-0.057	-0.025	-0.006
LV	0.095	0.046	-0.085	-0.074	-0.027	-0.028
LT	0.084	0.018	-0.079	-0.075	-0.019	-0.031
Average Elspot prices	0.251	0.021	-0.045	-0.059	-0.080	-0.012
UK day-ahead prices	0.094	0.038	-0.024	-0.046	0.098	0.004

Notes: The Nord Pool Spot computes the reference price used for financial trading purposes that is known as the System Price (SYS), i.e., the price that would be charged if there were no transmission restrictions within the Nordic region. SE1, SE2, SE3 and SE4 represent the four bidding areas in Sweden. FI denotes the bidding area in Finland. DK1 and DK2 stand for the two bidding areas in Denmark. Oslo, Kristiansand, Bergen, Molde, Trondheim and Tromsø represent the five bidding areas in Norway (Molde and Trondheim belong to the same bidding area NO3). EE, LV and LT correspond to the bidding areas of Estonia, Latvia and Lithuania, respectively. Average Elspot prices express an additional variable (price) representing the arithmetic average of the Elspot prices. Finally, UK day-ahead prices represent the auction prices in the United Kingdom. The last column of the table refers to the full sample period (01-Jan-2015 to 01-Jun-2020).

Table H.2: Historical correlation between the listed electricity returns and the Henry Hub natural gas returns.

	2015	2016	2017	2018	2019	All
SYS	-0.008	0.316	0.028	0.058	0.591	0.459
SE1	0.027	0.428	0.075	0.003	0.509	0.471
SE2	0.028	0.428	0.075	0.003	0.509	0.471
SE3	-0.025	0.403	0.019	0.033	0.485	0.435
SE4	0.012	0.418	0.042	0.050	0.400	0.425
FI	-0.004	0.219	-0.035	-0.018	0.124	0.299
DK1	0.018	0.364	0.028	0.063	0.254	0.381
DK2	0.064	0.371	0.062	0.032	0.278	0.382
Oslo	-0.025	0.275	0.044	0.054	0.601	0.445
Kristiansand	-0.015	0.329	-0.018	0.103	0.604	0.457
Bergen	-0.018	0.280	-0.040	0.062	0.603	0.444
Molde	0.036	0.410	0.060	0.003	0.598	0.466
Trondheim	0.036	0.410	0.060	0.003	0.598	0.466
Tromsø	0.102	0.311	0.027	-0.012	0.603	0.425
EE	0.042	0.185	-0.044	0.031	0.062	0.257
LV	-0.131	0.124	0.002	0.003	0.082	0.237
LT	-0.133	0.103	0.013	0.006	0.085	0.241
Average Elspot prices	-0.005	0.357	0.031	0.030	0.472	0.437
UK day-ahead prices	0.414	0.247	0.109	0.158	0.649	0.512

Notes: The Nord Pool Spot computes the reference price used for financial trading purposes that is known as the System Price (SYS), i.e., the price that would be charged if there were no transmission restrictions within the Nordic region. SE1, SE2, SE3 and SE4 represent the four bidding areas in Sweden. FI denotes the bidding area in Finland. DK1 and DK2 stand for the two bidding areas in Denmark. Oslo, Kristiansand, Bergen, Molde, Trondheim and Tromsø represent the five bidding areas in Norway (Molde and Trondheim belong to the same bidding area NO3). EE, LV and LT correspond to the bidding areas of Estonia, Latvia and Lithuania, respectively. Average Elspot prices express an additional variable (price) representing the arithmetic average of the Elspot prices. Finally, UK day-ahead prices represent the auction prices in the United Kingdom. The last column of the table refers to the full sample period (01-Jan-2015 to 01-Jun-2020).

4. Modeling commodity prices under alternative jump processes and fat tails dynamics

Abstract: The recent fluctuations in commodity prices affected significantly Oil & Gas (O&G) companies' returns. However, integrated O&G companies are not only exposed to the downturn of oil prices since a high level of integration allows these firms to obtain non-perfectly positive correlated portfolio. This paper aims to test several different stochastic processes to model the main strategic commodities in integrated O&G companies: brent, natural gas, jet fuel and diesel. The competing univariate models include the log-normal and double exponential jump-diffusion model, the Variance-Gamma process and the geometric Brownian motion with nonlinear GARCH volatility. Given the effect of correlation between these assets, we also estimate multivariate models, such as the Dynamic Conditional Correlation (DCC) GARCH, DCC-GJR-GARCH and the DCC-EGARCH models. Overall, we find that: (i) the asymmetric conditional heteroskedasticity model substantially improves the performance of the univariate jump-diffusion models; and (ii) the multivariate approaches are the best models for our strategic energy commodities, in particular the DCC-GJR-GARCH model.

JEL Classification: C52, C58, Q40, Q41

Keywords: Commodities, Fat tails, Jumps, Maximum likelihood

4.1 Introduction

The attention paid by notable economists to energy markets is not recent. Following the prominent contributions of Keynes (1936), Kaldor (1939), Working (1948) and Working (1949), Brennan and Hughes (1991) recover the findings on the theory of storage and denominate it as the Kaldor–Working hypothesis, where the comparison between owning physically a commodity and writing a future contract on it is analyzed. Afterwards, the developments of the option pricing theory fully influenced the research on energy markets.

Motivated by the seminal research of Black (1976), Gibson and Schwartz (1990) describe the spot price of the crude oil following a log-normal diffusion process, i.e., a GBM for pricing options on this commodity. Other references follow this idea for some exhaustible natural resources, such as Slade (1988), MacKie-Mason (1990), Pindyck (2001) and Lund (1992). Years later, some studies introduced mean-reverting processes to replace the usual GBM approach to model spot prices of commodities, e.g., Bessembinder et al. (1995), Schwartz (1997) and Eydeland and Geman (1998). More recently, Geman and Shih (2009) examine and test alternative stochastic processes (including the Constant Elasticity of Variance (CEV, hereafter) theoretical framework of Cox (1975) and their mean-reverting processes) for modeling the spot prices of four strategic commodities: crude oil, gold, copper and coal. The estimation of the authors for these commodities occurred for two subsamples: 1990-1999 and 2000-2007 and they achieve three relevant findings: (i) the log-returns of the spot prices have become closer to the features of skewness and kurtosis of a normal distribution; (ii) the mean-reverting processes disappeared between 2000-2007 as long as the spot prices increases; and (iii) the importance of the CEV theoretical framework emerges due to the increasing volatility. Dias and Nunes (2011) also suggest the use of the CEV

diffusion for pricing real options on commodity markets. Comparing with the standard GBM approach, the authors show that firms using the assumption of the log-normal behaviour for the prices of the underlying asset may result to non-optimal investment (or disinvestment) policies.

More complex alternative stochastic models have been tested recently in commodity markets. Askari and Krichene (2008) study the dynamics of crude oil prices and use for this purpose the jump-diffusion model of Merton (1976) and the Variance-Gamma process suggested by Madan and Milne (1991) and Madan et al. (1998). In the field of the infinite and finite jump-diffusion, Cao et al. (2018) examine these jump processes in commodity futures prices, in particular for crude oil and natural gas futures. These authors document that futures prices can be decomposed into infinity small jumps and infrequent larger jump-diffusion in these commodity futures markets. Another relevant finding from the authors is that there is no evidence to eliminate the Brownian motion behaviour for each futures series.

The volatility in commodities markets has not only been modeled based on stochastic processes adopted from the option pricing theory. Recognizing that GARCH models are widely used to model the volatility in energy markets, several empirical studies emerged recently and use more complex models than the standard GARCH. For example, while Nomikos and Andriosopoulos (2012) investigate the pertinence of modeling the volatility of several NYMEX commodity series using the exponential GARCH (EGARCH, hereafter) to face the standard GARCH approach, Youssef et al. (2015) examine the adoption of three long-memory frameworks: the Fractional Integrated GARCH (FIGARCH), the Hyperbolic GARCH (HYGARCH) and the Fractional Integrated APARCH (FIAPARCH). More recently, Chan and Grant (2016) test a battery of GARCH-family and stochastic volatility (hereafter, SV) models under Bayesian estimation for the several commodity prices, including crude oil, natural gas and several

refined products. The list of the tested models includes standard, jump-diffusion, fat tails and asymmetric frameworks. Their empirical research has found that SV models generally outperform their GARCH-family counterpart models.

Another recent field in energy markets is the application of multivariate analysis. In order to capture the changes in correlations between variables, the dynamic conditional correlation GARCH (DCC-GARCH, hereafter) model suggested by Engle (2002) has been applied for energy markets too. Creti et al. (2013) investigate the link between the commodities and stocks markets and find that the last financial crisis has emphasized the financialization of commodity markets. A similar empirical analysis was conducted by Basher and Sadorsky (2016) by modeling the volatility of emerging stock markets, crude oil, VIX, gold and bond prices with the DCC-GARCH model. This setup has been combined with the multivariate heteroscedastic autoregressive model to investigate the relationship between the volatility of the US crude oil and the Chinese agricultural markets has been investigated by Luo and Ji (2018). The volatility linkage between energy and agricultural Germany markets was studied by Cabrera and Schulz (2016) with the adoption of the DCC-GARCH.

Hence, the main goal of this paper is to test the performance of four univariate stochastic processes and three multivariate models to capture the price movements for the main assets of an integrated O&G company using different time periods of analysis. More specifically, this paper offers three contributions to the current literature on modeling commodity prices. First, and to the best of our knowledge, these models have not been explored yet for the main strategic commodities of integrated O&G firms: crude oil, natural gas, jet fuel and diesel. Although some researchers used the standard stochastic processes (GBM, CEV and others) to model prices of some individual commodities, this paper studies different univariate and multivariate jump-diffusion and fat tails models. Second, to support the stylized-fact of discontinuous variations in com-

modity prices, this research tests empirically the pertinence of jumps by incorporating the log-normal and the double exponential jump-diffusion models and others pure jumps processes of finite variations, however with infinitely jump-diffusion, such as the VG process. The traditional conditional heteroskedasticity phenomena is also tested by introducing the nonlinear generalized autoregressive conditional heteroskedasticity (NGARCH) volatility to the standard GBM. Third, since the correlation effects matter for integrated O&G companies, we test three different multivariate approaches based on the Dynamic Conditional Correlation: the DCC-GARCH, DCC-GJR-GARCH and the DCC-EGARCH. Additionally, we also study a large period of analysis in order to include the recent fluctuations in the prices of our commodities. Our examination for these commodities allow us to find which features are pertinent for commodity prices, thus providing useful empirical findings for investors and energy firms.

The remainder of this paper is organized as follows. Section 4.2 presents a brief overview on the data. Section 4.3 reports the jump-diffusion and fat tails univariate processes and the corresponding statistical implementation with the estimation results. Section 4.4 presents multivariate approaches for our strategic commodities. Finally, section 4.5 presents some concluding remarks and proposals for future research.

4.2 Data

This section presents the main features of the data set chosen for an integrated O&G company. More specifically, we consider the (usual) daily spot prices typically used by these firms, namely: brent, natural gas and the main refined products included in the refining margin. In the case of exploration and production activities, the main driver for the performance of these business units is the market risk of brent. As expected, fluctuations in the prices of natural gas affect the prices of brent. Furthermore, the

refining margin is considered as the most crucial and exogenous variable in the downstream business unit. Since the refining margin is not a spot price—i.e., it is a weighting price of several refined products as output and taking the initial cost of the crude oil as input—, we adopt the jet fuel and diesel as proxies for the refined products. Hence, our data is constituted by four assets: brent, natural gas, jet fuel and diesel.

The prices of the light North Sea (physical) crude oil—measured in US$/barrel (henceforth, US$/bbl)—are usually considered as the benchmark for the daily (spot) prices of brent. Therefore, we follow this market standard throughout this paper. For natural gas daily prices, we adopt the UK National Balancing Point (hereafter, NBP) gas market, which is the longest-established spot-traded natural gas market in Europe—the prices are measured in GB Pence/Therm. Finally, for the downstream operations and the refining margin, we consider a benchmark refining margin for companies based on hydrocracking, cracking, base oils and aromatic margins, which includes the jet fuel and the ULSD/diesel.[4.1] These two commodities are measured in US$/Ton (henceforward, US$/T).

All data is collected from the Standard & Poor's Global Platts database. The time series for the daily prices of brent is collected from January 1990 to December 2017. Since the first available price for the UK NBP gas market is August 1996, the data set period for this commodity is from August 1996 to December 2017. For the spot prices of jet fuel and diesel, we consider the period between January 1990 and December 2017 and from December 2002 to December 2017, respectively.

To calibrate each stochastic differential equation, we divide the full data set 1990-2017 into three subsamples: 1990-1999, 2000-2007 and 2008-2017. The entire sample is provided for an analysis of long-term estimations. The choice made for the first two

[4.1] ULSD is diesel fuel with significantly lowered sulfur content which was recently adopted for almost all European and North America O&G companies.

subperiods (i.e., 1990-1999 and 2000-2007) follows from the insights of Geman and Shih (2009) and is justified by the changes observed in the commodity price behaviour after 2000 for the period between 1990-2007. In fact, an increasing trajectory of the brent and crude oil is observed after 2000 until the beginning of the subprime crisis. The following subsample (i.e., 2008-2017) contains the two most relevant drops in the crude oil prices in the latest years. Table 4.1 provides the descriptive statistics for the prices and log-returns of the four strategic commodities under analysis.

Table 4.1: Descriptive statistics of the four strategic commodities for integrated O&G firms.

	Brent	Natural gas	Jet fuel	Diesel
Panel A: Prices				
Average	47.59	34.47	463.88	655.92
Std. deviation	33.60	19.57	308.14	246.23
Median	32.39	30.63	341.88	605.50
Minimum	9.13	4.20	105.75	227.75
Maximum	144.22	187.50	1,466.50	1,354.00
Panel B: Log-returns				
Average	0.00015	0.00024	0.00013	0.00021
Std. deviation	0.02303	0.07786	0.01859	0.01935
Median	0.00055	0.00000	0.00000	0.00037
Minimum	-0.45319	-1.11045	-0.32333	-0.08735
Maximum	0.19454	1.17826	0.15369	0.10905
Observations	7,125	5,370	7,062	3,781

4.3 Jump-diffusion and fat tails processes

This section addresses the estimation of jump-diffusion and fat tails processes for our portfolio of commodities.

4.3.1 The jump-diffusion model of Merton (1976)

It is commonly accepted that realistic approaches for modeling the behaviour of commodity prices should contain both diffusion and jump components. In order to model the spot prices of our commodities, we start considering the jump-diffusion model proposed by Merton (1976) in which the asset price dynamics is governed by

$$dS_t = \mu S_t dt + \sigma S_t dW_t + S_t dJ_t, \tag{4.1}$$

where S_t, μ and σ represent the spot price, the corresponding drift and the instantaneous volatility per unit of time, respectively, and $\{W_t; t \geq t_0\}$ is a standard Brownian motion under the real probability measure $\mathbb{P}$. The univariate jump process defined by

$$J_t = \sum_{j=1}^{N_T} (Y_j - 1), \tag{4.2}$$

where the parameters N_t and J_t denotes a Poisson process and the log-jump size, respectively. Y_j describes the size of the j-th jump. $(N_T)_{T\geq 0}$ follows a homogeneous Poisson process with intensity λ. Given this Poisson distribution with parameter λT, the Poisson probability mass function is represented by

$$f_P(x, \lambda T) = \frac{\exp(-\lambda T)(\lambda T)^x}{x!}, x = 0, 1, 2, ... \tag{4.3}$$

Under this stochastic differential equation (SDE, hereafter), the log-jump size J_t is represented by a Gaussian random variable which is characterized by the mean value μ_J and standard deviation σ_J. For simplicity, we are assuming that W_t, N_t and J_t are independent variables in this model. We define the set of parameters, θ, of this

Poisson-based jump-diffusion model as follows

$$\theta \equiv (\mu, \sigma, \lambda, \mu_J, \sigma_J), \tag{4.4}$$

which is an unknown parameter represented in the bounded set $\Theta \subset \mathbb{R}^5$. For comparison purposes, we compare the performance of the jump-diffusion model of Merton (1976) against the standard GBM process.

Regarding estimation purposes, Aït-Sahalia (2004) explored the estimation of the Merton (1976) jump-diffusion model based on Poisson jumps (JGBM, henceforth)—as well as for other Lévy processes—through the Generalized Method of Moments (GMM, hereafter). One of the key conclusions obtained from Aït-Sahalia (2004) is that GMM estimators using absolute moment of various noninteger orders are not as efficient as the Maximum Likelihood (ML, hereafter) estimation. Hence, we adopt the ML procedure to estimate jump-diffusion and fat tails models. For the sake of completeness, Appendix I.1 of provides further details about the estimation under ML for both the GBM and JGBM processes.

The probability density function (pdf) results from the sum of the conditional probability density, which is weighted by the probability of the conditioning variable, i.e., the jumps occurrence. The ML estimates the parameter set on the log-returns conditioning on the jumps as

$$_{\{\mu^\star, \mu_J, \lambda>0, \sigma>0, \sigma_J>0\}} L^\star = \log(L), \tag{4.5}$$

where the parameter set is represented by $\theta \equiv (\mu, \mu_J, \lambda, \sigma, \sigma_J)$. Thus, we can define the log-likelihood (LL, hereafter) function for $X_{t_i} := \log(S_{t_i}) - \log(S_{t_{i-1}})$ as

$$L^\star(\Theta) = \sum_{i=1}^{n} \log f(x_i; \mu, \mu_J, \lambda, \sigma, \sigma_J), \tag{4.6}$$

and

$$f(x_i;\mu,\mu_J,\lambda,\sigma,\sigma_J)=\sum_{j=0}^{\infty}\mathbb{P}(n_t=j)f_N(x_i;(\mu-\frac{1}{2}\sigma^2)\Delta t+j\mu_J,\sigma^2\Delta t+j\sigma_J^2), \tag{4.7}$$

where Δt is the time step in the discretisation, x_i represents the vector for the values x_1,...,x_n and for t_1,...,t_n. From equation (4.7) it is easy to understand that this expression is an (infinite) product between Gaussian random variables and a Poisson probability defined by $\mathbb{P}(n_t = j) = f_p(j;\Delta t\lambda)$. For example, for small values of Δt usually the Poisson process jumps at most once. When this scenario occurs, equation (4.7) is simplified to

$$\begin{aligned} & f(x_i;\mu,\mu_J,\lambda,\sigma,\sigma_J) \qquad (4.8)\\ = \;& (1-\lambda\Delta t)f_N(x_i;(\mu-\frac{1}{2}\sigma^2)\Delta t,\sigma^2\Delta t)+\lambda\Delta t f_N(x_i;(\mu-\frac{1}{2}\sigma^2)\Delta t+\mu_J,\sigma^2\Delta t+\sigma_J^2). \end{aligned}$$

and results in a combined product of two Gaussian random variables by the probabilities of no jumps in Δt or one jump in Δt.

The parameter set for both the GBM and JGBM processes are estimated via ML for brent, natural gas, jet fuel and diesel. The aforementioned subsamples are also used to perform this estimation.[4.2] Table 4.2 reports the estimation for the parameter set under the JGBM process, whereas the estimates under the GBM diffusion are displayed in Table I.1 of the appendix I.

[4.2] All the numerical results are obtained through Matlab (R2015a 32 bit) running on an Intel Core i7 2.40GHz personal computer. The application of the ML is executed with the "*fminsearch*" algorithm. By default, we set the maximum number of iterations and maximum number of function evaluations to be 100,000. The termination tolerance on the function value is 1e-4.

Table 4.2: Estimation of the parameters under the jump-diffusion model of Merton (1976) and via the ML approach.

		μ	σ	μ_J	σ_J	λ	LL
Brent	1990-2017	0.0000312	0.0216000	0.0706000	0.0008480	0.0113000	16,885
	1990-1999	0.0000475	0.0230000	0.0848000	0.0004795	0.0095000	5,927
	2000-2007	0.0006833	0.0223000	0.0704000	0.0008732	0.0046000	4,859
	2008-2017	-0.0000635	0.0194000	0.0740000	0.0007642	0.0166000	6,142
Natural gas	1996-2017	0.0002462	0.0658000	0.2679000	0.0075000	0.0172000	6,571
	1996-1999	0.0000107	0.0639000	0.2521000	0.0101000	0.0177000	1,051
	2000-2007	0.0006055	0.0910000	0.3632000	0.0067000	0.0168000	1,831
	2008-2017	0.0000211	0.0390000	0.1675000	0.0009419	0.0132000	4,398
Jet fuel	1990-2017	0.0001066	0.0175000	0.0688000	0.0008681	0.0076000	18,278
	1990-1999	-0.0001544	0.0172000	0.0690000	0.0008963	0.0077000	6,615
	2000-2007	0.0006403	0.0190000	0.0808000	0.0004987	0.0015000	5,119
	2008-2017	-0.0001603	0.0163000	0.0550000	0.0015000	0.0181000	6,567
Diesel	2002-2017	0.0004222	0.0187000	0.0875000	0.0003726	0.0046000	9,584
	2002-2007	0.0010000	0.0204000	0.0743000	0.0007144	0.0021000	3,156
	2008-2017	-0.0001710	0.0170000	0.0542000	0.0011000	0.0200000	6,461

Several interesting findings can be drawn from these results. First, since μ_J is not larger than one, jumps in the log-returns of our commodities will not assume to be only strictly positive. The role of this finding is particularly relevant since the price behaviour of our strategic commodities also shows negative jumps. However, the estimated mean value of the jumps is positive, which is also coherent with our series. The mean value of jumps in natural gas exceeds the corresponding mean values for jumps for the other commodities. This fact is in line with the extreme spikes observed in 2005 and 2006.

Second, the estimation of the parameters is consistent with the descriptive statistics. For example, the estimation of μ in the period 1990-2017 for brent and via the ML approach is 0.0001502, which compares with the average of the log-return of this commodity for the same period, i.e., 0.000147. The correlation between our commodities is also evident in the results. Since the spot prices of brent, jet fuel and diesel are highly correlated, the estimation for the drift in the period 2008-2017 assume always negative values (once again, it is consistent with the average daily log-returns). Comparing with

the natural gas and for the same subsample, the estimation for the drift component assumes a positive value, given a lower correlation between the spot price of brent (as well as other refined products) and natural gas prices. The estimated volatility in our strategic commodities shows that a lower volatility can be identified in the last subsample.

Finally, a brief comment on the parameter λ. Since the intensity of the jump-diffusion plays a significant role in the framework suggested by Merton (1976), indeed we find higher estimations for λ in the subsamples where occurred the most significant (positive and negative) jumps. In fact, the subsample 2008-2017 represents the period in which we find higher values for the intensity of jump-diffusion, which is explained by the most two relevant drops in the price of brent (and consequently on the refined products, such as the jet fuel and the diesel) over the last decade.[4.3] As usual, the exception occurs for natural gas, which reports similar values for $\hat{\lambda}$ in each subsample.

Table I.2. of the appendix I reports the usual information criteria, i.e., the Akaike Information Criteria (AIC, hereafter) and Bayesian Information Criteria (BIC, henceforth). In fact, introducing Poisson jumps in the standard GBM process allows a better performance in fitting these models to real data in accordance with the AIC. This finding is valid for both the entire sample and each subsample, which justifies the preference of the JGBM process when compared with the standard GBM diffusion. Using the BIC, the previous results also remain for the major of subsamples.

Another goodness-of-fit test is introduced to validate this jump-diffusion approach: the Q-Q plot. The parameter set of the jump-diffusion model with compound Poisson jumps

[4.3]The first relevant drop in this subsample was motivated by the uncertainty of the global financial crisis in 2007-2009. In fact, during the first semester of 2008 the spot prices of petroleum products (brent or crude oil) achieved 140$/bbl and few months later these prices dropped abruptly to 35$/bbl in the global markets. In April of 2011 the spot prices of petroleum products achieved 120$/bbl as the recovery of the global economy occurred. However, in June of 2014 the spot prices of this commodity dropped once again, until 27$/bbl in the beginning of 2016. A large period of higher prices encouraged oil production by the major countries/firms, so there was an oil glut in 2014 after demand from emerging markets declined.

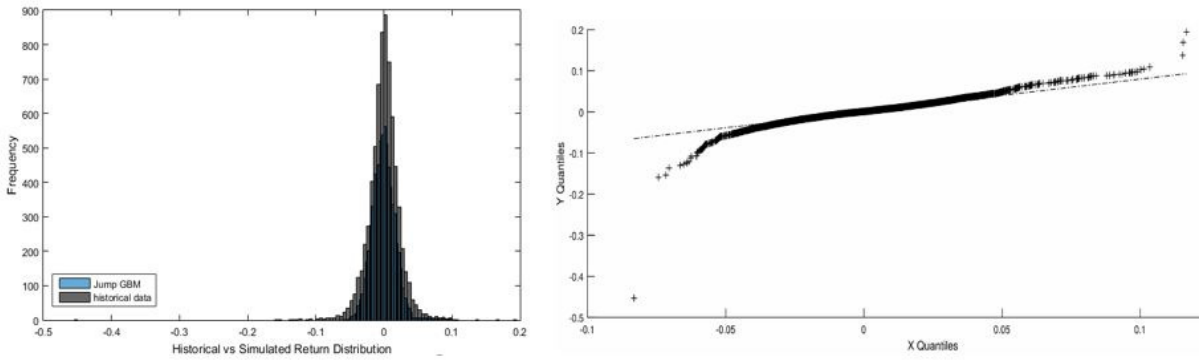

Figure 4.1: Histogram of brent log-returns during 1990-2017 and simulated JGBM process using estimated parameters and Q-Q plot of the series.

estimated via ML for brent during 1990-2017 is used to simulate the stochastic paths of this framework. This goodness-of-fit is depicted in Figure 4.1 by showing the Q-Q plot of the simulated returns from the JGBM process against the historical continuous returns of brent. The quantiles of the empirical distribution are plotted in the Y-axis, whereas the quantiles of the Merton (1976) distribution are presented in the X-axis. Even though the JGBM process provides a slightly better performance when compared with the standard GBM—as documented in Table I.2—, this Q-Q plot shows that the model suggested by Merton (1976) does not capture all features of the empirical distribution. Similar conclusions are achieved for the others strategic commodities.

4.3.2 The jump-diffusion model of Kou (2002)

In this subsection, we present and test the Double Exponential Jump-Diffusion (DEJD, hereafter) model suggested by Kou (2002). The DJED model is a particular case of Lévy processes with two-sided jumps. Comparing with the Poisson jump-diffusion approach introduced by Merton (1976), the DEJD model incorporates a highly skewed and leptokurtic distribution for the log-returns and, consequently, allows to model the spot prices of commodity prices.

In this paper, we adopt this DEJD approach to model our integrated O&G commodity prices for two reasons. First, the statistical nature of the double exponential distribution allows to capture the leptokurtic feature in the jump size distribution. Second, the double exponential distribution has the advantage of incorporating the memoryless property, which explains the success of this approach for both modeling and pricing under the DEJD approach Kou (2007).

This special case of Lévy processes with two-sided jumps is governed by the following SDE (under the physical measure $\mathbb{P}$)

$$dS_t = \mu S_{t-} dt + \sigma S_{t-} dW_t + S_{t-} d(\sum_{i=1}^{N_t} (Y_i - 1)), \tag{4.9}$$

and solving this SDE using the Itô's lemma, the following solution is obtained

$$S_{t+\Delta t} = S_t \exp\left[(\mu - \frac{1}{2}\sigma^2)\Delta t + \sigma W_{\Delta t}\right] \prod_{i=1}^{N_{\Delta t}} Y_i, \tag{4.10}$$

where μ, σ and W_t have the same meaning as before, S_{t-} is the value of the underlying asset just before the possible jump event, N_t is the usual Poisson process with intensity λ and $\{Y_i\}$ denotes a sequence of independent and identically distributed (iid, hereafter) random variables assuming non-negative values. The parameters μ and σ are constant over time, while the standard Brownian motion and the jumps are one-dimensional Kou (2002). The introduction of randomness occurs by considering N_t, W_t and $\log Y$ (hereafter, $\Upsilon := \log Y$), which we assume to be independent.

Therefore, Υ has the following density based on an asymmetric double exponential distribution

$$f_\Upsilon(y) = p\eta_1 e^{-\eta_1 y} \mathbf{1}_{\{y \geq 0\}} + q\eta_2 e^{-\eta_2 y} \mathbf{1}_{\{y<0\}}, \tag{4.11}$$

where $\eta_1 > 1$, $\eta_2 > 0$, p and q represent the probability of upward and downward jumps,

respectively, and the constrains p, $q \geq 0$ and $p + q = 1$ are needed. In order to impose that $\mathbb{E}$(Y) and $\mathbb{E}(S_t) < \infty$, we need to use the assumption that $\eta_1 > 1$. Without these requirements, we cannot ensure that the average upward jump exceed 100%, which is not reasonable in commodity markets. Hence, $\frac{1}{\eta_1}$ and $\frac{1}{\eta_2}$ represent the mean values of the two exponential distributions, respectively. The estimation of the parameters for the DEJD model involves the inverse Fourier transform of the characteristic function to compute an approximation for the density of the model since it is not known in a closed-form setting. Hence, the (unique) representation of the characteristic function and the corresponding inverse Fourier transform are expressed respectively by

$$\begin{aligned} \phi_{x_{\Delta t}}(u) &= \mathbb{E}[e^{iuX_{\Delta t}}] \\ &= \exp\left[\Delta t\left(iu\mu - \frac{\sigma^2 u^2}{2} + \lambda\left\{\frac{p\eta_1}{\eta_1 - iu} + \frac{p\eta_2}{\eta_2 - iu} - 1\right\}\right)\right] \end{aligned} \tag{4.12}$$

and

$$\begin{aligned} f_{X_{\Delta t}}(X) &= \frac{1}{2\pi}\int_{-\infty}^{\infty}(e^{iuX}\phi_{X_{\Delta t}}(u))du \\ &= \frac{1}{\pi}\int_{0}^{\infty}(e^{iuX}\phi_{X_{\Delta t}}(u))du. \end{aligned} \tag{4.13}$$

The implementation and evaluation of the integral in equation (4.13) is performed using the built-in function *quadgk* available in *Matlab*. Table 4.3 shows the parameter estimates under the DEJD model for our O&G commodities and via the ML approach. Overall, the estimated parameters have realistic values and are coherent with the previous processes. For all commodities under analysis, the probabilities of upward and downward jumps are quite similar in each subsample. Additionally, we find that the average upward jump did not exceed 100%, given the estimates for η_1, which is true for all the commodities. In the second step of this analysis, we provide in Figure 4.2 the graphical performance of the DEJD process comparing with the real data. For this pur-

pose, we use the histogram of entire sample of brent and compare with the simulated DEJD process.

Similarly to the case of the jump-diffusion model with compound Poisson jumps, the Q-Q plot of the empirical returns of brent in the entire sample and the simulated DEJD returns show that this jump-diffusion framework offers similar results to the Merton (1976) model, i.e., it does not capture all features of the empirical distribution since the Q-Q-plot does not fully approximates a straight line.

Table 4.3: Estimation of the parameters under the jump-diffusion model of Kou (2002) and via the ML approach.

		μ	σ	η_1	η_2	p	λ
Brent	1990-2017	0.0010	0.0256	125,171,402	94,755,845	0.4996	380,382
	1990-1999	0.0014	0.0249	92,087,251	65,698,804	0.5174	273,185
	2000-2007	-0.0000	0.0240	171,281,116	191,366,571	0.4950	588,230
	2008-2017	0.0006	0.0268	153,180,987	130,028,887	0.5049	472,783
Natural gas	1996-2017	0.0032	0.0779	101,932,483	131,681,718	0.5006	98,137
	1996-1999	0.0023	0.0732	131,078,029	224,979,723	0.4901	278,963
	2000-2007	0.0119	0.0434	113,034,397	248,767,439	0.4956	119,435
	2008-2017	0.0007	0.0451	65,031,631	63,467,985	0,5571	205,869
Jet fuel	1990-2017	0.0002	0.0255	95,776,081	124,855,153	0.4561	370,455
	1990-1999	-0.0002	0.0224	38,870,816	52,992,392	0.4962	152,076
	2000-2007	0.0000	0.0223	22,843,633	36,267,233	0.5000	97,865
	2008-2017	-0.0003	0.0216	131,955,369	161,829,333	0.4998	493,296
Diesel	2002-2017	0.0008	0.0225	84,900,204	67,506,820	0.4991	245,908
	2002-2007	0.0020	0.0233	55,589,651	33,743,654	0.5017	135,984
	2008-2017	0.0012	0.0219	89,279,721	41,259,725	0.5126	200,203

4.3.3 The VG model

Jump-diffusion models have two relevant drawbacks to model commodity prices: (i) they do not include the features of time-varying and stochastic volatility models; and

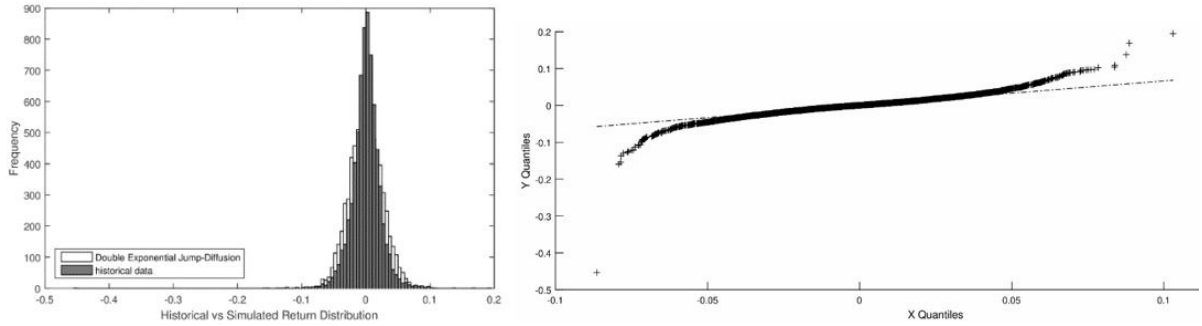

Figure 4.2: Histogram of brent log-returns during 1990-2017 and simulated DEJD process using estimated parameters and Q-Q plot of the series.

(ii) they only allow to model finite large jumps. Although the good performance shown by the jump-diffusion models, both limitations are significant disadvantages since commodity markets exhibit skewness and leptokurtosis features and probably shows infinite small jumps.

The VG process, introduced by Madan and Seneta (1990), Madan et al. (1998) and Seneta (2004), belongs to the subclass of the generalized hyperbolic distributions and allows to complement the class of fat tails models. In fact, the VG process has exponential tails and the rate for the tail decay is smaller than for the normal distribution. This allows to introduce more flexibility in order to capture the fat tails phenomenon and the high kurtosis exhibited in the commodity markets. Compared with other theoretical frameworks—e.g. the GARCH family or jump-diffusion models where we can find state-dependent volatility and by introducing randomness considering jumps, respectively—the VG process exhibits market activity time (also known as a subordinator), which is an increasing process and has independent and stationary increments. Moreover, this process can be considered a mixture of normal distributions, where the weighting density is given by the Gamma distribution of the market time. Indeed, this philosophy is similar to the framework of the GBM with jump-diffusion since the return process is a mixture too.

The SDE which governs the continuous log-returns of our commodity prices under the VG process is expressed as

$$d\log(S_t) = \bar{\mu}dt + \bar{\theta}dg_t + \bar{\sigma}dW(g_t), \tag{4.14}$$

where $\bar{\mu} \in \mathbb{R}$, $\bar{\theta} \in \mathbb{R}$ and $\bar{\sigma} \in \mathbb{R}_+$ represent the log-return drift in calendar-time, the log-return drift in market-activity-time and the volatility, respectively, and g_t denotes a positive and increasing random process, the market time. For $u \geq t \geq 0$, this random process has stationary increments $g_u - g_t$. Since $\mathbb{E}[g_u - g_t] = u - t$ and conditional on the market time's g, it follows that

$$\bar{\sigma}(W(g_u) - W(g_t))|_g \sim \bar{\sigma}\sqrt{(g_u - g_t)\epsilon}, \tag{4.15}$$

where ϵ represents the traditional Gaussian shock and, consequently,

$$\left(\log\left(\frac{S_u}{S_t}\right) - \bar{\mu}(u-t)\right)|_g \sim N\left(\bar{\theta}(g_u - g_t), \bar{\sigma}^2(g_u - g_t)\right). \tag{4.16}$$

Table 4.4 shows the estimations of the VG process via the ML approach.[4.4] The estimated volatility parameters for each commodity $\hat{\bar{\sigma}}$ show higher estimates that the ones for the mean value of returns and this finding is coherent with the previous results and the descriptive statistics for the continuous log-returns. Excluding the entire sample, the analysis of each subsample shows that the volatility in the last subsample is lower than the previous subsamples. This finding is aligned with the results of the previous stochastic models.

The symmetry feature of the log-returns of our commodities is tested with the estimation of the parameter θ. The estimates for θ confirm the asymmetric nature of the

[4.4] Appendix J of the provides the technical details of the VG estimation through ML.

log-returns, since the estimation for almost all subsamples is negative. Exemplifying for brent, we obtain negative estimations for θ, which are consistent with the skewness estimations in these subsamples—the unique exception is the subsample 2008-2017, where the skewness is close to zero.

Finally, we find a significant value for the time change parameter ν, which controls the tail fatness. The subsample which is showing a higher level of kurtosis is the first one for brent, natural gas and jet fuel (it is not applicable for diesel since this empirical analysis only starts in 2002). For diesel, we find a higher level of tail fatness in the last subsample, i.e., in 2008-2017. In fact, this is coherent with the kurtosis of the continuous log-returns for the same period of analysis.

The fit of the simulated continuous returns from the VG process is performed in the left-hand side of Figure 4.3. The leptokurtic and the fat tails features identified in commodity markets are better achieved with the VG process, though not completely replicating the original data. In the right-hand side of Figure 4.3, the quantiles from the simulated returns of the VG distribution are closer to the quantiles of the historical empirical distribution of brent's returns. Given this goodness-of-fit test, the VG process achieves a better performance when compared with the previous two jump-diffusion models by allowing for infinitely many jumps in finite time interval. Similar observations are also found in the other commodities.

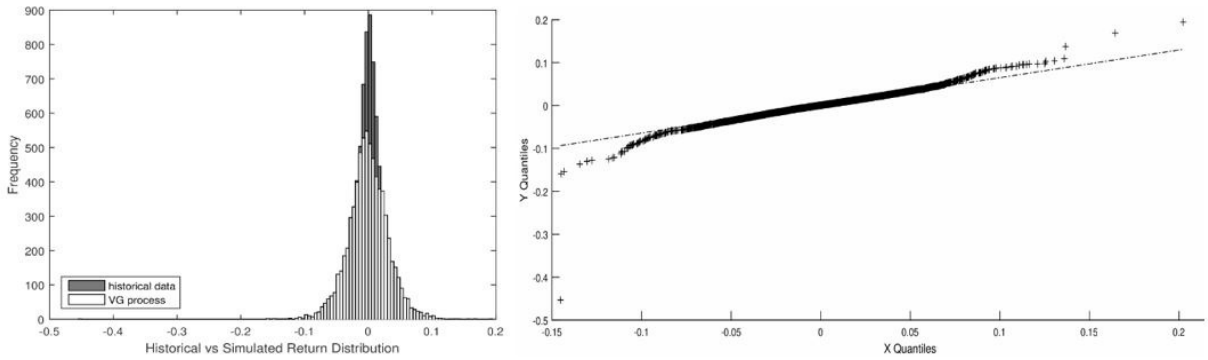

Figure 4.3: Histogram of brent log-returns during 1990-2017 and simulated VG process using estimated parameters and Q-Q plot of the series.

Table 4.4: Estimation of the parameters under the VG process and via the ML approach.

		$\bar{\mu}$	$\bar{\sigma}$	θ	ν
Brent	1990-2017	0.0013040	0.0221	-0.0011570	0.7954
	1990-1999	0.0005270	0.0225	-0.0004810	1.0351
	2000-2007	0.0077140	0.0222	-0.0070500	0.3865
	2008-2017	0.0003520	0.0211	-0.0005270	0.8913
Natural gas	1996-2017	0.0007665	0.0650	-0.0009357	1.8654
	1996-1999	0.0044445	0.0804	-0.0366245	2.4996
	2000-2007	-0.0042000	0.0938	0.0055000	1.3539
	2008-2017	0.0000000	0.0402	-0.0007000	1.6490
Jet fuel	1990-2017	0.0000000	0.0190	0.0000327	3.3386
	1990-1999	0.0028000	0.1727	-0.0104000	5.2855
	2000-2007	0.0023280	0.0191	-0.0017410	0.2501
	2008-2017	0.0007010	0.0177	-0.0008600	0.8290
Diesel	2002-2017	0.0032160	0.0206	-0.0022750	0.3503
	2002-2007	0.0009850	0.0193	-0.0007780	0.6758
	2008-2017	0.0002660	0.0185	-0.0004360	0.8155

4.3.4 GBM with nonlinear GARCH volatility

Over the years, several models have followed the seminal research of Bollerslev (1986) on GARCH models, which are considered to be an important modeling tool when dealing with high frequency financial data. These models capture the autocorrelation in

the volatility (volatility clustering). In other words, a period of high (resp., low) volatility will be followed by high (resp., low) volatility. Three popular extensions of the traditional GARCH models are the threshold GARCH (hereafter, TGARCH), the exponential GARCH (henceforth, EGARCH) and NGARCH models. In particular, the NGARCH model suggested by Engle and Ng (1993) plays a significant role in the literature since this model captures the asymmetric feature in the volatility. Thus, it implies that positive (resp., negative) returns yield subsequently lower (resp., higher) volatility.

The GBM with NGARCH volatility is expressed as

$$\Delta S_{t_i} = \mu S_{t_i} \Delta t_i + \sigma_{t_i} S_{t_i} \Delta W_{t_i}, \tag{4.17}$$

$$\sigma_{t_i}^2 = \omega + \alpha \sigma_{t_{i-1}}^2 + \beta(\epsilon_{t_{i-1}} - \gamma \sigma_{t_{i-1}})^2 \tag{4.18}$$

and

$$\epsilon_{t_i}^2 = (\sigma_{t_i} \Delta W_{t_i})^2, \tag{4.19}$$

where α, β and ω are positive parameters and γ is defined such that the inequality $\beta(\gamma^2 + 1) + \alpha < 1$ is valid. In the framework of the GBM with NGARCH, the parameter γ denotes an adjustment to the return innovations. Hence, a particular case of this framework is obtained when $\gamma = 0$, since it yields the symmetric GARCH(1,1) process. The statistical significance of this parameter implies that positive and negative return innovations have not the similar effect on the conditional variance, which is coherent with most financial and energy markets. On the other hand, when γ is positive, it increases the impact of negative returns on the variance.

For estimation purposes, the LL function for the sample of continuous log-returns is given by

$$L^{\star}(\Theta) = \sum_{i=1}^{n} log f_{\Theta}(x_i; x_{i-1}), \tag{4.20}$$

$$
\begin{aligned}
f_{\Theta}(x_i; x_{i-1}) &= fN(x_i; \mu, \sigma_i^2) \\
&= \frac{1}{\sqrt{2\pi\sigma_i^2}} \exp\left(-\frac{(x_i-\mu)^2}{2\sigma_i^2}\right)
\end{aligned} \tag{4.21}
$$

and

$$
L^{\star}(\Theta) = k + 0.5(-\log\sigma_i^2 - (x_i-\mu)^2/\sigma_i^2), \tag{4.22}
$$

where $x_1, x_2, x_3, ..., x_n$ represent the sample of continuous log-returns, f_{Θ} is the density function of the normal distribution and k is a constant. The set of parameters is represented by $\theta \equiv (\mu, \omega, \alpha, \beta, \gamma)$, where θ is an unknown parameter represented in the bounded set $\Theta \subset \mathbb{R}^5$.

Table 4.5 reports the estimations of the GBM with the NGARCH approach and via the ML prodedure. From the results of this estimation and since γ plays a significant role in this framework, it is relevant to focus on the signal related to $\hat{\gamma}$. Considering all the entire samples for brent, natural gas and diesel, all the $\hat{\gamma}$ assume positive estimates. Hence, it implies that this adjustment to the continuous log-return innovations reduces the impact of positive returns and increases the effect of negative returns. Considering the natural gas market, we can find an exception in the subsample of 1990-1999. Indeed, the historical data covering this period also supports the idea that this parameter allows a reduction in the impact of negative returns. As previously mentioned, the seasonality effect covering this commodity may explain this finding. For the jet fuel market, we find two subsamples with negative estimates for $\hat{\gamma}$: 1990-2017 and 1990-1999. While the estimate for 1990-1999 is almost zero—denoting that this data is governed by a GBM with symmetric effects, i.e., positive and negative innovations have the same effect on the conditional variance—, the second one clearly shows that the parameter is increasing the impact of good news in the volatility.

The histogram of the simulated continuous returns against the historical data for brent in 1990-2017 depicted in Figure 4.4 shows that the GBM with NGARCH volatility

achieve a significantly better performance when compared with the previous jump-diffusion model (JGBM or DEJD) and even the infinite-activity jump model of the VG approach. Analyzing the Q-Q plot in Figure 4.4, we confirm the quantiles of the simulated GBM with NGARCH volatility distribution are much more coherent with the quantiles of the empirical return distribution for the entire sample for this commodity. To validate these results against the standard Gaussian distribution, the information criteria for the GBM and GBM with NGARCH is provided in the Appendix K.1. The results show that the GBM with the NGARCH volatility outperforms the standard GBM model. Consequently, the autocorrelation in volatility and the asymmetric feature of the GARCH models are two powerful drivers in our strategic commodities.

Table 4.5: Estimation of the parameters under the GBM with NGARCH volatility process and via the ML approach.

		μ	ω	α	β	γ	LL
Brent	1990-2017	-0.00012860	0.00000182	0.9363	0.0216	1.3474	17,587
	1990-1999	-0.0007712	0,00008424	0.4844	0.4714	0.2668	6,208
	2000-2007	0.00120000	0.00031161	0.2134	0.2126	0.0780	4,883
	2008-2017	-0.00001706	0.00007507	0.4578	0.5079	0.1796	6,267
Natural gas	1996-2017	0.00017379	0.00002502	0.8723	0.1244	0.0478	8,283
	1996-1999	0.00360000	0.00055336	0.3516	0.6343	-0.0196	1,347
	2000-2007	0.00110000	0.00042924	0.8396	0.1351	0.0709	1,999
	2008-2017	-0.00066432	0.00003264	0.7908	0.1977	0.1652	5,044
Jet fuel	1990-2017	0.00026781	0.00000325	0.9230	0.0673	-0.1273	19,150
	1990-1999	-0.00016645	0.00005328	0.3972	0.5936	-0.0092	7,063
	2000-2007	0.00077217	0.00023702	0.1937	0.1705	0.2447	5,134
	2008-2017	-0.00055149	0.00006897	0.3735	0.3986	0.6010	6,647
Diesel	2002-2017	0.00006429	0.00009993	0.4191	0.3456	0.4242	9,668
	2002-2007	0.00130000	0.00033606	0.0773	0.1323	0.0251	3,168
	2008-2017	-0.00045225	0.00000048	0.9551	0.0187	1.1692	6,746

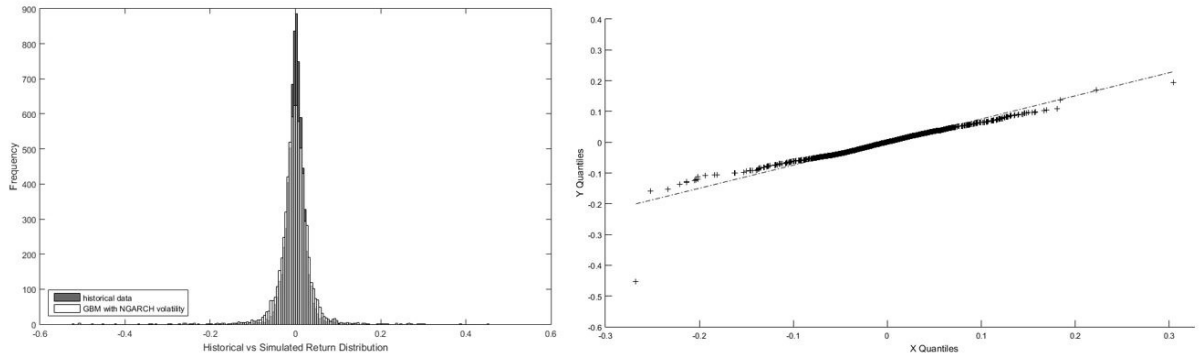

Figure 4.4: Histogram of brent log-returns during 1990-2017 and simulated GBM with NGARCH volatility using estimated parameters and Q-Q plot of the series.

4.4 Multivariate processes

This section addresses the estimation of multivariate processes for our portfolio of commodities.

4.4.1 The DCC-GARCH

Correlations between the spot prices in the portfolio of integrated O&G companies are crucial for decision makers. A relevant example of the role of correlations is for hedging purposes: if the structure of correlations is changing, the hedge ratio should incorporate the recent information. Until now, we modeled our strategic commodities individually and, therefore, we do not use multivariate processes, such as the multivariate ARCH family or multivariate stochastic volatility models. Hence, we consider now the DCC-GARCH family models.

This choice is motivated by the flexibility of the univariate GARCH estimators but avoiding the higher complexity of multivariate GARCH models. The flexibility and the simplicity is ensured by the two-step procedure proposed by Engle (2002): (i) univariate

GARCH models are fitted to the data set of our commodities and then (ii) the standardized residuals are used to estimate the time-varying correlation matrix.

According to the DCC-GARCH approach suggested by Engle (2002), this model can be expressed as

$$y_t = Cx_t + \epsilon_t, \tag{4.23}$$

and

$$\epsilon_t = H_t^{\frac{1}{2}} \nu_t, \tag{4.24}$$

where y_t is a $m \times 1$ vector which represents the dependent variables, x_t is a $k \times 1$ vector representing the independent variables, which incorporates the lags of y_t, C denotes the parameters by a $m \times k$ matrix and ν is a vector of iid innovations with dimension $m \times 1$. Moreover, the matrix generalization of univariate GARCH models, H_t, is expressed as

$$H_t = D_t^{\frac{1}{2}} R_t D_t^{\frac{1}{2}}, \tag{4.25}$$

$$R_t = diag(Q_t)^{-\frac{1}{2}} Q_t diag(Q_t)^{-\frac{1}{2}} \tag{4.26}$$

and

$$Q_t = (1 - \lambda_1 - \lambda_2)R + \lambda_1 \tilde{\epsilon}_{t-1} \tilde{\epsilon}'_{t-1} + \lambda_2 Q_{t-1}, \tag{4.27}$$

where $H_t^{\frac{1}{2}}$ denotes the Cholesky factor of the time-varying conditional covariance matrix H_t, Q_t represents the dynamic of the correlation coefficient (where λ_1 and λ_2 denote the two dynamics that determine the conditional quasicorrelations) and D_t is the diag-

onal matrix of conditional variances, which can be described by

$$D_t = \begin{bmatrix} \sigma_{1,t}^2 & 0 & \dots & 0 \\ 0 & \sigma_{2,t}^2 & \dots & 0 \\ \vdots & \vdots & \ddots & \vdots \\ 0 & 0 & \dots & \sigma_{m,t}^2 \end{bmatrix}, \tag{4.28}$$

and where $\sigma_{i,t}^2$ changes in accordance to a standard univariate GARCH family framework such as

$$\sigma_{i,t}^2 = \omega_i + \sum_{j=1}^{q_i} \alpha_j \epsilon_{i,t-j}^2 + \sum_{j=1}^{q_i} \beta_j \sigma_{i,t-j}^2. \tag{4.29}$$

Table 4.6 reports the DCC-GARCH parameter estimates for our commodities obtained via the ML approach. Appendix L provides the parameter estimations for the adjustment parameters λ_1 and λ_2. We are assuming that the error term follows a normal distribution. For comparison purposes, we have estimated the same model with the error term assuming a student-t distribution, but both models show similar results (outputs are available upon request). Furthermore, the technical conditions needed for stability and required by the parameters that affect the dynamics of the conditional quasicorrelations are satisfied, since $\lambda_1 > 0$, $\lambda_2 > 0$ and $0 \leq \lambda_1 + \lambda_2 < 1$ as shown in Panel A of Table L.1 of the corresponding appendix. In addition, λ_1 and λ_2 are largely statistically significant and a usual Wald test can reject the null hypothesis $\lambda_1 = \lambda_2 = 0$ and, therefore, the assumption that time-invariant conditional correlations is too restrictive for our commodities and the use of the DCC-GARCH is pertinent.

Table 4.6: Estimation of the parameters under the DCC-GARCH framework in 2002-2017 and via the ML approach.

	Brent	Natural gas	Jet fuel	Diesel
Mean equation:				
μ	0.000387	0.000062	0.000311	0.000272
Variance equation:				
ω	0.000001	0.000007	0.000001	0.000001
α	0.042088	0.169638	0.039954	0.042553
β	0.955489	0.869268	0.958552	0.955717
LL	9,624.46	6,112.75	10,108.84	9,921.90
AIC	-19,240.91	-12,217.49	-20,209.68	-19,835.81
BIC	-19,215.96	-12,192.54	-20,184.73	-19,810.86

The historical conditional correlations using the DCC-GARCH approach for the pairs of our strategic commodities are available in Figure L.1 of the corresponding appendix. The graphical analysis shows a similar dynamic conditional correlation between the pairs jet fuel-diesel, brent-jet fuel and brent-diesel, however it is different for the dynamic correlation between brent-natural gas, jet fuel-natural gas and diesel-natural gas. Besides the different dynamic, the correlation between brent (or its derivatives) and natural gas reveals that an obvious relationship between both commodities is not found. Indeed, for the most of the trading days, this dynamic correlations assumes values between -0.4 and 0.6.

In order to explain the price signal between both commodities, we note that it depends on several effects, such as the fuel substitution and resource competition. First, since integrated O&G companies produce both brent and natural gas, a positive shock in brent prices may likely lead to an increase in natural gas extraction and production which would likely exert downward pressure on natural gas prices. However, the same movement in brent prices may lead to increase oil drilling which would decrease natural gas drilling, potentially leading to higher natural gas prices. This effect is an example of

the uncertainty effect of the crude oil prices in the natural gas. Second, fuel substitution also matters since some refined products are competitive substitutes to natural gas. As a consequence, an increase in brent prices would likely promote the substitution of natural gas for some refined products, which would increase the natural gas demand and, consequently, the spot prices.[4.5]

In this part, it is also interesting to compare the fitting results of the DCC-GARCH model with the performance of the best model presented in the previous section, i.e., GBM with non-linear GARCH effect in volatility. For this purpose we adopt the AIC and BIC rules. Exemplifying with the brent case and re-estimating the univariate GBM with the NGARCH volatility for the period 2002-2017, we achieve 9,460 for the maximum LL and it corresponds to -18,802.20 for the AIC and -18,771.01 for the BIC. In other words, the standard DCC-GARCH seems to present a slightly better performance than the best univariate model, since this approach allows to model the joint dynamics of integrated O&G commodities. The same conclusion is valid for natural gas, jet fuel and diesel.

4.4.2 Alternative multivariate approaches

In order to complement the previous multivariate processes, we also test alternative frameworks in the DCC framework. More specifically, we adopt the following asymmetric approaches to capture the leverage effects in commodity markets in two different ways: (i) the GJR-GARCH model suggested by Glosten et al. (1993) and the EGARCH model proposed by Nelson (1991). Both univariate processes allow for threshold ef-

[4.5] In fact, some refined products obtained from brent or crude oil are competitive substitutes to natural gas. For example, notice that the residual fuel oil competes with natural gas for electric power generation purposes. Therefore, a positive shock in brent prices would likely encourage the substitution between natural gas and some refined products, which would increase the demand for natural gas and, consequently, the corresponding price of this commodity. This substitution effect is also known in the literature as the burner-tip parity.

fects, though with alternative powers of variance in the variance equation.

The GJR-GARCH model is intended to capture the potential presence of an asymmetric leverage effect, which is known to potentially improve the forecast performance of the standard GARCH approach, as documented, for instance, in Wei et al. (2010). In this model setup, the variance equation is given by

$$\sigma_t^2 = \omega + (\alpha + \gamma \mathbf{1}_{\{\varepsilon_{t-1}<0\}})\varepsilon_{t-1}^2 + \beta\sigma_{t-1}^2. \tag{4.30}$$

where γ is the parameter that controls the asymmetric leverage effect and $\mathbf{1}_{\{.\}}$ is the indicator function. When $\gamma = 0$, the GJR-GARCH model is reduced to the standard GARCH framework. The usual restrictions on the parameters are $\omega, \alpha, \gamma, \beta > 0$.

The EGARCH approach assumes a specific parametric form for the conditional heteroskedasticity. More specifically, we say $\varepsilon_t \sim$ EGARCH if the variance equation is governed by

$$\log(\sigma_t^2) = \omega + \alpha\frac{\varepsilon_{t-1}}{\sqrt{\sigma_t}} + \gamma\frac{\varepsilon_t}{\sqrt{\sigma_t}} + \beta\log(\sigma_{t-1}^2). \tag{4.31}$$

Given the log variance feature of the univariate EGARCH, the model does not require any restrictions on the parameters.

Despite being models of asymmetric leverage effect, a particular feature matters for the stylized facts of our strategic commodities: in the GJR-GARCH approach, if the condition $\alpha + \frac{\gamma}{2} + \beta < 1$ is valid, the volatility itself shows the mean-reverting feature and it fluctuates around the square root of the unconditional variance, which is defined as $\sigma_t^2 = \frac{\omega}{1-\alpha-\frac{\gamma}{2}-\beta}$.

Since the standard DCC-GARCH does not incorporate asymmetries, the theoretical framework is modified to include the asymmetries and the corresponding impact of news. These further developments are detailed in the research of Cappiello et al.

(2006), where the authors considered an asymmetric form of the standard DCC approach. Therefore, following Cappiello et al. (2006) we show the numerical results of the estimates for the DCC-GJR-GARCH and the DCC-EGARCH in Tables 4.7 and 4.8, respectively.

Table 4.7: Estimation of the parameters under the DCC-GJR-GARCH framework in 2002-2017 and via the ML approach.

	Brent	Natural gas	Jet fuel	Diesel
Mean equation:				
μ	0.000087	-0.000401	0.000144	0.000136
Variance equation:				
ω	0.000001	0.000007	0.000001	0.000001
α	0.009203	0.138275	0.023305	0.030501
γ	0.048336	0.064176	0.029764	0.021643
β	0.964837	0.869356	0.961313	0.957653
LL	9,650.47	6,118.25	10,119.02	9,926,55
AIC	-19,290.94	-12,226.51	-20,228.04	-19,843.11
BIC	-19,259.76	-12,195.32	-20,196.85	-19,811.92

Table 4.8: Estimation of the parameters under the DCC-EGARCH framework in 2002-2017 and via the ML approach.

	Brent	Natural gas	Jet fuel	Diesel
Mean quation:				
μ	-0.000073	0.000141	0.000104	0.000021
Variance equation:				
ω	-0.098809	-5.108350	-0.106009	-0.122564
α	-0.079612	0.010000	0.089766	0.098892
γ	-0.041511	0.010000	-0.026227	-0.022822
β	0.995281	0.010000	0.995502	0.994237
LL	9,647.72	4,326.03	10,115.97	9,916.66
AIC	-19,285.44	-8,642,07	-20,221.94	-19,823.32
BIC	-19,254.25	-8,610.88	-20,190.75	-19,792.14

Two concluding remarks can be drawn from this tables. First, the inclusion of asym-

metric effects contributes for improving the performance of the standard DCC-GARCH (and the best univariate model as well). More specifically, the performance of the DCC-GJR-GARCH seems slightly better than the remaining models. In other words, our numerical results show that negative multivariate innovations at time $t-1$ have a stronger impact in the variance at time t than positive multivariate innovations. Since the DCC-GJR-GARCH highlights in the fitting performance of our strategic commodity prices, there is evidence that the volatility of our commodities is mean-reverting for brent, jet fuel and diesel.

The second finding is relevant for the pertinence of the DCC in both setups. Panels B and C of Table L.1 of the corresponding appendix show that a Wald test rejects the null hypothesis that $\lambda_1 = \lambda_2 = 0$ at all conventional statistical levels and, therefore, there is no evidence to support the idea that the DCC approach reduces to constant conditional correlation between the volatility of our strategic commodity prices. This finding is coherent to the standard DCC-GARCH, where we obtained the same conclusion for all commodities.

4.4.3 Out-of-sample multivariate forecasting results

This subsection performs an out-of-sample forecasting exercise to evaluate the performance of the multivariate models in our strategic commodities. Here we compare the last three multivariate models using the Root Mean Square Error (RMSE). More specifically, given the data of 2016 for our commodity log-returns, we compute the one-step ahead predictive variance in 2017. The predicted variance is then compared with the real volatility. The evaluation period for the forecasting exercise is from January 2017 to the end of the sample (November 2017). The results are reported in Table 4.9.

These out-of-sample forecasting results are broadly similar to the model comparison

results using the LL, AIC and BIC. In particular, the DCC-GJR-GARCH multivariate models provide better forecasts than their GARCH counterparts (the standard DCC-GARCH and the DCC-EGARCH) for all the strategic commodities. Other evaluation metrics such as the Mean Absolute Error (MAE) and the Mean Absolute Percent Error (MAPE) have highlighted that the best forecasting performance is achieved for the DCC-GJR-GARCH and are available upon request. As previously mentioned, the relevance of the DCC-GJR-GARCH is related to the mean-reverting feature of our commodity prices.

Table 4.9: Root mean square error from the out-of-sample forecasting exercise.

	Brent	Natural gas	Jet fuel	Diesel
DCC-GARCH	0.015882	0.033569	0.013590	0.014336
DCC-GJR-GARCH	0.015844	0.033514	0.013559	0.014292
DCC-EGARCH	0.015898	0.033729	0.013559	0.014306
Out-of-sample trading days	224	224	224	224

4.5 Concluding remarks

Much of the research on modeling spot prices in commodity markets considers each commodity individually. This paper uses a standard integrated O&G company with a portfolio of assets representing the main strategic commodities in the industry: brent for the exploration and production activities, natural gas for trading purposes and the main refined products to represent the refining margin in downstream operations. We tested a few classes of alternative models, including the log-normal and the double exponential jump-diffusion approaches, the VG process and the GBM with nonlinear GARCH volatility. We obtain two relevant concluding remarks for the literature.

The first contribution is about the jump-diffusions in our strategic commodities. It is well known that several market anomalies affect commodity prices, such as jumps, bubbles and other plausible reasons which cause structural breaks. We find strong evidence to support the idea that jumps heavily affect the results of the standard GBM and the features of the Gaussian distribution. Under these frameworks, one fat tails model emerges as the preferable one: the GBM with non-linear effects. Its fitting performance shows that all commodities exhibit returns with asymmetric behaviour in the volatility.

Second, we also contribute by testing the pertinence of three different multivariate models in a context of non-perfectly positive correlated commodities. The nonlinear combination of univariate GARCH models (standard GARCH, GJR-GARCH and EGARCH) and the conditional covariance matrix of the errors modeled by time-varying cross-equation weights allows to obtain a better fitting performance than univariate frameworks. Overall, the DCC-GJR-GARCH is the best model for our four strategic commodity prices.

Given these promising findings, future research should incorporate the performance of the jump-diffusion and fat tails processes to pricing the most usual financial derivatives for the O&G companies, such as spread options and swing options. This avenue for future research is particularly relevant for hedging purposes in integrated O&G companies. To introduce more realistic assumptions, these findings also allow to expand the evaluation of investment projects in the O&G industry based on the incorporation of the jump-diffusion processes in the real options theory. The events of the following decade in the O&G industry, namely with some disinvestment in upstream activities and the new challenges with the energy transition will require the update of our results.

Appendix I

For stochastic processes, the Markov property is generally sufficient to define the likelihood along a time series of observations as a product of transition probabilities on single time steps between two adjacent periods. Consequently, for a Markov process x_t, we can write the likelihood function, $L(\Theta)$, based on the probability density f of the vector random sample, as

$$\begin{aligned} L(\Theta) &= f_{X(t_0),X(t_1)\,,\ldots,X(t_n);\Theta} \\ &= f_{X(t_n)|X(t_{n-1});\Theta} \times f_{X(t_{n-1})|X(t_{n-2});\Theta} \times \ldots \times f_{X(t_1)|X(t_0);\Theta} \times f_{X(t_0);\Theta}\,. \end{aligned} \tag{I.1}$$

A particular case occurs for independent and identically distributed (hereafter, iid) data, in which we can simplify the problem since the likelihood function $L(\Theta)$ is represented by the product of the probability density of each data point in our sample. For the GBM framework, it occurs if and only if the Maximum Likelihood (henceforth, ML) is implemented based on the log-returns of the prices (in opposition to the series in levels, i.e., prices), that is

$$X_{t_i} := \log(S_{t_i}) - \log(S_{t_{i-1}}), \tag{I.2}$$

and since these returns respect the iid assumption, we do not need to apply equation (I.1) through transitions. Therefore, for iid random variables, the likelihood function is described by

$$\begin{aligned} L(\Theta) &= f_\Theta(x_1, x_2, \ldots, x_n) \\ &= \prod_{n=1}^{n} f_\Theta(x_i). \end{aligned} \tag{I.3}$$

In order to avoid numerical problems in the maximization of the likelihood function (the resulting product of density values could tend to zero), the likelihood function is frequently adapted to the log-likelihood (LL, hereafter) framework as follows

$$L^{\star}(\Theta) = \sum_{i=1}^{n} \log f_{\Theta}(x_i), \tag{I.4}$$

where $L^{\star}(\Theta)$ denotes the LL. Notice that the transformation to the LL function is valid since maxima is not affected by monotone changes. Hence, the parameter set of the GBM framework is determined as

$$m = \left[\hat{\mu} - \frac{1}{2}\sigma^2\right] \Delta t \tag{I.5}$$

and

$$v = \hat{\sigma}^2 \Delta t. \tag{I.6}$$

Based on Gaussian iid samples, the ML method allows to achieve closed-form solutions for m and v. The estimations for m and v result from the differentiation of the Gaussian density function with respect to the set of parameters individually and thus equaling to zero. Therefore, the estimations for the mean and variance for the log-returns x_i— taking $X_i = \log(S_t) - \log(S_{t-1})$—are described as

$$\hat{m} = \sum_{i=1}^{n} \frac{x_i}{n}, \tag{I.7}$$

and

$$\hat{v} = \sum_{i=1}^{n} \frac{(x_i - \hat{m})^2}{n}. \tag{I.8}$$

Focusing now on the jump-diffusion model with compound Poisson jumps, we first

rewrite the stochastic equation with logarithm of the asset price as

$$d\log S_t = (\mu - \frac{1}{2}\sigma^2)dt + \sigma dW_t + \log(Y_{N_t})dN_t, \tag{I.9}$$

which is equivalent to

$$d\log S_t = (\mu + \lambda\mu_J - \frac{1}{2}\sigma^2)dt + \sigma dW_t + \left[\log(Y_{N_t})dN_t - \mu_J\lambda dt\right], \tag{I.10}$$

where the jump-diffusion component (inside the square brackets on the right-hand side of the previous expression) and the diffusion shock (given by the standard Brownian motion) have null mean.

Similarly to the standard GBM process, we apply also the ML method in log-returns space to the JGBM process. Integrating both sides, the solution for the SDE incorporating a jump-diffusion for S_t is given by

$$S_T = S_0 \exp\left[(\mu - \frac{1}{2}\sigma^2)T + \sigma W_T\right] \prod_{j=1}^{N_T} Y_j, \tag{I.11}$$

which can be discretized as

$$S_t = S_{t-\Delta t} \exp\left[(\mu - \frac{1}{2}\sigma^2)\Delta t + \sigma\sqrt{\Delta t}\epsilon_t\right] \prod_{j=1}^{n_t} Y_j, \tag{I.12}$$

where Δt represents the time step, ε follows a normal distribution with zero mean and variance one and n_t denotes the number of jumps during $t - \Delta t$ and is described by $n_t = N_t - N_{t-\Delta t}$. The discretization is also valid for the expression in log-returns, that is

$$\begin{aligned} X_t &= \Delta\log(S_t) \\ &= \mu^\star\Delta t + \sigma\sqrt{\Delta t}\epsilon_t + \Delta J_t^\star, \end{aligned} \tag{I.13}$$

where X_t represents the returns, described by

$$\begin{aligned} X_t &:= \Delta \log(S_t) \\ &= \log(S_t) - \log(S_{t-\Delta t}), \end{aligned} \tag{I.14}$$

and where the jump disturbance in Δt and the $\mu^\star$ are given by

$$\Delta J_t^\star = \sum_{j=1}^{n_t} log(Y_j) - \lambda \Delta t \mu_J, \tag{I.15}$$

and

$$\mu^\star = (\mu - \frac{1}{2}\sigma^2 + \lambda \mu_J). \tag{I.16}$$

Since the estimation of the parameter set is performed in discrete time and assuming that the number of jump innovations occurring in the fixed small time interval Δt has the expectation $\lambda \Delta t$, we get

$$\mathbb{E}[\Delta J_t^\star] = E(n_t \mu_J) - \lambda \Delta t \mu_J = 0. \tag{I.17}$$

Moreover, the jump disturbance $J_t^\star$—which is conditional on the jumps occurrence—is normally distributed, that is

$$\Delta J_t^\star|_{n_t} \sim N((n_t - \lambda \Delta t)\mu_J, n_t \sigma_J^2). \tag{I.18}$$

Therefore, the conditional distribution of X_t is also normally distributed and we can

write the two most relevant moment conditions—mean and variance—as follows

$$\begin{aligned}\mathbb{E}\left[\Delta \log(S_t|n_t)\right] &= \mu^{\star}\Delta t + (n_t - \lambda\Delta t)\mu_J \\ &= (\mu - \frac{1}{2}\sigma^2)\Delta t + n_t\mu_J \end{aligned} \tag{I.19}$$

and

$$Var\left[\Delta \log(S_t|n_t)\right] = \sigma^2\Delta t + n_t\sigma_J^2. \tag{I.20}$$

Table I.1: Estimation of the parameters under the GBM diffusion and via the ML approach.

		μ	σ	LL
Brent	1990-2017	0.0001502	0.0230	16,756
	1990-1999	0.0000484	0.0246	5,867
	2000-2007	0.0006672	0.0228	4,855
	2008-2017	-0.0001718	0.0215	6,059
Natural gas	1996-2017	0.0002360	0.0779	6,088
	1990-1999	0.0000112	0.0731	1,003
	2000-2007	0.0006255	0.1066	1,666
	2008-2017	0.0000071	0.0444	4,231
Jet fuel	1990-2017	0.0001240	0.0186	18,121
	1990-1999	0.0000373	0.0187	6,517
	2000-2007	0.0005844	0.0192	5,116
	2008-2017	-0.0001585	0.0180	6,493
Diesel	2002-2017	0.0002084	0.0194	9,548
	2002-2007	0.0009368	0.0206	3,155
	2008-2017	-0.0001738	0.0187	6,403

Table I.2: Information criteria for GBM and JGBM processes.

		AIC		BIC	
		GBM	JGBM	GBM	JGBM
Brent	1990-2017	-33,508	-33,767	-33,495	-33,727
	1990-1999	-11,730	-11,850	-11,719	-11,814
	2000-2007	-9,706	-9,714	-9,696	-9,680
	2008-2017	-12,113	-12,280	-12,102	-12,245
Natural Gas	1996-2017	-12,172	-13,137	-12,159	-13,098
	1990-1999	-2,003	-2,099	-1,993	-2,069
	2000-2007	-3,329	-3,659	-3,318	-3,625
	2008-2017	-8,458	-8,792	-8,447	-8,757
Jet Fuel	1990-2017	-36,239	-36,552	-36,225	-36,513
	1990-1999	-13,030	-13,225	-13,019	-13,190
	2000-2007	-10,229	-10,234	-10,218	-10,200
	2008-2017	-12,983	-13,129	-12,971	-13,095
Diesel	2002-2017	-19,093	-19,164	-19,080	-19,126
	2002-2007	-6,307	-6,308	-6,296	-6,276
	2008-2017	-12,802	-12,919	-12,790	-12,884

Appendix J

We notice that the VG framework assumes a Gamma process, such that $\{g_t\} \sim \Gamma(\frac{t}{\nu}, \nu)$ and where the parameter ν is an independent parameter from $\{W_t; t \geq t_0\}$. For any values of u and t and since $\mathbb{E}[g_u - g_t] = u - t$ and $Var(g_u - g_t) = \nu(u - t)$, then $\{g_u - g_t\} \sim \Gamma(\frac{u-t}{\nu}, \nu)$. Given the law of iterated expectations, it is easy to check that

$$\mathbb{E}\left[\log S_u - \log S_t\right] = (\bar{\mu} + \bar{\theta})(u - t) \tag{J.1}$$

and

$$Var\left[\log S_u - \log S_t\right] = (\bar{\sigma}^2 + \bar{\theta}^2\nu)(u - t). \tag{J.2}$$

Using equation (4.16) of the paper and integrating out the term g through its Gamma density, we can obtain the unconditional density. By setting $\Delta t := u - t$ and $X_{\Delta t} := \log(S_{t+\Delta t}/S_t)$, it is possible to obtain the density function as follows

$$f_{(X\Delta t)}(x) = \int_0^\infty f_N(x; \bar{\theta}g, \bar{\sigma}^2 g) f_\Gamma(g; \frac{\Delta t}{\nu}, \nu) dg. \tag{J.3}$$

As previously mentioned, this is an infinite mixture of Gaussian densities weighted by Gamma densities. In fact, the integral in equation (J.3) converges and the pdf of a VG model is described by

$$f_{(X\Delta t)}(x) = \frac{2e^{\frac{\theta(x-\bar{\mu})}{\bar{\sigma}^2}}}{\bar{\sigma}\sqrt{2\pi}\nu^{\frac{\Delta t}{\nu}}\Gamma\frac{1}{\nu}} \left(\frac{|x - \bar{\mu}|}{\sqrt{\frac{2\bar{\sigma}^2}{\nu} + \bar{\theta}^2}}\right)^{\frac{\Delta t}{\nu} - \frac{1}{2}} K_{\frac{\Delta t}{\nu} - \frac{1}{2}} \left(\frac{|s - \bar{\mu}|\sqrt{\frac{2\bar{\sigma}^2}{\nu} + \bar{\theta}^2}}{\bar{\sigma}^2}\right), \tag{J.4}$$

where k_η (.) denotes a modified bessel function of the third kind with index η described

by

$$K_\eta(x) = 0.5 \int_0^\infty y^{\eta-1} \exp\left\{-\frac{x}{2}(y^{-1}+y)\right\} dy. \tag{J.5}$$

Once again, we introduce the assumption of independence in the continuous returns $(x_1, x_2, x_3, ..., x_n)$ and we define the pdf of a VG process by $\Theta \equiv (\bar{\mu}, \bar{\sigma}, \bar{\theta}, \nu)$ to estimate under the ML technique. Thus, the moment generating function $\mathbb{E}\left[e^{zX}\right]$ for $X_{\Delta t}$ is expressed as

$$M_X(z) = e^{\bar{\mu}z}(1 - \bar{\theta}\nu z - 0.5\nu\bar{\sigma}^2 z^2)^{-\frac{\Delta t}{\nu}}, \tag{J.6}$$

where the moments of the returns in the period Δt are given by

$$\mathbb{E}\left[X\right] = \bar{X} = (\bar{\mu} + \bar{\theta})\Delta t, \tag{J.7}$$

$$\mathbb{E}\left[(X - \bar{X})^2\right] = (\nu\bar{\theta}^2 + \bar{\sigma}^2)\Delta t, \tag{J.8}$$

$$\mathbb{E}\left[(X - \bar{X})^3\right] = (2\bar{\theta}^3\nu^2 + 3\bar{\sigma}^2\nu\bar{\theta})\Delta t, \tag{J.9}$$

and

$$\mathbb{E}\left[(X - \bar{X})^4\right] = (3\nu\bar{\sigma}^4 + 12\bar{\theta}^2\bar{\sigma}^2\nu^2 + 6\bar{\theta}^4\nu^3)\Delta t + (3\bar{\sigma}^4 + 6\bar{\theta}^2\bar{\sigma}^2\nu + 3\bar{\theta}^4\nu^2)(\Delta t)^2, \tag{J.10}$$

where the skewness and kurtosis are equal to

$$S = \frac{\Delta t 3\bar{\theta}\nu}{((\nu\bar{\theta}^2 + \bar{\sigma^2})\Delta t)^{\frac{3}{2}}}, \tag{J.11}$$

and

$$K = \frac{3\nu\bar{\sigma}^4 + 12\bar{\theta}^2\bar{\sigma}^2\nu^2 + 6\bar{\theta}^4\nu^3)\Delta t + (3\bar{\sigma}^4 + 6\bar{\theta}^2\bar{\sigma}^2\nu + 3\bar{\theta}^4\nu^2)(\Delta t)^2}{((\nu\bar{\theta}^2 + \bar{\sigma}^2)\Delta t)^2}. \tag{J.12}$$

Using the assumption that $\bar{\theta}$ assumes small values and, hence, ignoring the terms $\bar{\theta}^2$,

$\bar{\theta}^3$ and $\bar{\theta}^4$, it is possible to simplify the skewness and kurtosis to

$$S = \frac{3\bar{\theta}\nu}{\sqrt{\Delta t}\bar{\sigma}} \tag{J.13}$$

and

$$K = 3 + \frac{3\nu}{\Delta t}. \tag{J.14}$$

Finally, we consider the following initial values in order to solve the optimization problem

$$\bar{\sigma} = \sqrt{\frac{V}{\Delta t}}, \tag{J.15}$$

$$\nu = \Delta t(\frac{K}{3} - 1), \tag{J.16}$$

$$\bar{\theta} = \frac{\sqrt{\Delta t}S\bar{\sigma}}{3\nu} \tag{J.17}$$

and

$$\bar{\mu} = \frac{\bar{X}}{\Delta t} - \bar{\theta}. \tag{J.18}$$

Appendix K

Table K.1: Information criteria for GBM with NGARCH volatility.

		AIC	BIC
Brent	1990-2017	- 35,163	- 35,128
	1990-1999	- 12,406	- 12,377
	2000-2007	- 9,755	- 9,727
	2008-2017	- 12,523	- 12,494
Natural gas	1996-2017	- 16,555	- 16,522
	1996-1999	- 2,685	- 2,661
	2000-2007	- 3,987	- 3,959
	2008-2017	- 10,078	- 10,049
Jet fuel	1990-2017	- 38,289	- 38,254
	1990-1999	- 14,116	- 14,087
	2000-2007	- 10,258	- 10,230
	2008-2017	- 13,283	- 13,254
Diesel	2002-2017	- 19,325	- 19,293
	2002-2007	- 6,326	- 6,300
	2008-2017	- 13,482	- 13,453

Appendix L

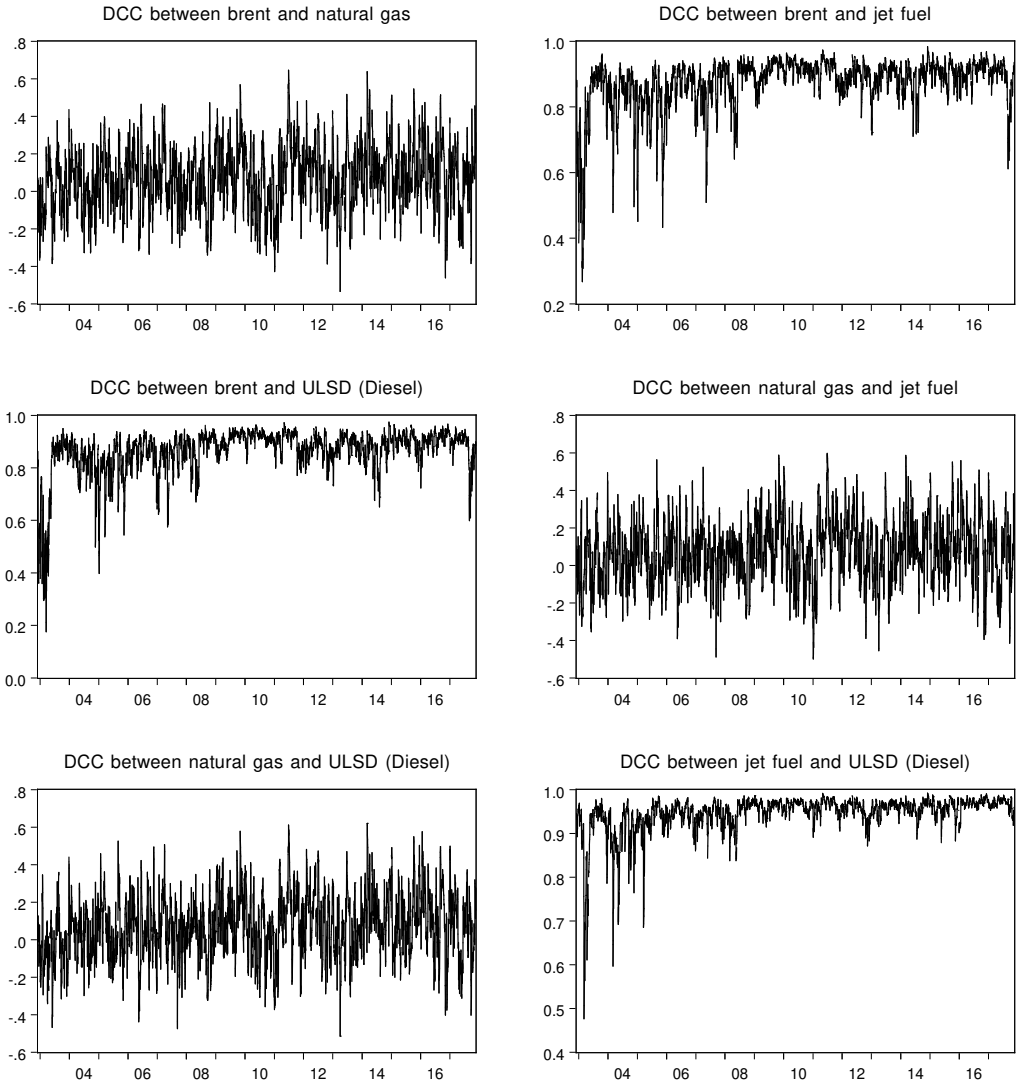

Figure L.1: Dynamic conditional correlation between the returns of our commodities.

Table L.1: Estimation of the parameters under the DCC models.

	Coefficient	Standard error	z-statistic	p-value
Panel A: DCC-GARCH model				
λ_1	0.100072	0.0000	10,057.27	0.0000
λ_2	0.850230	0.0000	15,359.31	0.0000
Panel B: DCC-GJR-GARCH model				
λ_1	0.099979	0.0000	9,652.20	0.0000
λ_2	0.849969	0.0000	14,840.26	0.0000
Panel C: DCC-EGARCH model				
λ_1	0.100110	0.0000	17,217.91	0.0000
λ_2	0.850361	0.0000	20,015.06	0.0000

5. Conclusion

This thesis provides important results concerning on modeling energy prices with time-varying volatility and jumps in three separate articles.

The first paper tests several time-varying volatility processes based on a formal Bayesian model comparison exercise for modeling the volatility of future contracts for energy firms: oil, natural gas and electricity. This paper offers four relevant findings for the current literature. First, by adopting the Bayes factor criteria to rank our list of models, we find that SV models almost always outperform the corresponding GARCH models. This finding consolidates the main conclusion of Chan and Grant (2016) for a list of similar models but applied to spot prices in several commodity markets. Second, the SV model with a t-distribution seems to be the best model to replicate the volatility of futures contracts on the adopted commodities and utilities. Third, the maturity of future contracts seems significant since it impacts the fitting performance of our models. Finally, given the previous concluding remarks, these findings have relevant implications for hedging purposes, mainly when investors and risk managers are computing extreme risk measures, such as the CVaR. Our results show the relevance of adopting the accurate stochastic process for computing the corresponding risk measures for both hedged and unhedged positions.

In the second paper, we have proposed a stochastic framework for modeling electricity (and natural gas) prices in a context of energy transition. The model allows to capture

the three most relevant features in these markets: the mean reversion in the prices, the spikes and drops modeled as a jump-diffusion process and the seasonality effects. Our empirical analysis was addressed for the day-ahead prices of the Nord Pool electricity market and natural gas prices. Using the suggested stochastic model for multiple day-ahead prices, we estimate the parameters under ML estimation. The out-of-sample exercise shows that the mean-reverting and jump-diffusion process outperforms the corresponding standard geometric Brownian motion with jumps and the GARCH-EVT.

Given the recent forecasts about the increasing in the global demand of natural gas (and liquefied natural gas) and since this is the unique fossil fuel in the context of energy transition (and the goals for decreasing the CO_2 emissions), we propose a copula approach (by incorporating mean reversion and jumps) to model a simulated portfolio of electricity (from renewable energy sources) and natural gas assets. Our estimations for several copula functions show the best suitable copulas are the Gumbel's and the t-Student's. Our findings are also relevant for risk management purposes. Based on extreme risk measures, the portfolio risk analysis simulates multiple energy portfolios in a context of energy transition by decreasing the energy sources from fossil fuels (i.e., natural gas) and increasing the weight of electricity assets (representing renewable energy sources). One of the main findings is about the relevance of the accurate copula-stochastic approach: when the unitary results of the adopted risk measures are transposed to a real portfolio of an energy firm, the importance of fitting the accurate model to the underlying prices becomes crucial.

To complement the risk analysis, we have performed an optimization problem to compute the optimal energy mix of energy based on a portfolio manager that seeks to maximize his return-risk ratio. The results show that decision makers tend to avoid a high level of exposure to electricity prices, since electricity is known to be an high-volatility utility. This finding has relevant implications in energy transition since the most relevant

investments enhancing carbon neutrality involve electricity production with renewable energy sources (assets). Therefore, in addition to the large required capital expenditures in renewable projects, the high level of volatility in electricity markets highlights that the existence of incentive schemes provided by governments to new investments in renewable projects are of pivotal importance or, in the absence of such mechanisms, an accurate risk management policy is needed for hedging electricity positions as long as energy transition is done based on electricity assets.

Finally, the last paper provides several findings about the dynamics of several univariate and multivariate approaches to model the commodity prices. Much of the research on modeling spot prices in commodity markets considers each commodity individually. This paper uses a standard integrated O&G company with a portfolio of assets representing the main strategic commodities in the industry: brent for the exploration and production activities, natural gas for trading purposes and the main refined products to represent the refining margin in downstream operations. We tested a few classes of alternative models, including the log-normal and the double exponential jump-diffusion approaches, the VG and the GBM with nonlinear GARCH volatility. In this paper we obtain two relevant concluding remarks for the literature.

The first contribution is about the jump-diffusions in our strategic commodities. It is well known that several market anomalies affect commodity prices, such as jumps, bubbles and other plausible reasons that causes structural breaks. We find strong evidence to support the idea that jumps heavily affect the results of the standard GBM and the features of the Gaussian distribution. Under these frameworks, one fat tails model highlights: the GBM with nonlinear effects. Their fitting performance show that all commodities exhibit returns with asymmetric behaviour in the volatility.

Second, we also contribute by testing the pertinence of three different multivariate models in a context of non-perfectly positive correlated commodities. The nonlinear com-

bination of univariate GARCH models (standard GARCH, GJR-GARH and EGARCH) and the conditional covariance matrix of the errors modeled by time-varying cross-equation weights allows to obtain a better fitting performance than univariate frameworks. Overall, the DCC-GJR-GARCH is the best model for our four strategic commodity prices.

Bibliography

Aït-Sahalia, Y., 2004. Disentangling diffusion from jumps. Journal of Financial Economics 74, 487–528.

Aloui, C., Mabrouk, S., 2010. Value-at-risk estimations of energy commodities via long-memory, asymmetry and fat-tailed GARCH models. Energy Policy 38, 2326–2339.

Ang, B.W., Su, B., 2016. Carbon emission intensity in electricity production: A global analysis. Energy Policy 94, 56–63.

Artzner, P., Delbaen, F., Eber, J.M., Heath, D., 1999. Coherent measures of risk. Mathematical Finance 9, 203–228.

Askari, H., Krichene, N., 2008. Oil price dynamics (2002-206). Energy Economics 30, 2134–2153.

Barbosa, L., Ferrão, P., Rodrigues, A., Sardinha, A., 2018. Feed-in-tariffs with minimum price guarantees and regulatory uncertainty. Energy Economics 72, 517–541.

Basher, S.A., Sadorsky, P., 2016. Hedging emerging market stock prices with oil, gold, VIX, and bonds: A comparison between DCC, ADCC and GO-GARCH. Energy Economics 54, 235–247.

Benth, F.E., Benth, J.Š., Koekebakker, S., 2008. Stochastic Modeling of Electricity and

Related Markets. volume 11 of *Advanced Series on Statistical Science and Applied Probability*. World Scientific.

Bessembinder, H., Coughenour, J.F., Seguin, P.J., Smoller, M.M., 1995. Mean reversion in equilibrium asset prices: Evidence from the futures term structure. Journal of Finance 50, 361–375.

Black, F., 1976. The pricing of commodity contracts. Journal of Financial Economics 3, 167–179.

Bollerslev, T., 1986. Generalized autoregressive conditional heteroskedasticity. Journal of Econometrics 31, 307–327.

Brennan, M.J., Hughes, P.J., 1991. Stock prices and the supply of information. Journal of Finance 46, 1665–1691.

Brooks, C., Prokopczuk, M., 2013. The dynamics of commodity prices. Quantitative Finance 13, 527–542.

Cabrera, B.L., Schulz, F., 2016. Volatility linkages between energy and agricultural commodity prices. Energy Economics 54, 190–203.

Cao, W., Guernsey, S.B., Linn, S.C., 2018. Evidence of infinite and finite jump processes in commodity futures prices: Crude oil and natural gas. Physica A: Statistical Mechanics and its Applications 502, 629–641.

Cappiello, L., Engle, R.F., Sheppard, K., 2006. Asymmetric dynamics in the correlations of global equity and bond returns. Journal of Financial Econometrics 4, 537–572.

Chan, J.C., 2013. Moving average stochastic volatility models with application to inflation forecast. Journal of Econometrics 176, 162–172.

Chan, J.C., Eisenstat, E., 2015. Marginal likelihood estimation with the cross-entropy method. Econometric Reviews 34, 256–285.

Chan, J.C., Grant, A.L., 2016. Modeling energy price dynamics: GARCH versus stochastic volatility. Energy Economics 54, 182–189.

Chan, K.F., Gray, P., 2006. Using extreme value theory to measure value-at-risk for daily electricity spot prices. International Journal of Forecasting 22, 283–300.

Choroś, B., Ibragimov, R., Permiakova, E., 2010. Copula estimation, in: Jaworski, P., Durante, F., Härdle, W., Rychlik, T. (Eds.), Copula Theory and Its Applications. Springer, Berlin, Heidelberg. volume 198 of *Lecture Notes in Statistics*. chapter 3, pp. 77–91.

Clayton, D.G., 1978. A model for association in bivariate life tables and its application in epidemiological studies of familial tendency in chronic disease incidence. Biometrika 65, 141–151.

Clewlow, L., Strickland, C., 2000. Energy Derivatives: Pricing and Risk Management. Lacima Publications, London.

Conejo, A.J., Contreras, J., Espínola, R., Plazas, M.A., 2005. Forecasting electricity prices for a day-ahead pool-based electric energy market. International Journal of Forecasting 21, 435–462.

Couture, T., Gagnon, Y., 2010. An analysis of feed-in-tariff remuneration models: Implications for renewable energy investment. Energy Policy 38, 955–965.

Cox, J.C., 1975. Notes on option pricing I: Constant elasticity of variance diffusions. Working Paper, Stanford University. Reprinted in *Journal of Portfolio Management*, 23 (1996), 15-17.

Creti, A., Joëts, M., Mignon, V., 2013. On the links between stock and commodity markets' volatility. Energy Economics 37, 16–28.

Deng, S.J., Oren, S.S., 2006. Electricity derivatives and risk management. Energy 31, 940–953.

Dias, J.C., Nunes, J.P., 2011. Pricing real options under the constant elasticity of variance diffusion. Journal of Futures Markets 31, 230–250.

Embrechts, P., McNeil, A.J., Straumann, D., 2002. Correlation and dependence in risk management: Properties and pitfalls, in: Dempster, M.A.H. (Ed.), Risk Management: Value at Risk and Beyond. Cambridge University Press, Cambridge, United Kingdom. chapter 7, pp. 176–223.

Engle, R.F., 1982. Autoregressive conditional heteroscedasticity with estimates of the variance of United Kingdom inflation. Econometrica , 987–1007.

Engle, R.F., 2002. Dynamic conditional correlation: A simple class of multivariate generalized autoregressive conditional heteroskedasticity models. Journal of Business and Economic Statistics 20, 339–350.

Engle, R.F., Ng, V.K., 1993. Measuring and testing the impact of news on volatility. Journal of Finance 48, 1749–1778.

European Wind Energy Association, 2012. Wind in Power: 2011 European Statistics. Technical Report. Brussels, Belgium.

Eydeland, A., Geman, H., 1998. Pricing power derivatives. Risk 11, 71–73.

Fang, H.B., Fang, K.T., Kotz, S., 2002. The meta-elliptical distributions with given marginals. Journal of Multivariate Analysis 82, 1–16.

Frank, M.J., 1979. On the simultaneous associativity of $f(x, y)$ and $x + y - f(x, y)$. Aequationes Mathematicae 19, 194–226.

Fusai, G., Roncoroni, A., 2008. Implementing Models in Quantitative Finance: Methods and Cases. Springer-Verlag, Berlin Heidelberg.

Geman, H., Roncoroni, A., 2006. Understanding the fine structure of electricity prices. Journal of Business 79, 1225–1261.

Geman, H., Shih, Y.F., 2009. Modeling commodity prices under the CEV model. Journal of Alternative Investments 11, 65–84.

Ghorbel, A., Trabelsi, A., 2014. Energy portfolio risk management using time-varying extreme value copula methods. Economic Modelling 38, 470–485.

Gianfreda, A., Bunn, D., 2018. A stochastic latent moment model for electricity price formation. Operations Research 66, 1189–1203.

Gibson, R., Schwartz, E.S., 1990. Stochastic convenience yield and the pricing of oil contingent claims. Journal of Finance 45, 959–976.

Glosten, L.R., Jagannathan, R., Runkle, D.E., 1993. On the relation between the expected value and the volatility of the nominal excess return on stocks. Journal of Finance 48, 1779–1801.

Gumbel, E.J., 1960. Bivariate exponential distributions. Journal of the American Statistical Association 55, 698–707.

Hammoudeh, S., Li, H., 2004. The impact of the Asian crisis on the behavior of US and international petroleum prices. Energy Economics 26, 135–160.

Hammoudeh, S., Li, H., Jeon, B., 2003. Causality and volatility spillovers among petroleum prices of WTI, gasoline and heating oil in different locations. The North American Journal of Economics and Finance 14, 89–114.

Haugom, E., 2011. Some stylized facts about high-frequency Nord Pool forward electricity prices. Journal of Energy Markets 4, 21–49.

Huang, B.N., Yang, C.W., Hwang, M.J., 2009. The dynamics of a nonlinear relationship between crude oil spot and futures prices: A multivariate threshold regression approach. Energy Economics 31, 91–98.

Huisman, R., Mahieu, R., 2003. Regime jumps in electricity prices. Energy Economics 25, 425–434.

Joe, H., 1997. Multivariate Models and Dependence Concepts. volume 73 of *Monographs on Statistics and Applied Probability*. Chapman and Hall, London, UK.

Kaldor, N., 1939. Speculation and economic stability. Review of Economic Studies 7, 1–27.

Kaminski, V., 1997. The challenge of pricing and risk managing electricity derivatives, in: The US Power Market. Risk Publications, London, pp. 149–171.

Kayalar, D.E., Küçüközmen, C.C., Selcuk-Kestel, A.S., 2017. The impact of crude oil prices on financial market indicators: Copula approach. Energy Economics 61, 162–173.

Keynes, J.M., 1936. The General Theory of Employment, Interest, and Money. Harcourt Brace, New York, NY.

Kök, A.G., Shang, K., Yücel, S., 2018. Impact of electricity pricing policies on renewable energy investments and carbon emissions. Management Science 64, 131–148.

Koopman, S.J., Hol Uspensky, E., 2002. The stochastic volatility in mean model: empirical evidence from international stock markets. Journal of Applied Econometrics 17, 667–689.

Kou, S.G., 2002. A jump-diffusion model for option pricing. Management Science 48, 1086–1101.

Kou, S.G., 2007. Jump-diffusion models for asset pricing in financial engineering, in: Birge, J.R., Linetsky, V. (Eds.), Handbooks in Operations Research and Management Science. Elsevier. volume 15. chapter 2, pp. 73–116.

Larsson, K., Nossman, M., 2011. Jumps and stochastic volatility in oil prices: Time series evidence. Energy Economics 33, 504–514.

Lee, L.F., 1983. Generalized econometric models with selectivity. Econometrica 51, 507–512.

Lin, S.X., Tamvakis, M.N., 2001. Spillover effects in energy futures markets. Energy Economics 23, 43–56.

Lindström, E., Regland, F., 2012. Modeling extreme dependence between European electricity markets. Energy Economics 34, 899–904.

Lu, X.F., Lai, K.K., Liang, L., 2014. Portfolio value-at-risk estimation in energy futures markets with time-varying copula-GARCH model. Annals of Operations Research 219, 333–357.

Lucia, J.J., Schwartz, E.S., 2002. Electricity prices and power derivatives: Evidence from the Nordic power exchange. Review of Derivatives Research 5, 5–50.

Lund, D., 1992. Petroleum taxation under uncertainty: Contingent claims analysis with an appplication to Norway. Energy Economics 14, 23–31.

Luo, J., Ji, Q., 2018. High-frequency volatility connectedness between the US crude oil market and China's agricultural commodity markets. Energy Economics 76, 424–438.

MacKie-Mason, J.K., 1990. Do taxes affect corporate financing decisions? Journal of Finance 45, 1471–1493.

Madan, D.B., Carr, P.P., Chang, E.C., 1998. The variance gamma process and option pricing. European Finance Review 2, 79–105.

Madan, D.B., Milne, F., 1991. Option pricing with VG martingale components. Mathematical Finance 1, 39–55.

Madan, D.B., Seneta, E., 1990. The variance gamma (V.G.) model for share market returns. Journal of Business 63, 511–524.

Markowitz, H., 1952. Portfolio selection. Journal of Finance 7, 77–91.

Merton, R.C., 1976. Option pricing when underlying stock returns are discontinuous. Journal of Financial Economics 3, 125–144.

Nelsen, R.B., 2006. An Introduction to Copulas. Springer, New York, NY. 2nd edition.

Nelson, D.B., 1991. Conditional heteroskedasticity in asset returns: A new approach. Econometrica 59, 347–370.

Nomikos, N., Andriosopoulos, K., 2012. Modelling energy spot prices: Empirical evidence from NYMEX. Energy Economics 34, 1153–1169.

Ordoudis, C., Delikaraoglou, S., Kazempour, J., Pinson, P., 2020. Market-based coordination of integrated electricity and natural gas systems under uncertain supply. European Journal of Operational Research 287, 1105–1119.

Ordoudis, C., Pinson, P., Morales, J.M., 2019. An integrated market for electricity and natural gas systems with stochastic power producers. European Journal of Operational Research 272, 642–654.

Pindyck, R.S., 2001. The dynamics of commodity spot and futures markets: A primer. Energy Journal 22, 1–29.

Quintino, A., Catalão-Lopes, M., Lourenço, J.C., 2019. Can switching from gasoline to aromatics mitigate the price risk of refineries? Energy Policy 134, 110963.

Ritzenhofen, I., Spinler, S., 2016. Optimal design of feed-in-tariffs to stimulate renewable energy investments under regulatory uncertainty - a real options analysis. Energy Economics 53, 76–89.

Rockafellar, R.T., Uryasev, S., 2000. Optimization of conditional value-at-risk. Journal of Risk 2, 21–42.

Rubinstein, R.Y., 1997. Optimization of computer simulation models with rare events. European Journal of Operational Research 99, 89–112.

Rubinstein, R.Y., Kroese, D.P., 2004. The cross-entropy method: a unified approach to combinatorial optimization, Monte-Carlo simulation, and machine-learning. Springer-Verlag, New York.

Sadorsky, P., 2006. Modeling and forecasting petroleum futures volatility. Energy Economics 28, 467–488.

Schwartz, E.S., 1997. The stochastic behavior of commodity prices: Implications for valuation and hedging. Journal of Finance 52, 923–973.

Schwartz, E.S., Smith, J.E., 2000. Short-term variations and long-term dynamics in commodity prices. Management Science 46, 893–911.

Seifert, J., Uhrig-Homburg, M., 2007. Modelling jumps in electricity prices: Theory and empirical evidence. Review of Derivatives Research 10, 59–85.

Seneta, E., 2004. Fitting the variance-gamma model to financial data. Journal of Applied Probability 41, 177–187.

Silvapulle, P., Moosa, I.A., 1999. The relationship between spot and futures prices: evidence from the crude oil market. Journal of Futures Markets 19, 175–193.

Sklar, A., 1959. Fonctions de répartition à n-dimensions et leurs marges. Publications de l`Institut Statistique de l`Université de Paris 8.

Slade, M.E., 1988. Grade selection under uncertainty: Least cost last and other anomalies. Journal of Environmental Economics and Management 15, 189–205.

Taylor, S.J., 1994. Modeling stochastic volatility: a review and comparative study. Mathematical Finance 4, 183–204.

Trolle, A.B., Schwartz, E.S., 2009. Unspanned stochastic volatility and the pricing of commodity derivatives. Review of Financial Studies 22, 4423–4461.

U.S. Energy Information Administration, 2016. International Energy Outlook 2016. Technical Report. Washington, DC, USA.

Van Ophem, H., 1999. A general method to estimate correlated discrete random variables. Econometric Theory 15, 228–237.

Wei, Y., Wang, Y., Huang, D., 2010. Forecasting crude oil market volatility: further evidence using GARCH-class models. Energy Economics 32, 1477–1484.

Wind Europe, 2019. Wind Energy in Europe in 2018: Trends and Statistics. Technical Report. Brussels, Belgium.

Working, H., 1948. Theory of the inverse carrying charge in futures markets. Journal of Farm Economics 30, 1–28.

Working, H., 1949. The theory of price of storage. American Economic Review 39, 1254–1262.

Wozabal, D., Rameseder, G., 2020. Optimal bidding of a virtual power plant on the Spanish day-ahead and intraday market for electricity. European Journal of Operational Research 280, 639–655.

Youssef, M., Belkacem, L., Mokni, K., 2015. Value-at-Risk estimation of energy commodities: A long-memory GARCH-EVT approach. Energy Economics 51, 99–110.

Zhou, Y., Scheller-Wolf, A., Secomandi, N., Smith, S., 2016. Electricity trading and negative prices: Storage vs. disposal. Management Science 62, 880–898.

Zhou, Y., Scheller-Wolf, A., Secomandi, N., Smith, S., 2019. Managing wind-based electricity generation in the presence of storage and transmission capacity. Production and Operations Management 28, 970–989.